

December 2016



## **Project Report No. 565**

### **Exploiting yield maps and soil management zones**

Shibu Muhammed<sup>1</sup>, Alice Milne<sup>1</sup>, Ben Marchant<sup>2</sup>, Simon Griffin<sup>3</sup> and Andrew Whitmore<sup>1</sup>

<sup>1</sup> Rothamsted Research, Harpenden, Hertfordshire AL5 2JQ, UK

<sup>2</sup> British Geological Survey, Keyworth, Nottingham NG12 5GG, UK

<sup>3</sup> SOYL Precision Farming, Newbury, RG14 5PX

This is the final report of an 18 month project (RD-2012-3875) which started in January 2013 and was carried out part-time over three years. The work was funded by a contract for £202,308 from AHDB Cereals & Oilseeds and an in-kind contribution of £4,200 from SOYL.

While the Agriculture and Horticulture Development Board seeks to ensure that the information contained within this document is accurate at the time of printing, no warranty is given in respect thereof and, to the maximum extent permitted by law, the Agriculture and Horticulture Development Board accepts no liability for loss, damage or injury howsoever caused (including that caused by negligence) or suffered directly or indirectly in relation to information and opinions contained in or omitted from this document.

Reference herein to trade names and proprietary products without stating that they are protected does not imply that they may be regarded as unprotected and thus free for general use. No endorsement of named products is intended, nor is any criticism implied of other alternative, but unnamed, products.

AHDB Cereals & Oilseeds is a part of the Agriculture and Horticulture Development Board (AHDB).



# CONTENTS

<b>1.</b>	<b>ABSTRACT</b> .....	<b>6</b>
<b>2.</b>	<b>INTRODUCTION</b> .....	<b>6</b>
<b>3.</b>	<b>METHODS</b> .....	<b>9</b>
<b>3.1.</b>	<b>Protocols for reliable yield maps</b> .....	<b>9</b>
<b>3.2.</b>	<b>Delineating management zones</b> .....	<b>18</b>
3.2.1.	Smoothed fuzzy k-means cluster analysis .....	19
<b>3.3.</b>	<b>Compare the merits of managing soil nutrients at different scales</b> .....	<b>21</b>
3.3.1.	<i>Modelling phosphorus in soil</i> .....	22
3.3.2.	<i>Modelling yield and quantifying its spatial variation</i> .....	24
3.3.3.	<i>Yield response model</i> .....	24
3.3.4.	<i>Management scales</i> .....	26
3.3.5.	<i>Using metrics of variation to guide sampling strategies</i> .....	26
<b>3.4.</b>	<b>Assess the extent to which yield maps can be used to manage soil variation at the scale of soil management zones</b> .....	<b>27</b>
3.4.1.	<i>Potential for Variable Rate Management based on Lark et al. (2003)</i> .....	27
3.4.1.1	<i>Variance ratio (VR)</i> .....	29
3.4.1.2	<i>The normalized classification entropy (NCE)</i> .....	30
3.4.1.3	<i>Standard deviation (SD)</i> .....	30
3.4.2.	<i>Opportunity index (Yi)</i> .....	30
3.4.3.	<i>Variable Rate Management Score</i> .....	31
<b>4.</b>	<b>RESULTS</b> .....	<b>32</b>
<b>4.1.</b>	<b>Comparison of yield cleaning software</b> .....	<b>32</b>
<b>4.2.</b>	<b>Delineating management zones to understand the causes of yield variation</b>	<b>40</b>
4.2.1.	Field-BD .....	41
4.2.2	Field-BF .....	45
4.2.3	Field-CC.....	50
4.2.4	Field-CP.....	55
4.2.5	Field-ER.....	59
4.2.6	Field-EL .....	63

4.2.7	Field-HM .....	67
4.2.8	Field-HS .....	70
4.2.9	Field-LM .....	74
4.2.10	Field-PA .....	78
4.2.11	Field-TK .....	81
<b>4.3.</b>	<b>Compare measuring soil nutrients by different sampling methods .....</b>	<b>83</b>
4.3.1.	<i>Comparison of P estimated by the sampling schemes.....</i>	83
4.3.2.	<i>Assessing the extent to which yield maps can be used to predict the most appropriate sampling scheme .....</i>	84
<b>4.4.</b>	<b>Usefulness of yield maps to manage soil variation at the scale of soil management zones .....</b>	<b>89</b>
4.4.1.	<i>Potential for variable rate (PVRM) based on Lark et al. (2003) .....</i>	89
4.4.2.	<i>Opportunity index (Yi).....</i>	90
4.4.1.	Variable Rate Management Score .....	93
<b>5.</b>	<b>DISCUSSION .....</b>	<b>94</b>
5.1	Comparison of yield cleaning software.....	94
5.2	Delineating management zones to understand the causes of yield variation	95
5.3	Compare measuring soil nutrients by different sampling methods .....	96
5.4	Usefulness of yield maps to manage soil variation at the scale of soil management zones .....	97
<b>6.</b>	<b>CONCLUSIONS .....</b>	<b>98</b>
6.1.	Guidance for farmers.....	100
6.2.	Future research and knowledge transfer.....	101
6.2.1.	<i>Integrating farmer's knowledge with hard data to inform management zones.....</i>	101
6.2.2.	<i>Validation of soil management zones by the yield determining factors at field.....</i>	101
6.2.3.	<i>Investigate new methods of sampling.....</i>	101
6.2.4.	<i>Developing an integrated model that farmers can use.....</i>	101
<b>7.</b>	<b>REFERENCES .....</b>	<b>102</b>
<b>8.</b>	<b>APPENDICES .....</b>	<b>104</b>

<b>8.1.</b>	<b>Description of variogram.....</b>	<b>104</b>
<b>8.2.</b>	<b>Mathematical symbols and abbreviations used.....</b>	<b>106</b>
<b>8.3.</b>	<b>Summary statistics for P in each field according to zone and the probability that the observed variation in P was explained by the classifications. ....</b>	<b>107</b>
<b>8.4.</b>	<b>Parameters of different variograms models for various fields.....</b>	<b>108</b>
<b>8.5.</b>	<b>Opportunity index (<math>Y_i</math>) and its components for different years for different fields.</b>	<b>110</b>

## 1. Abstract

Combine harvesters often have yield monitors fitted as standard, and many farmers use them to create yield maps for their fields. These maps contain important information about the spatial and temporal variation of fields. Understanding the variation of a field helps the farmer to make more informed management decisions on how he or she might vary inputs such as fertilizer. The objectives of this project were to establish robust and accessible protocols for the production of reliable yield maps from yield monitor data and create management zones, compare the merits of measuring soil nutrients (a) at the field scale, (b) using management zones and (c) using grids, and to assess the extent to which yield maps can be used to inform the management of soil variation. In the first instance, we reviewed some of the existing software available for cleaning the yield maps and evaluated those including the one we have developed (ROTH-YE). A novel statistical method developed to filter the values associated with flow delay was included in the ROTH-YE software. ROTH-YE performed as well or better than any of the other yield cleaning software we have compared in this study. We then went on to use the cleaned monitor data to create management zones using a spatially smoothed version of a fuzzy k-means classification. This method identifies areas of the field that vary similarly to one another across seasons. In practice, identifying these zones is useful for the farmer as it highlights and quantifies differences in yield that should be explored further.

Farmers sample their fields periodically to assess the nutrient concentration and pH to formulate the fertilizer application rates to the crop. We compared the cost effectiveness of three soil sampling schemes: field-based, management zone-based and grid-based. The advantages of using grid- and zone-based sampling strategies over field-based ones varied from field to field in our study, although for most of the fields grid-based sampling performed better than zone-based sampling. We found that the spatial variation of the yield monitor data (quantified by estimating a variogram) could be used to predict which sampling scheme was likely to be most profitable. We also explored the use of metrics derived from the variogram to help farmers to decide on whether to use uniform or variable rate management within a given field. We reviewed two methods from the literature and, based on our findings, proposed a new method for farmers to rank their fields for the potential for variable management based on these metrics.

## 2. Introduction

Yield mapping on British arable farms has been possible since the early 1990s, and coupled systems of yield monitors and global positioning systems are now routinely fitted on many makes of combine harvester. This means that farmers are gathering a plethora of data on the variation of yields within their fields and because this variation often results from variation in soil properties, it holds valuable

information that could inform site-specific management. However, the raw data collected from farmers' combine harvesters in the form of yield maps consists of complex signals and there are several difficulties associated with the generation and interpretation of these maps. Firstly, yield monitor data are often noisy and contain artefacts with various systematic and random sources of variation (Stafford *et al.*, 1996; Arslan and Colvin, 2002). These include naturally occurring yield variation due to climate and soil-landscape features, management-induced yield variation, and measurement errors caused by the yield-monitoring process itself (Simbahan *et al.*, 2004). To be of use it is important, as far as possible, to remove the erroneous measurements without losing the true variation in the observed yield. A proper understanding of the true variation in the field helps the farmer to decide on a uniform or variable rate management within the field. For a variable rate management, farmers may wish to manage their land by dividing their fields into management zones according to the inherent fertility of the soil or actual crop performance over several years. They can then adjust the amount of fertilizer or other agricultural inputs applied to each management zone in accordance with each zone's potential to yield. Several properties of the soil or observations of yield are likely to contribute to a farmer's judgement and to the division of his fields into management zones, and many methods have been proposed for this purpose (Milne *et al.*, 2012). In dividing large fields into smaller zones for precise management we take into account several factors that a farmer would want to consider:

- a) Each individual zone should be sufficiently homogeneous that the farmer could treat it as uniform
- b) Each zone should be substantially less variable than the field as a whole;
- c) Each zone should be large enough for the farmer to manage separately from the others;
- d) Each zone should be spatially coherent and have smooth boundaries.

Algorithms to identify these factors are not necessarily compatible. In particular, spatial coherence and the demand for smooth boundaries might mean that the zones are more variable than they would be if they were allowed to be more fragmented with intricate boundaries, and large zones are likely to be more variable than small ones. So, delineating zones for management almost inevitably requires compromise. Mathematical algorithms exist that use yield monitor data covering several seasons and other sensor data to select management zones within which the yield is fairly constant for each individual season. Many approaches simply partition the field into areas that constantly yield better than average, consistently poorer than average or lie somewhere between. Such strategies are based on the assumption that permanent characteristics of soil always lead to the same behaviour in each year (Blackmore *et al.*, 2003). Perhaps, the average yield for a particular zone might fluctuate between seasons depending on weather, management and variation in the factors that limit yield. Therefore, if one wants to understand the observed variation in the field, algorithms based on understanding of the processes that account for both within field and year to year variation and quantify both are arguably better.

Once management zones have been identified, a farmer is faced with the questions:

- (i) what is causing the differences between the zones? and
- (ii) are these differences large enough to consider variable rate management?

Often the reason for the variation between zones will be obvious to the farmer. For example, he or she will know if a particular part of the field is prone to drought, and that the effect of this is causing the observed variation in yield between the zones. In other cases, the reason might not be clear, and the farmer might wish to sample the soil to see if there is some nutrient deficiency or some local problem with the pH of the soil.

Generally, fertilizer application rates (uniform or variable) are decided based on soil sampling results. It is well accepted that the average soil nutrient concentration within a reasonably uniform area can be established by measuring at 10-15 locations on a 'W' design across the area. Marchant (2012) confirmed that this sampling strategy was adequate for uniform fertilizer applications. However, it is not clear how a farmer should establish when the nutrient concentration within a field is sufficiently uniform to follow this strategy or whether it would be better to divide the field into smaller management zones or even to vary nutrient inputs at the finest scale permitted by the fertilizer spreader. If the fertilizer inputs are to vary on a fine scale then continuous maps of soil nutrient concentrations on an equally fine scale are required. These could be produced by grid-based sampling of the field. There is no general consensus about whether grid-based sampling should be used or whether sampling should be based on management zones. The best approach will vary from field to field. We have investigated the plausibility of using the variation within yield maps to give some indication of which of the sampling strategies is most appropriate.

Understanding the variation on production constraints in the field leads the farmer to decide on whether uniform or variable rate management is appropriate in his field. In the latter situation, the farmer will vary the inputs (seeds, fertilizer, pesticides, etc.) across each field. Yield monitor data can be used as a proxy for variation in the field and it has been proposed that it could be used to make a decision on whether variable rate management is likely to be cost effective. Lark *et al.* (2003) describes a methodology for allocating rankings for the 'potential for variable rate management' based on the variation captured in yield monitor data. Similarly, de Oliveira (2009) presents a method for calculating an 'opportunity index' that scores the 'opportunity' for variable rate management. This is based on the variation in yield monitor data and characteristics of the machinery used to apply variable rate inputs. We investigated these methods using a number of case studies to see whether they could be of potential value to UK farmers.

Here we explore the usefulness of yield monitor data to understand both spatial and temporal yield variation and act accordingly. The specific objectives include

- I. To establish robust and accessible protocols for the production of reliable yield maps from yield monitor data
- II. To devise protocols for the robust and efficient implementation of management zones
- III. To compare the merits of measuring soil nutrients (a) at the field scale, (b) using management zones and (c) using grids. Determine the situations in which each is appropriate.
- IV. To assess the extent to which yield maps can be used to inform the management of soil variation within fields.

### **3. Methods**

We collated yield and soil information from fields from a number of arable farms in the UK. The precision agriculture company, SOYL, provided most of the data we used. These data comprised sets of yield monitor data from fields in the UK dating back to 2000 for different crops (winter wheat, oil seed rape and spring barley). The yield-monitor files contained measurements of latitude, longitude, yield ( $\text{Mg ha}^{-1}$ ), time stamps of when the measurements were made (s), the speed of the combine ( $\text{km h}^{-1}$ ), GPS satellite information, the date, moisture content of the grain (%), cut height (m), working width or swath (m), partial working width, a calibration factor (correction value for too little or too much weight), a code that defines the crop being harvested, engine revolutions, angle of roll, angle of pitch and harvesting rate ( $\text{Mg h}^{-1}$ ). Some monitor files did not include all of this information. For some fields, we also had measurements of nutrient concentrations (P, K, and Mg) and pH recorded on 100-m grids at five-yearly intervals and other sensor measurements such as electrical conductivity.

#### **3.1. Protocols for reliable yield maps**

We reviewed the current literature to identify methods designed to remove artefacts from yield monitor data. Of the methods found, programs were available from Sudduth and Drummond (2007) (*Yield Editor*), Sun *et al.* (2013) and the Auto-N project (Kindred *et al.*, 2015). These were tested on the yield-monitor files that we had collated and are described below.

One of the most common sources of error in yield-monitor data is caused by the delay between the crop entering the harvester and its flow (which is used to estimate local yield) being recorded by the sensor and is called flow delay. In a commercial combine harvester, the flow delay can be of around 15-20 seconds (Searey, 1989). Some commercially available yield monitors automatically achieve correction for flow delay by applying a time-shift to the data that is specified by either the user or the

combine harvester manufacturer. However, the use of such a time-shift is generally not recorded in yield monitor files and even when we know that one has been applied, we cannot be sure it was of the appropriate number of seconds. Therefore, we require a method to examine the yield data for evidence of artefacts due to the flow delay and then to correct the data if necessary.

The use of sub-optimal procedures can make a substantial difference to the yield maps produced and hence to the management decisions inferred from them (Griffin, 2010). Therefore we also developed our own program, which we called Roth-YE, for cleaning yield monitor data which included many of the standard filters used in other programs, and a novel flow delay filter which was used to estimate the true delay. We now briefly describe each of the programs we obtained from the literature search and compare them.

### ***Yield Editor***

Yield Editor was developed by Sudduth and Drummond (2007) to simplify the process of applying the filtering techniques for yield monitor data outlier detection and removal. The software allows the user to visualise the yield data in the form of a map. It includes twelve filters, which are listed in Table 3.1.1. The filters are based on extensive literature review by the authors and their own experiences.

The user may choose which of the filters to apply, and these are then applied in a stepwise manner to remove the erroneous data. The first filter is a grain-flow-delay filter which adjusts the position of the data to account for the time it takes for the grain to travel from the header to the yield monitor. The value of the delay is set by the user based on visual inspection of the yield map. Similarly, start of pass and end of pass delay filters are set by the user based on visual inspection. Thresholds for minimum and maximum combine speeds may be defined by the user, as can minimum and maximum yield values. There is a filter to eliminate yield measurements taken where rapid changes of velocity have occurred. This again is set by the user but an example of a ratio of 0.2 is given in the paper (Sudduth and Drummond, 2007). If the combine operator can record the swath width changes during harvest, then that too can be used as a filter. Yield measurements associated with widths below a user-set threshold are then removed. Sudduth and Drummond (2007) also included a filter to remove yield measurements that lay outside of a given number of standard deviations from the mean. This is arguably one of the most commonly used filter in yield-monitor cleaning protocols and its values are 2 to 3 standard deviations from the mean. In Yield Editor, the authors suggest to choose the standard deviation by systematically changing the value to remove the outliers without removing the values that appeared to be part of the true variation in the yield. Users can also remove points that lie outside of a defined boundary and remove individual points or areas manually.

The input file to the Yield Editor program **must** include: latitude and longitude information (which is converted to Easting (m) and Northing (m) by the program), flow or harvest rate ( $\text{lb sec}^{-1}$ ), logging

interval (sec), distance (inches), swath (inches) and pass number. Yield monitor data collected on from UK harvesters may not record all of the necessary information and typically yield is recorded in Mg ha<sup>-1</sup> rather than as a flow rate and metric units might be used over imperial. Therefore we needed to convert the yield monitor data before it could be used in the input file. For example, distance travelled by the harvester between each time stamp interval was calculated from the observed speed (km h<sup>-1</sup>) values by multiplying them by the logging interval (s)

$$\text{Distance (m)} = \frac{1000}{3600} \times \text{speed (km ha}^{-1}\text{)} \times \text{logging interval (s)}$$

Harvest rate was estimated from the yield data (Mg ha<sup>-1</sup>) by using data on swath (assumed a standard width of 8.89 m), distance travelled (m) and the logging interval.

$$\text{Harvest rate (kg s}^{-1}\text{)} = \frac{1000 \text{ Yield (Mg ha}^{-1}\text{)} \times \text{swath (m)} \times \text{distance (m)}}{\text{logging interval (s)}}$$

Harvest rate (kg s<sup>-1</sup>) is converted to lb s<sup>-1</sup> by multiplying with 2.205.

Pass number is another variable that may need to be calculated if it is not directly available from the harvester. Pass number is the number of passes (or transects) made by the harvester during the course of harvesting a field. Usually, it is calculated by the yield monitor software by counting the number of times the header has been raised during its course of travel. Since the header status was not available in our monitor files, we estimated the pass number by assuming a new pass was started when the harvester turned by more than 90°.

Table 3.1.1 The filters used by Yield Editor, Sun et al. (2013) , Auto-N and Roth-YE programs for cleaning monitor data.

Filters	Yield Editor	Sun et al. (2013)	Auto-N method	ROTH-YE
Flow delay	✓			✓
Moisture correction	✓		✓	✓
Start pass delay	✓			
End pass delay	✓			
Max velocity	✓		✓	✓
Min velocity	✓		✓	✓
Smooth velocity	✓			
Minimum swath	✓			
Maximum yield	✓	✓		✓
Minimum yield	✓	✓	✓	✓
Distance between rows		✓		✓
Distance between points		✓		
Direction change			✓	✓
Positional outliers	✓			✓
Manual selection of points	✓			
Standard deviation: Remove points $n$ standard deviations from the mean	✓	✓	✓	✓

### ***Sun et al. (2013) program***

Sun et al (2013) report on an integrated framework for yield data cleaning and estimating an ‘opportunity index’ for site specific management which provides farmers with the means to assess whether the observed variation in yield warrants further investigation. Here we focus on the yield data cleaning software. The software requires yield measured as mass per area or data on mass flow, distance travelled, harvest width, grain moisture to calculate yield as mass per area. The longitude and latitude of these measurements are also required. The order of the variables in the input file can be specified by the user as can the units of measurement.

The longitude and latitude are converted to Easting and Northing using the Universal Transverse Mercator projection. Yield values are discarded above upper and lower thresholds that can be set by the user. The default values are given as 0.1 and 10 t ha<sup>-1</sup>. By default, the program assumes that the upper and lower limits of the yield are  $\pm 2.5$  standard deviations from the mean, although this parameter may be adjusted by the user. Values that lie outside of this range are marked for deletion. To remove the local extremes in the yield data, a local application of the standard deviation filter is included. A local neighbourhood with a search radius of 25m is identified at the nodes of 5 m grid across the field. Yield values that lie outside the thresholds are marked for deletion. They are then removed when the whole filtering process is completed. The program removes points where the distance between two successive measurements on a transect is smaller than a defined limit. This accounts for situations where the combine harvester is moving too quickly. It also removes points where the distance between neighbouring passes is too small. This accounts for the situation where the combine harvester cuts over an area that has been cut in a previous pass. Here, of the two passes, the points cut second are removed as these will have erroneous yields estimates.

### **Auto-N**

The Auto-N program was developed in Excel for cleaning the yield monitor data used in the Auto-N project (Kindred *et al.*, 2015). The yields are converted to a yield with standard moisture content (15% for wheat) before cleaning. Yield values are screened based on the speed of the combine. The program then uses some of the standard filters described above (see Table 3.1.1). Yield values associated with speeds less than 0.6 m s<sup>-1</sup> or greater than 2.2 m s<sup>-1</sup> are marked for deletion. In addition there is a filter for removing the yield data measured at the field margins where measurements are likely to be erroneous or unrepresentative. The filter works by detecting changes in direction of the combine harvester with the assumption that this will happen at the field margins. Three co-ordinates are used to estimate the direction of movement of the combine harvester. If the absolute change in direction from consecutive estimates of direction is greater than 0.6 radians corresponding values of yield are marked for deletion. Yield values that lie outside the mean  $\pm 3$  times the standard deviation of the total population are also marked for deletion.

## ROTH-YE program

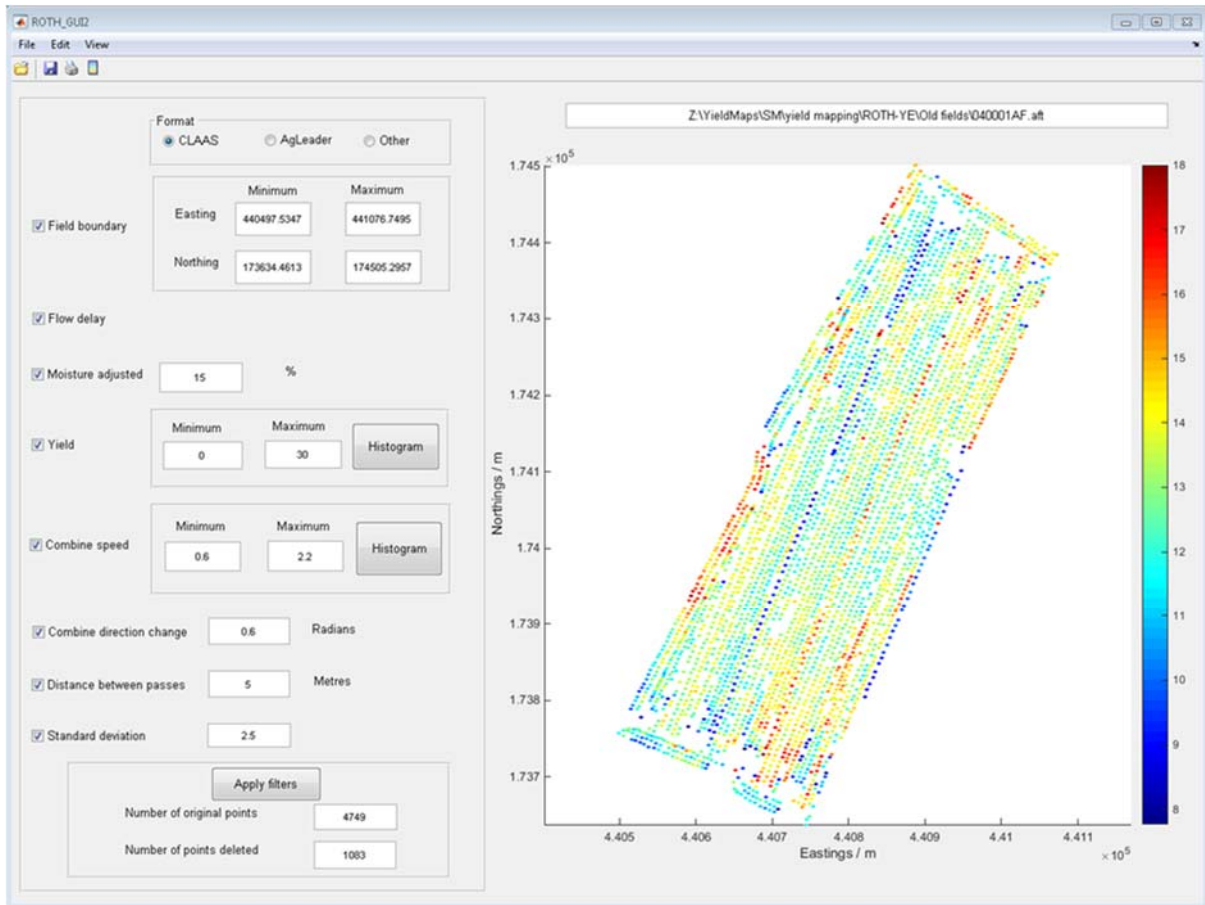


Figure 3.1.1 ROTH-YE program showing the different filters that can be applied and a cleaned yield map.

The Roth YE program uses the same filters as the Auto-N program but with additional filters for maximum yield, the distance between passes, positional outliers and a flow delay filter (Table 3.1.1). The program converts latitude and longitude to easting and northings using the ellipsoid and the Transverse Mercator projection (Ordnance-Survey, 2015). Default values for the moisture adjustment (15%), minimum and maximum combine harvester speed (0.6 m s<sup>-1</sup> and 2.2 m s<sup>-1</sup>), the threshold for the change of direction of the combine harvester (0.6 radians), the distance between passes (5 m) and the standard deviation filter (mean  $\pm$  2.5 SD) are given but the user can adjust each of these. The program allows the user to view histograms of the yield measurements and the combine harvester speed to help them decide suitable maximum and minimum values (Figure 3.1.2).

If the combine harvester is moving in opposite directions along two adjacent rows, then the flow delay can lead to distortions of features in the yield map that cross both rows. For example, Figure 3.1.3 (a) shows some yield data where there is a large jump in yield 200 m along the row. The combine harvester direction alternates for adjacent rows and a flow delay led to this horizontal linear feature being badly distorted (Figure 3.1.3 (a)).

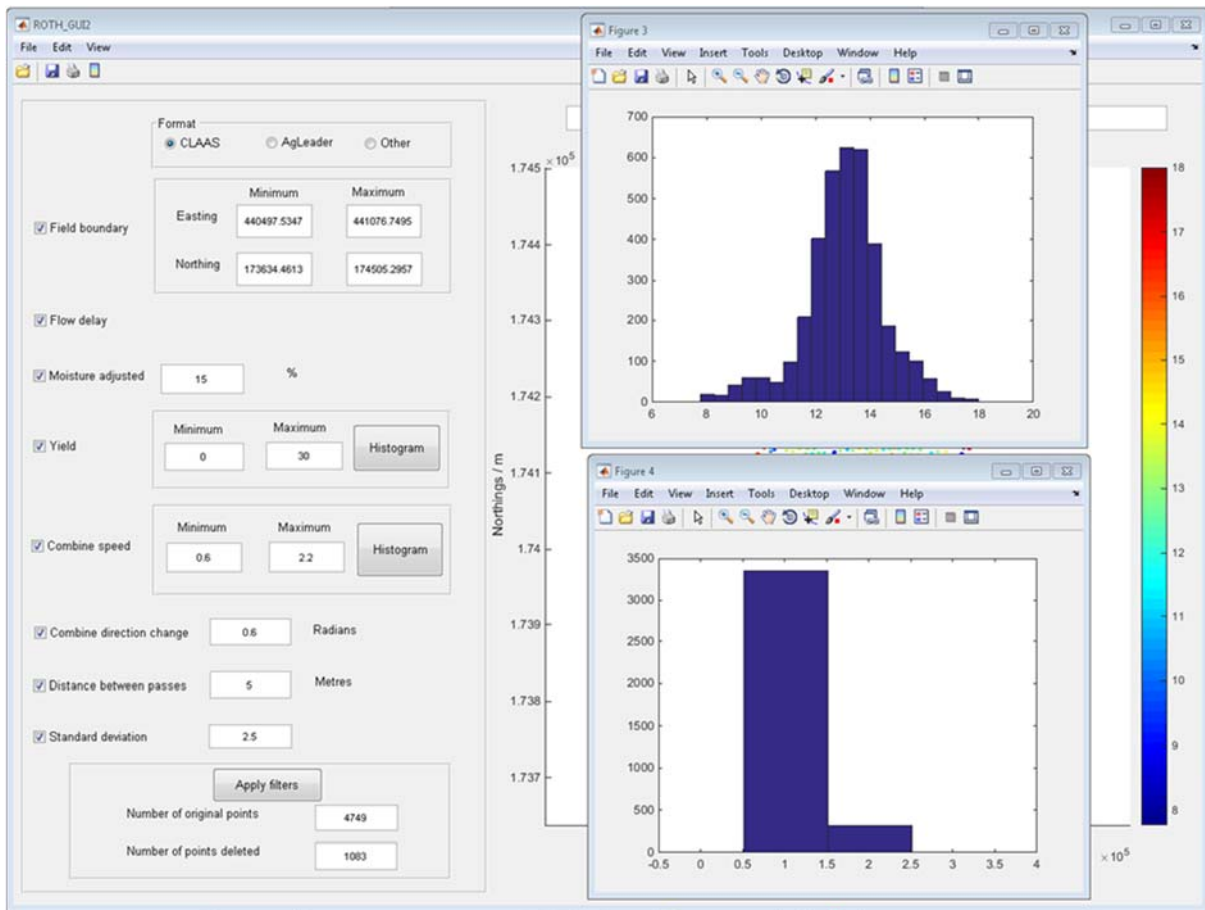


Figure 3.1.2. Roth-YE program showing histograms of yield and the combine speed.

The flow delay filter included in Roth-YE is an improvement on existing approaches. The flow delay is a parameter included in this model, and its value is automatically derived using a measure of the yield recorded in adjacent rows. The parameter could be made to vary with the speed of the harvester, but in our implementation we have assumed that it is a constant value.

One measure of the similarity between the variation in yield along adjacent rows is the average squared difference between pairs of yield measurements recorded at the same distance along the rows which we denote  $v_{adj}$ . If, as we would expect, the yield is spatially correlated, then  $v_{adj}$  will be less than the averaged squared difference between two randomly chosen points along the rows. However, in the simulated example shown in Figure 3.1.3(a) the flow delay has caused adjacent yield values to differ greatly and has therefore inflated the value of  $v_{adj}$ . In Figure 3.1.3(c) we apply a series of time-shifts to the data and then recalculate  $v_{adj}$ . We consider both positive and negative time-shifts to account for the possibility that too severe a delay has already been applied to the data. We assume that the yield data are correctly aligned when  $v_{adj}$  is minimized as in this example, when a delay of 10 time units has been applied. Indeed, in Figure 3.1.3(b) we see that when this delay is applied to the yield data that the horizontal linear features in the yield map is evident.

We have included an algorithm within Roth-YE to automatically test whether by applying a realistic (<30 second) time-shift to the yield data is it possible to decrease the value of  $v_{adj}$ . If this is the case, then this shift is applied as part of the data pre-processing.

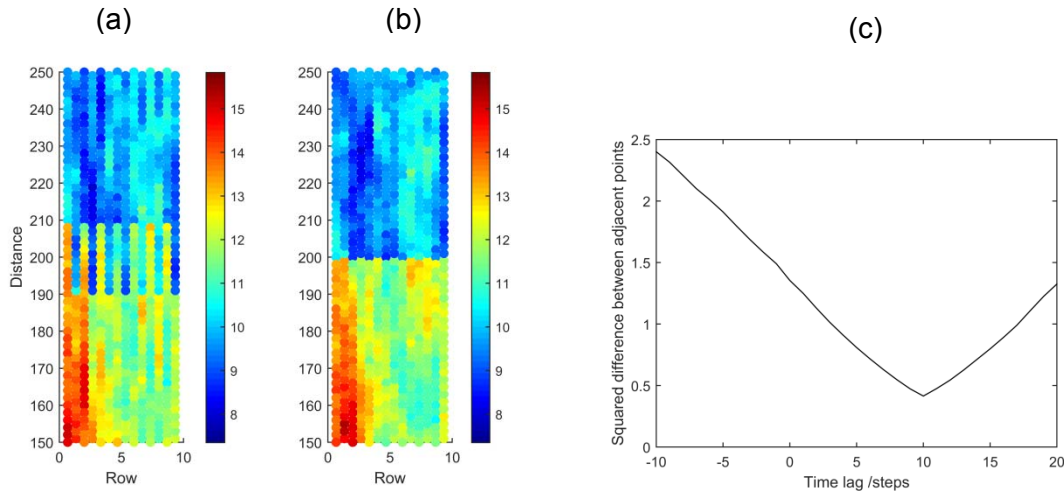


Figure 3.1.3. Examples of maps showing the effect of flow delay before (a) and after correction (b) and the time shifts applied in terms of the squared difference between points and the time lag (c)

We tested the accuracy of each program for UK conditions, and the ability to produce reliable maps from data collected from different combine harvesters yield monitors. Like many programs for cleaning yield monitor data, Yield Editor, Sun *et al.* (2013) and Roth-YE require the user to select parameter values that control the removal of artefacts, whereas the parameter values for the Auto-N program were fixed (see Table 3.1.4). We used two protocols to evaluate Yield Editor. In the first of these, we used the set of default values to eliminate points from each yield monitor file (method A) Table 3.1.2. In the second, we made judgments based on visual inspection and statistical distributions of the yield and combine harvester speed data to set the thresholds. We also set the parameter for the standard deviation filter to 2.5 which was the smallest default of the other methods tested (method B) Table 3.1.2. No start pass or end pass filters were applied in method A, but they were applied in method B where we found any anomalies at the beginning or end of the rows. For the Sun *et al.* (2013) program we used the default parameter values for all but max and min yield Table 3.1.3. These values were not suitable for the UK situation and so we based our parameter values on visual inspections of the distributions of the yield data. Similarly, we based the parameter values of Roth-YE on default values except for the minimum and maximum for yield and combine speed, which we based on visual inspections of the data Table 3.1.5

Table 3.1.2. Filter parameter values used in the evaluation of the Yield Editor

Filters	Method A	Method B				
		Fields				
		<i>040001AF</i>	<i>040001B1</i>	<i>040001B3</i>	<i>040001BA</i>	<i>02000157</i>
Flow delay	0	0	0	0	0	0
Start pass delay	0	0	0	0	0	0
End pass delay	0	0	0	0	0	0
Max velocity (mph <sup>-1</sup> )*	7	5.0(8)	5.0(8)	5.8(9.3)	5.5(8.9)	4.9(7.9)
Min velocity (mph <sup>-1</sup> )	2(0.16)	0.3(0.5)	0.4(0.6)	0.8(1.3)	0.8(1.3)	0.6(1.0)
Smooth velocity (mph <sup>-1</sup> )	0.2	Not applied				
Minimum swath (in)	Not applied	Not applied	Not applied	Not applied	Not applied	Not applied
Maximum yield (bu ac <sup>-1</sup> ) <sup>†</sup>	250(16.8)	268 (18)	327(22)	268(18)	245(16.5)	283(19)
Minimum yield (bu ac <sup>-1</sup> ) <sup>†</sup>	0 (0.0)	1.5 (0.1)	1.5(0.1)	1.5 (0.1)	1.5(0.1)	1.5 (0.1)
Standard deviation	4.0	2.5	2.5	2.5	2.5	2.5

\*Values in parenthesis shows velocity in km h<sup>-1</sup>

<sup>†</sup>Values in parenthesis shows yield in Mg ha<sup>-1</sup> (1 bushel/acre = 0.0673 Mg ha<sup>-1</sup>)

Table 3.1.3. Filter parameter values used in the evaluation of the Sun et al (2013) program.

Filters	Fields				
	<i>040001AF</i>	<i>040001B1</i>	<i>040001B3</i>	<i>040001BA</i>	<i>02000157</i>
Maximum Yield (Mg ha <sup>-1</sup> )	18	22	18	16.5	19
Minimum yield (Mg ha <sup>-1</sup> )	0.1	0.1	0.1	0.1	0.1
Global Standard deviation	2.5	2.5	2.5	2.5	2.5
Local Standard deviation	2.5	2.5	2.5	2.5	2.5
Distance between rows (m)	5	5	5	5	5
Distance between points (m)	1	1	1	1	1

Table 3.1.4. Filter parameter values used in the Auto-N program.

Filters	Values
Slope change (radians)	0.6
Maximum speed (m sec <sup>-1</sup> )*	2.2 (7.9)
Minimum speed (m sec <sup>-1</sup> )*	0.6(2.2)
Minimum yield (Mg ha <sup>-1</sup> )	>0
Standard deviation	3.0

\*Values in parenthesis shows velocity in km h<sup>-1</sup>

Table 3.1.5. Filter parameter values used in the evaluation of Roth-YE.

Filters	Fields				
	<b>040001AF</b>	<b>040001B1</b>	<b>040001B3</b>	<b>040001BA</b>	<b>02000157</b>
Max velocity (m sec <sup>-1</sup> )*	2.2 (7.9)	2.2 (7.9)	2.6 (9.3)	2.5 (8.9)	2.2 (7.9)
Min velocity (m sec <sup>-1</sup> )*	0.1 (0.5)	0.2 (0.6)	0.4 (1.3)	0.4 (1.3)	0.3 (1.0)
Maximum Yield (Mg ha <sup>-1</sup> )	18	22	18	16.5	19
Minimum yield (Mg ha <sup>-1</sup> )	0.1	0.1	0.1	0.1	0.1
Distance between rows (m)	5	5	5	5	5
Change of direction (radians)	0.6	0.6	0.6	0.6	0.6
Standard deviation	2.5	2.5	2.5	2.5	2.5

\*Values in parenthesis shows velocity in km h<sup>-1</sup>

### 3.2. Delineating management zones

We used yield monitor data that had been cleaned by Roth-YE to divide each field into soil management zones. The algorithm we chose to use was spatially smoothed version of a fuzzy k-means classification devised by Lark (1998). In a previous assessment we compared this method with other spatial-clustering methods and found it performed the best (Milne *et al.*, 2012). Commercially, simpler functions are used in precision farming software and by service providers to give yield performance maps, zoning areas that consistently perform well, badly or are inconsistent. To indicate the effectiveness of these approaches compared with the cluster analysis approach we also produced maps showing the areas of the field that consistently yielded better or worse than average in each year.

For many of the fields we studied, we had measurements of phosphorus (P), potassium (K), magnesium (Mg) and pH on an approximate 100m x 100m grid across the field. We used this data to determine the effectiveness of the resultant zones at explaining nutrient variation. The soil samples were not taken at random but on a grid, therefore we used restricted maximum likelihood (REML) for this analysis as oppose to an analysis of variance (ANOVA) as REML allows us to

account for any spatial correlation between measurements. We used the REML directive in Genstat (Payne *et al.*, 2011) to analyse the data. This returns a Wald statistic and usually an F-statistic which inform on the null hypothesis that the class means for the soil property are all equal. If the null hypothesis is rejected, then the zones can be regarded as different with respect to the particular soil property.

We also had other supporting information including soil maps produced by SOYL defining the texture and stone content and data on the electronic conductivity of the soil (EC) and elevation data measured from sensors. Where this information was available we tried to deduce what was causing the variation between zones.

### 3.2.1. Smoothed fuzzy k-means cluster analysis

For this type of classification we have measurements of  $p$  properties for a number of units which we want to classify. In our case, the properties consist of yields of wheat for  $p$  years and the units are the locations that they are associated with. In practice, the yield monitor data from each year are mapped onto a 10-m grid. The value of the yield for a given grid node in a particular year was assumed to be the average of the points that lay closest to that node. We denote the grid coordinates as  $x = \{x_1, x_2\}$  and the yields in the  $p$  years as  $y_1(x), y_2(x), \dots, y_p(x)$ . From these data we can create a classification. We standardize each of the  $y_j, j = 1, 2, \dots, p$  to zero mean and variance one. We choose  $k$ , the number of classes. Each class  $q, q = 1, 2, \dots, k$  is characterised by a centroid vector  $\bar{z}_q = \{\bar{z}_{1q}, \bar{z}_{2q}, \dots, \bar{z}_{pq}\}$ , where the elements of  $\bar{z}_q$  are the average values of the variates in class  $q$ . The Euclidean norm is used measure the distance between a unit  $z_{ij}$  and the class centroid

$$\delta_{i1} = \sqrt{\sum_{j=1}^p (z_{ij} - \bar{z}_{pq})^2} \quad (3.2.1)$$

where  $z_{ij}$  is the standardized yield at node  $i$  in the  $j$ th year, and  $\bar{z}_{pq}$  is the mean of  $z$  in class  $q$  in that year. We assume that each node belongs to some degree to every class, and we create a classification by minimizing a pooled 'belongingness':

$$b = \sum_{q=1}^k \sum_{i=1}^n \delta_{iq}^2 u_{iq}^\omega \quad (3.2.2)$$

in which  $u_{iq}$  is the degree of membership of node  $i$  to class  $q$ , and  $\omega$  is the fuzziness parameter. The membership across all classes must sum to 1:

$$\sum_{q=1}^k u_{iq} = 1 \quad (3.2.3)$$

The parameter  $\omega$  must lie between 1 (in which case we obtain a hard classification) and 2. We set  $\omega = 1.25$  to create our classifications.

As above, we must choose  $k$ . We do so by experimenting with several values between 2 and 5 (the most that a farmer is likely to distinguish). For each class we compute the normalized classification entropy  $\xi(k)$ , proposed by Dunn (1976):

$$\xi(k) = \frac{1}{\ln k} \sum_{q=1}^k \sum_{i=1}^n \frac{1}{n} u_{iq} \ln u_{iq} \quad (3.2.4)$$

We then plot  $\xi(k)$  against  $k$  and seek a value of  $k$  at which  $\xi(k)$  falls below the overall trend. Such a value is the one we choose.

The next step in the zonation is to smooth the classes. It turns out that the distributions of the memberships of the nodes are strongly bimodal, and so, following Lark (1998), we transformed them with the symmetric log-ratio to unimodal distributions. We denote the transformed memberships by  $\tilde{u}_{iq}$ , and we smooth them using a weighted average of the transformed memberships in circular neighbourhoods,  $R$ , of radius  $r$ :

$$\tilde{u}_{iq}^* = \sum_{j \in R} w(i, j) \tilde{u}_{iq} \quad (3.2.5)$$

Like the original memberships, the transformed memberships must lie in the range 0 to 1 and must sum to 1. This means that the weights in  $R$  must sum to 1.

The weights are derived from the variograms (see variogram description in Appendix 8.1). We can write a simple bounded model in general as

$$\gamma(\mathbf{h}) = c_0 + c_1 f(\mathbf{h}) \quad (3.2.6)$$

where  $c_0$  is a spatially uncorrelated variance, the 'nugget variance', corresponding to white noise,  $c_1$  is the spatially correlated component of variance, and  $f(\mathbf{h})$  is the functional form of the variogram containing a distance parameter. The weights are then obtained as

$$w(i, j) = \frac{1 - f(h_{ij})}{\sum_{j \in R} \{1 - f(h_{ij})\}} \quad \forall j \in R \quad (3.2.7)$$

where  $h_{ij}$  is the separation in distance and direction, the lag, between nodes  $i$  and  $j$ . Note that only the functional form of the variogram and its distance parameter affect the weights; neither  $c_0$  nor  $c_1$  do so. The neighbourhood  $R$  defines the region over which the membership values are smoothed,

unless the variogram reaches its sill within it. In the latter case the effective range of the variogram defines the smoothing region.

The farmer, of course, must have a hard classification; for practical management he or she must have each position in the field belonging to one class and one class only. So the final stage in the zonation is therefore to assign each node to the class for which its smoothed membership is greatest.

We note that the size of  $R$  affects the results. The larger it is the greater is the smoothing. If  $R$  is small then the classification is likely to be too fragmented; if it is too large then the memberships will be smoothed too much and the final classes not sufficiently homogeneous. Lark (1998) proposed a coherency index to identify an appropriate radius for  $R$  defined as

$$H = \frac{\eta_a}{\sum_{q=1}^k \psi_q^2} \quad (3.2.8)$$

where  $\eta_a$  is the proportion of pairs of nodes within a distance  $a$  that belong to the same class, and  $\psi_q$  is the proportion of nodes that belong to class  $q$ . The larger is the values of  $H$  the more spatially coherent are the classes. We chose  $a = 10\sqrt{2}$  m so that we were effectively comparing each node with its neighbours on the grid.

### **3.3. Compare the merits of managing soil nutrients at different scales**

We compared the cost effectiveness of three commonly used sampling approaches. The sampling schemes we considered were

- (i) a W-shaped design across the whole field,
- (ii) a zone-based scheme with W-shaped designs within each zone and
- (iii) a grid-based scheme with samples taken on a 100 m × 100 m grid.

In practice, soil samples taken according to schemes (i) and (ii) are bulked before analysis resulting in either a single value for each field or each zone within a field.

Previously, Marchant et al. (2012) compared the suitability of these sampling approaches for estimating the field-mean nutrient status. However, the adoption of one of these sampling approaches tends to imply that a farmer is aiming to vary fertiliser management at a particular spatial scale – the field scale, the management zone scale or the smallest scale at which the fertiliser rate can be adjusted. We now go beyond the Marchant et al. (2012) comparison of the sampling approaches to consider the cost effectiveness of managing nutrient inputs at these different scales.

It is not practical to compare sampling approaches in the field because (i) we would need to apply each sampling approach many times to determine its average profitability and (ii) we would need perfect knowledge of how the nutrients vary across the field to calculate which approach is most profitable. Therefore, we used a geostatistical model to simulate the variation in nutrients across fields. We then compared the effectiveness of the three sampling strategies in determining the nutrient requirement, and compared the cost effectiveness of each approach by taking into account the differences in nutrient inputs, yield and the cost of sampling. We did not expect that there would be a single best approach to sampling. We thought that the most cost effective approach would depend on the variation of the nutrients in the field. Therefore, we have a circular problem – the best sampling strategy varies according to the pattern and scale of nutrient variation in the field but the farmer will have little information about this variation before he has sampled. In situations where yield is limited by nutrient concentrations, it is reasonable to assume that the yield and nutrient maps are correlated and vary across similar spatial scales. Hence the pattern of observed yields would reflect the pattern of nutrients and could guide the farmer towards the best sampling approach. Therefore, we modelled the yield variation that would have been observed as a result of the variation in soil nutrient and explored whether parameters describing properties of the yield variation could be used to decide which sampling strategy was likely to be most cost-effective.

### 3.3.1. Modelling phosphorus in soil

We used P measurements (denoted  $z$ ) from fields named Field-BD, Field-ER, Field-GP, Field-LM, Field-MC and Field-RH, which are located near Newbury, UK to simulate realistic variation in P across the fields. Our data came from well managed fields, but we wanted our simulated values of P to limit the yield. Therefore, we scaled the measured data before fitting the models of spatial variation. First we used cluster analysis to define zones in each field, and in our model we allowed the mean and spatial variation of the nutrient to be different. We used a similar approach to that described by Marchant *et al.* (2012). We standardized the measurements to have a variance equal to one by dividing by the standard deviation,  $s$ , of the data to give values  $\tilde{z}_i, i = 1, 2, \dots, n$ . Then we characterized the mean and spatial variation within each of the  $p$  zones of the field by fitting a linear mixed model to the transforms,  $\tilde{z}$ :

$$\tilde{z} = M\beta + \eta \quad (3.3.1)$$

where  $M$  is an  $n \times p$  fixed effects design matrix which permits the mean concentrations to differ between zones. The vector  $\beta$  is of length  $p$  and contains the coefficients of the fixed effects (i.e. the mean concentration within each zone). The component  $\eta \sim UN(0, V)U$  where  $N(0, V)$  is a vector of spatially correlated random residuals with a normal distribution with zero mean and covariance matrix  $V$ , and  $U$  is a diagonal matrix where element  $U(i, i) = \sigma_j$  when the  $i$ th datum of  $z$  is in zone  $j$  (i.e. this is a zone-dependent scaling factor of the variance).

We assumed second-order stationarity, so that the fixed effects coefficients  $\beta$  and the variogram could be estimated simultaneously by residual maximum likelihood, REML (Patterson and Thompson, 1971). Here we have assumed that the spatial variation is represented by an isotropic exponential variogram model:

$$\gamma(h) = c_0 + c_1 \left(1 - \exp\left(-\frac{h}{a}\right)\right) \quad (3.3.2)$$

in which  $c_0$  and  $c_1$  are the nugget and spatially correlated components of the variance, as mentioned above, and  $a$  is a distance parameter. We simulated values for P on a 10 m  $\times$  10 m grid across each field using the Cholesky decomposition technique, also known as lower–upper or LU technique (Webster and Oliver, 2007). We used the variogram model that we fitted to the transformed data to create a  $t \times t$  covariance matrix  $C$  and scaled this for each zone independently as  $\widehat{U}C\widehat{U}$ , where  $t$  is the number of simulated points on the 10 m  $\times$  10 m grid and  $\widehat{U}$  is a diagonal matrix where element  $\widehat{U}(i, i) = \sigma_j$  when the  $i$ th simulated value is in zone  $j$ . This was then decomposed into its lower and upper triangular form where

$$\widehat{U}C\widehat{U} = LL^T \quad (3.3.3)$$

The simulated values,  $z^*$ , are then given by

$$z^* = s(Lg + M_{\text{sim}}\beta) \quad (3.3.4)$$

where  $g$  is a  $t \times 1$  vector of random numbers drawn from a standard normal distribution, and  $M_{\text{sim}}$  is a  $t \times p$  design matrix. Because  $g$  is a vector of random numbers we can simulate many different realisations of the field using the same basic covariance structure. This is a similar concept to drawing random numbers from a distribution and getting a different answer each time. Figure 3.3.1 shows examples of the simulated values of P. For ease of calculating the yield response (see section 3.3.3) we converted our simulated P values to  $\text{mg kg}^{-1}$  by assuming the soil has a bulk density of  $1.1 \text{ g cm}^{-3}$ . To simulate field measurements with larger variances than in the observed data, we also scaled the values of  $\sigma_j$  and simulated values of P. In each additional zone, concentrations of P were modified at four scales (0.5, 1, 2, 3) resulting in four sets of runs for fields with two zones and 16 sets of runs for fields with three zones.

### 3.3.2. Modelling yield and quantifying its spatial variation

For each realisation of simulated phosphorus,  $z^*$ , we simulated the associated yields using a yield response model for P. We then computed experimental variograms of the simulated yield values by the method of moments and fitted an exponential variogram model.

### 3.3.3. Yield response model

The yield response model for P was derived by Marchant *et al.* (2012) from published data (Johnston and Goulding, 1988; Johnston, 2005; Milford and Johnston, 2007; Syers *et al.*, 2008). For every 1 kg of P added in fertilizer, we assume that 0.18 kg is available to the crop. We also assumed that this addition is contained in the top 30 cm of soil and the soil has a bulk density of 1.1 g cm<sup>3</sup>. This means that an addition of 1 kg P ha<sup>-1</sup> leads to an increase in the concentration of this layer of  $k = 0.054$  mg kg<sup>-1</sup>.

Thus the total nutrient available after addition of a quantity of fertilizer  $z_{\text{fert}}$  is

$$z_{\text{total}} = kz_{\text{fert}} + z_{\text{soil}} \quad (3.3.5)$$

The yield response to added nutrients is modelled by

$$y_r = y_0(1 - AB^{z_{\text{total}}}) \quad (3.3.6)$$

where  $y_r$  is the realized yield,  $y_0$  is target yields and  $A$  and  $B$  are parameters. We set our target yield at 8.8 t ha<sup>-1</sup>. The model parameters were  $A = 1.33$  and  $B = 0.68$  (see Figure 3.3.2).

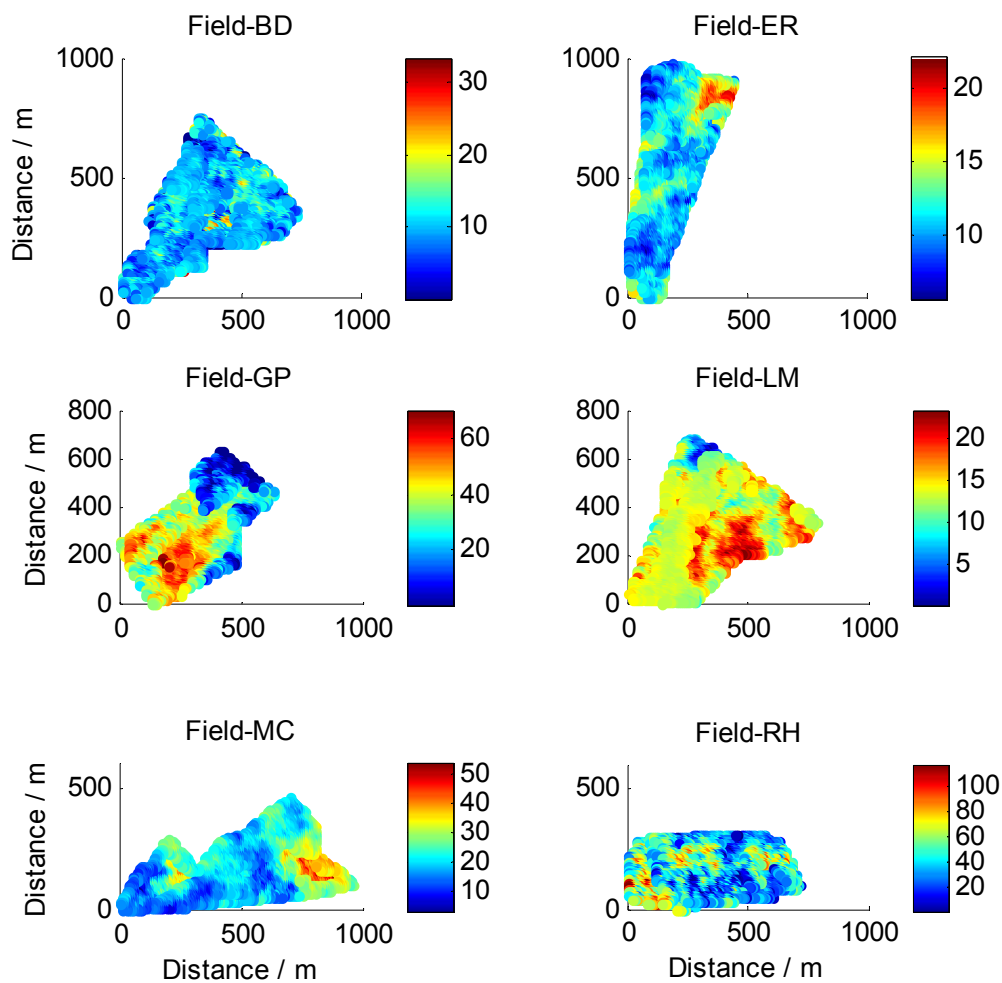


Figure 3.3.1. Realisations of the simulated phosphorus concentrations ( $\text{mg kg}^{-1}$ ). Note that the ranges of phosphorus change substantially from field to field. The scale bars vary accordingly, and so the colours that depict the levels of phosphorus cannot be compared between fields.

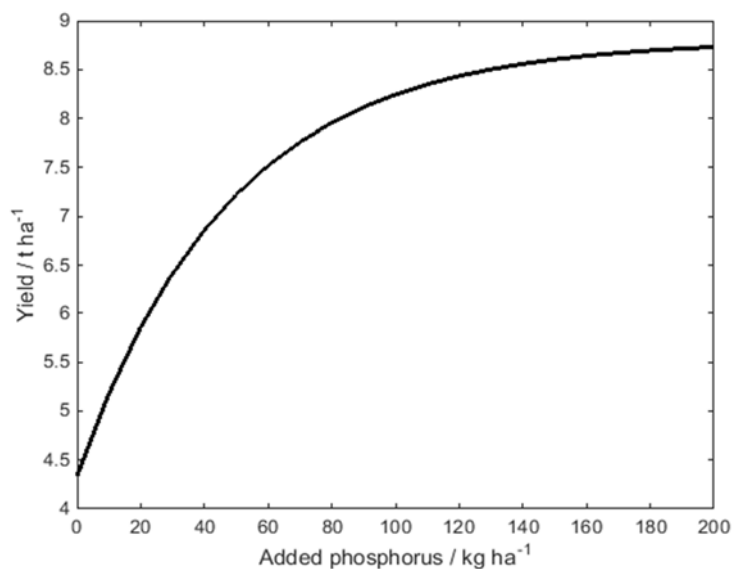


Figure 3.3.2. Response of yield to added P to a soil with an available P of  $2.5 \text{ mg kg}^{-1}$ .

### 3.3.4. Management scales

In each of the simulated fields, we compared three sampling schemes to see which would result in a treatment map that gave the greatest profit. Each W-shaped design comprised 10 sampling points. In practice, soil samples taken according to these different schemes are bulked before analysis resulting in either a single value for each field or each zone within a field. To simulate these we calculated the average of the nutrient values from the sample points on each W-shaped design. In grid-based designs the aim is to map the variation in a nutrient so that fertilizer rates can be adjusted accordingly. We followed the method typically used by precision agricultural consultants and used inverse distance weighting to predict the variation in the nutrient between the sampling points.

We estimated the nutrient concentration in the soil at each location on the 10 m × 10 m grid using each of the three sampling schemes. This resulted in a single estimate for the whole-field sampling scheme, an estimate for each zone for the zone-based scheme and a spatially varying estimate for the grid-based scheme. Using these estimates with equations (3.3.5), (3.3.6) and (3.3.7) we calculated the amount of fertilizer that should be added ( $\hat{z}_{\text{fert}}$ ), noting that this value is not the true optimum as it is based on the estimated nutrient supply and not the true nutrient supply,  $z_{\text{soil}}$ .

For each realisation,  $i$ , of the fields we calculated the profit margin under each sampling scheme and management scale. We computed the difference in profit margin given by the zone-based,  $\Delta_{\text{zone}}(i)$ , and grid-based,  $\Delta_{\text{grid}}(i)$ , schemes compared with that of the field-based  $\Delta_{\text{field}}(i)$  scheme. We also computed the excess fertilizer applied under the zone- and grid-based schemes and compared this with the field-based scheme. However, we did not consider the beneficial effect of excess P applications to the crop in the previous years to the following crop.

We then calculated the profit from applying the nutrient strategies to each field by

$$\Delta = yG_{\text{wheat}} - Z_{\text{fert}}G_{\text{fert}} - nG_{\text{sample}} \quad (3.3.7)$$

where  $G_{\text{wheat}}$  is the price of the grain, which we assumed to be £150 t<sup>-1</sup>,  $G_{\text{fert}}$  is the price of fertilizer P, assumed to be £0.31 kg<sup>-1</sup>,  $n$  is the number of individual soil samples analysed in the laboratory, each costing  $G_{\text{sample}} = £5$ , and  $y$  and  $Z_{\text{fert}}$  are the yield and quantity of fertilizer added, respectively (Appendix 8.2).

### 3.3.5. Using metrics of variation to guide sampling strategies

In our simulation experiments the effectiveness of each management scale is controlled by the model of nutrient variability in the field. A farmer will require simpler metrics to decide on the best approach. For each set of simulations, we therefore used multiple linear regression to see how much of the

variation in  $\Delta_{\text{grid}} - \Delta_{\text{field}}$  and  $\Delta_{\text{zone}} - \Delta_{\text{field}}$  could be explained by the distance parameter of the yield variogram  $a$  and the variance parameter  $c_1$ . More importantly, we wanted to compute the probability that the grid- or zone-based sampling strategies were more profitable than the field-based strategy for given parameters of  $a$  and  $c_1$ .

For each field we fitted the model

$$\Delta_{\text{scheme}} - \Delta_{\text{field}} = b_0 + b_1 a + b_2 c_1 + b_3 a c_1 \quad (3.3.8)$$

to the data, where 'scheme' is 'zone' or 'grid'. The assumption underlying the model is that the residuals are normally distributed about the mean prediction and that the standard error,  $s_{\text{obs}}$  for predicting a single observation is given by

$$s_{\text{obs}} = s^2 \text{mse} + \mathbf{b}^T \mathbf{V}(\mathbf{b}) \mathbf{b}, \quad (3.3.9)$$

where  $\mathbf{V}(\mathbf{b})$  the covariance function for the parameter is estimates  $\mathbf{b} \equiv \{b_0, b_1, b_2, b_3\}$  and  $s^2 \text{mse}$  is the mean square error. From this we could calculate the probability that  $\Delta_{\text{grid}} - \Delta_{\text{field}} > 0$  for any given combination of  $a$  and  $c_1$ . We did a similar analysis for excess fertilizer.

### **3.4. Assess the extent to which yield maps can be used to manage soil variation at the scale of soil management zones**

For variable management to be practical the variation in the field must be of sufficiently large magnitude and scale. Methods have been proposed to assess this by considering the variation captured in yield monitor data. We explored two such methods, the first was proposed by Lark *et al.* (2003) who derived a decision tree to determine a field's 'potential for variable rate management' (PVRM) and a second which was first proposed by Pringle *et al.* (2003) and later developed by de Oliveira (2009) which calculates a metric for the opportunity for variable rate management. After evaluation of both approaches, we propose a new method for ranking fields for their potential for variable rate management.

#### *3.4.1. Potential for Variable Rate Management based on Lark et al. (2003)*

The Lark *et al.* (2003) approach is based on the hypotheses that the scale and magnitude of variation in yield provide the basis for identifying fields where variable rate management is feasible. Variograms of the yield map from a particular field indicate the scale and magnitude of the yield variation in the field (see Appendix 8.1 for a description of the variogram). A variogram of yield data that rises steeply to the sill over a short lag indicates that the variation in yield is dominated by short-range processes, whereas one which rises less steeply indicates that the variation is dominated by

long-range processes (Figure 3.4.1). Similarly, a nugget which is large relative to the sill implies that a lot of variation in yield is happening at short spatial scales, and suggests that the variability is too intricate for variable rate management to be practical (Lark *et al.*, 2003). Lark *et al.* (2003) use metrics of the variogram and the normalized classification entropy (see Section 3.2) in a decision tree (Figure 3.4.2) to help farmers to decide whether variable rate management is likely to be appropriate for a given field. It was formed using a data mining exercise and so not all of the decision nodes are intuitive. The decision tree uses the variance ratio and the standard deviation and the normalized classification entropy (Figure 3.4.2).

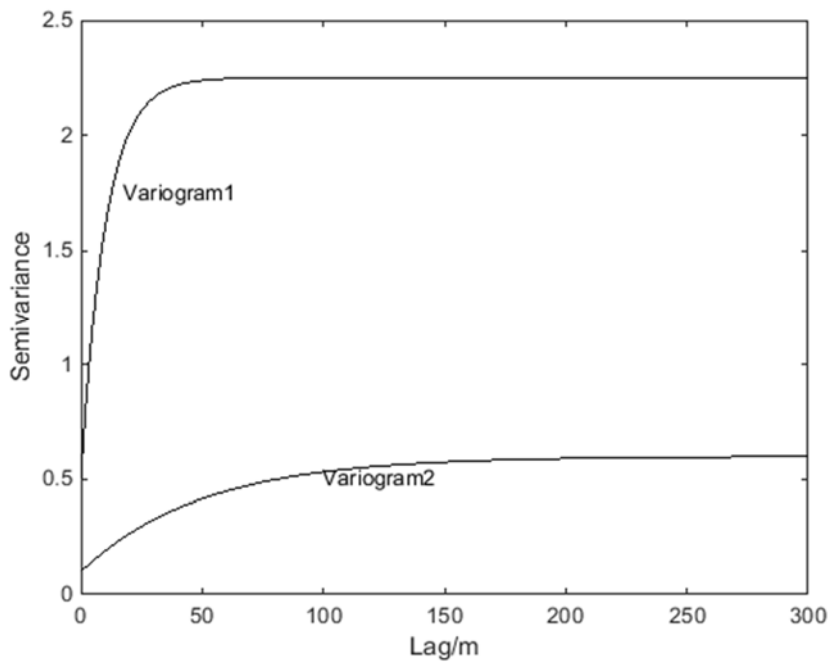


Figure 3.4.1 Hypothetical variograms indicating short and long range processes leading to the yield variability in the field.

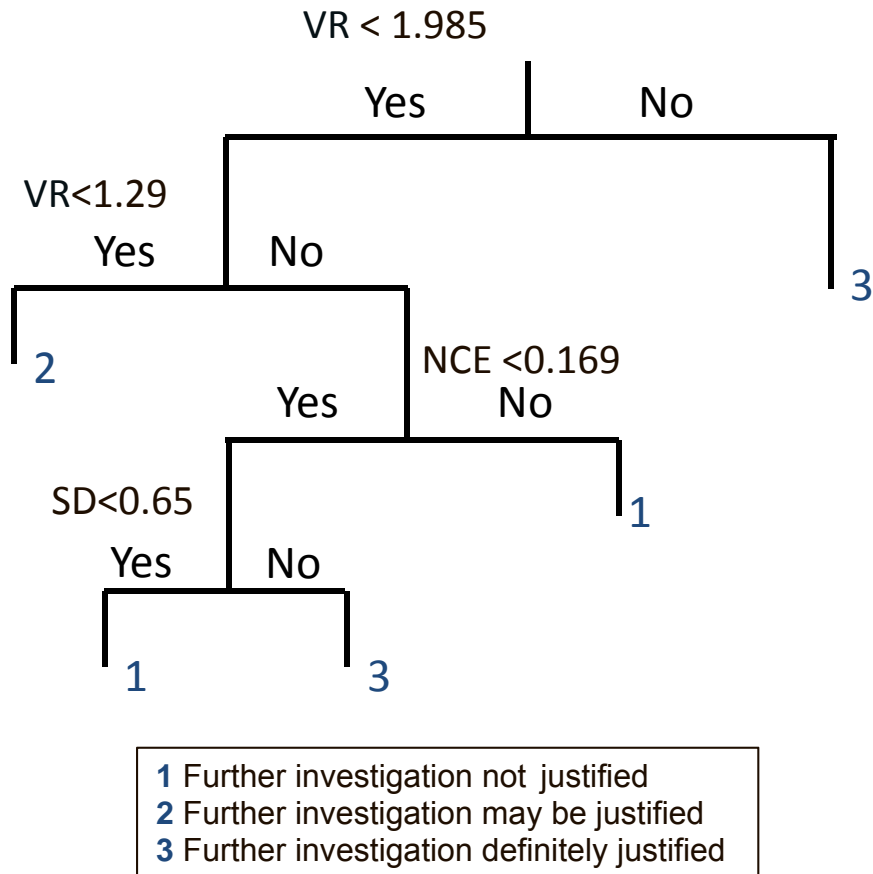


Figure 3.4.2 Decision tree diagram for potential variable rate of a field derived by Lark et al. (2003). The variance ratio (VR) is the ratio of the dispersion variances for a 1ha block to a 0.01ha block. The Normalised classification entropy (NCE) is a measure of how distinct management zones based on a cluster classification are and the standard deviation (SD) is the square root of the variance for a region excluding nugget.

### 3.4.1.1 Variance ratio (VR)

Regional dispersion variance is the ratio of the dispersion variance ( $\sigma^2_B$ ) for a 1ha block B to a 0.01ha block D

$$V_R = \frac{\sigma^2_{B=1}}{\sigma^2_{B=0.01}} \quad (3.4.1)$$

where  $\sigma^2_B$  is calculated by

$$\sigma^2_B = \iint_B \gamma(x_i - x_j) dx_i dx_j \quad (3.4.2)$$

The ratio has a minimum value of 1 which relates to the situation where the variance is entirely unstructured over these scales. The larger the value the greater the spatial structure of the variation in yield.

### 3.4.1.2 The normalized classification entropy (NCE)

The cluster analysis classification which we described above divides the field into zones that have similar season-to-season variation. The normalized classification entropy (see section 3.2) gives a measure of how distinct the classes are from one and other. The smaller the value of the normalized classification entropy the more distinct the class.

### 3.4.1.3 Standard deviation (SD)

Standard deviation is a measure of the variance which is manageable in a given block size (1 ha). We call it the regional standard deviation ( $S_B$ ). It is calculated by integrating the variogram without nugget of a 1 ha block B

$$S_B = \sqrt{\iint_B [(Y(x_i) - Y(x_j)) - c_0] dx_i dx_j} \quad (3.4.3)$$

where  $x_i$  and  $x_j$  are pairs of points within B.

By integrating over an area of standard size and shape means that this statistic can be meaningfully compared across fields. This standard deviation will be large for variable fields and small for more uniform ones.

### 3.4.2. Opportunity index ( $Y_i$ )

De Oliveira's (2009) presented an opportunity index ( $Y_i$ ), which enumerates the opportunity for site specific crop management in a given field. This is an improvement to Pringle's (2003) approach and estimates the ( $Y_i$ ) based on a set of statistical measures of the yield variogram. The opportunity index,  $Y_i$  is defined

$$Y_i = \sqrt{M_v \cdot S_v} \quad (3.4.4)$$

where  $M_v$  is the magnitude of the yield variation and  $S_v$  is the spatial structure of yield variation. The magnitude of variation depends on the coefficient of variation ( $C_v$ ), which is the average covariance of the total field estimated as half the squared yield differences between all pairs of locations in yield minus nugget as given below:

$$C_v = \frac{1}{n^2} ([\sum_{i=1}^n \sum_{j=1}^n (x_i - y_j)^2 / 2] - c_0) \quad (3.4.5)$$

To compare the variation in magnitude between fields  $C_v$  is standardised in to a new areal coefficient,  $aC_v$

$$aC_v = \left( \frac{\sqrt{C_v}}{\bar{y}} \right) \times 100 \quad (3.4.6)$$

where  $\bar{y}$  is the mean yield.

$M_v$  is calculated as the ratio of  $aC_v$  and the median of  $aC_v$  over all the available fields  $aC_{v50}$

$$M_v = \frac{aC_v}{aC_{v50}} \quad (3.4.7)$$

The spatial structure measure is given by

$$S_v = \frac{r}{O_L} \quad (3.4.8)$$

where  $r$  is the range of the variogram of the yield monitor data (in the case of the exponential variogram, the effective range,  $r = 2.966 \times$  the distance parameter Webster (1985) and if the field length is smaller than the range then  $r$  is assumed to be 95% of the half of the maximum field length).

The operational length  $O_L$  (ability of the variable rate machinery to react) is the product of the variable rate machinery characteristics such as swath ( $\beta$ ), speed ( $v$ ), and time to alter applications ( $t$ ) (Pringle et al., 2003) and is divided by 10000 to convert to hectares:

$$O_L = \frac{\beta vt}{10000} \quad (3.4.9)$$

In our analysis we assumed values of  $\beta, v, t$  are of 8m, 5  $\text{ms}^{-1}$ , 3 sec, respectively (Pringle 2003).

### 3.4.3. Variable Rate Management Score

We considered five different methods for ranking fields based on their potential for variable rate management. These were (i) the range ( $r$ ) multiplied by  $c_1$  parameter of the variogram (i.e.  $rc_1$ ), (ii)  $V_R S_B$ , (iii)  $c_1 \sqrt{r}$  (iv)  $V_R \sqrt{S_B}$  and (v)  $c_1 \log(r)$ . Using the simulation results described in section 3.3, we explored to see how much of the variation in the increased profit achieved from variable rate management (i.e.  $\Delta_{\text{grid}} - \Delta_{\text{field}}$  from section 3.3.5 above) could be explained by each of these metrics.

## 4. Results

### 4.1. Comparison of yield cleaning software

The parameter values used in the evaluation of the yield-monitor cleaning programs are shown in Tables 3.1.2 – 3.1.5. For Yield Editor (method B), the Sun *et al.* program and Roth-YE the maximum and minimum yield values were chosen from visual inspection of the yield monitor data (Figure 4.1.1). Figures 4.1.2 – 4.1.6 show the raw yield monitor data and the cleaned yield maps for each of the fields, and Table 4.1.1 reports the summary statistics of the cleaned data. The raw yield data ranges from 0–30 t ha<sup>-1</sup> (Table 4.1.1). It is clear that the projections used by Yield Editor and Sun *et al.* (2013) are not suitable for the UK. The field co-ordinates are warped and change their orientation.

Yield ranges were widest in Yield Editor method A. The range of yields were comparable for Yield Editor method B, Auto-N and ROTH-YE. Mean yields after cleaning were always higher under Yield editor method B, and the lowest coefficient of variation (CV) and standard deviation (SD) were given by the Sun *et al.* program. The Sun *et al.* program removes the largest number of points, but the yield maps tend to be visually more coherent than those produced by the other methods. For example, in Figure 4.1.2 there is a clear line of lower values and a clear line of higher values in all maps except that produced by Sun *et al.* These are removed by the local SD filter. However the maximum yields tend to be lower than from other programs. The performance of the Auto-N program and Roth-YE are similar. They have similar summary statistics and the numbers of points remaining after filtering (Table 4.1.1). Roth-YE filters slightly more points out because it has more filters.

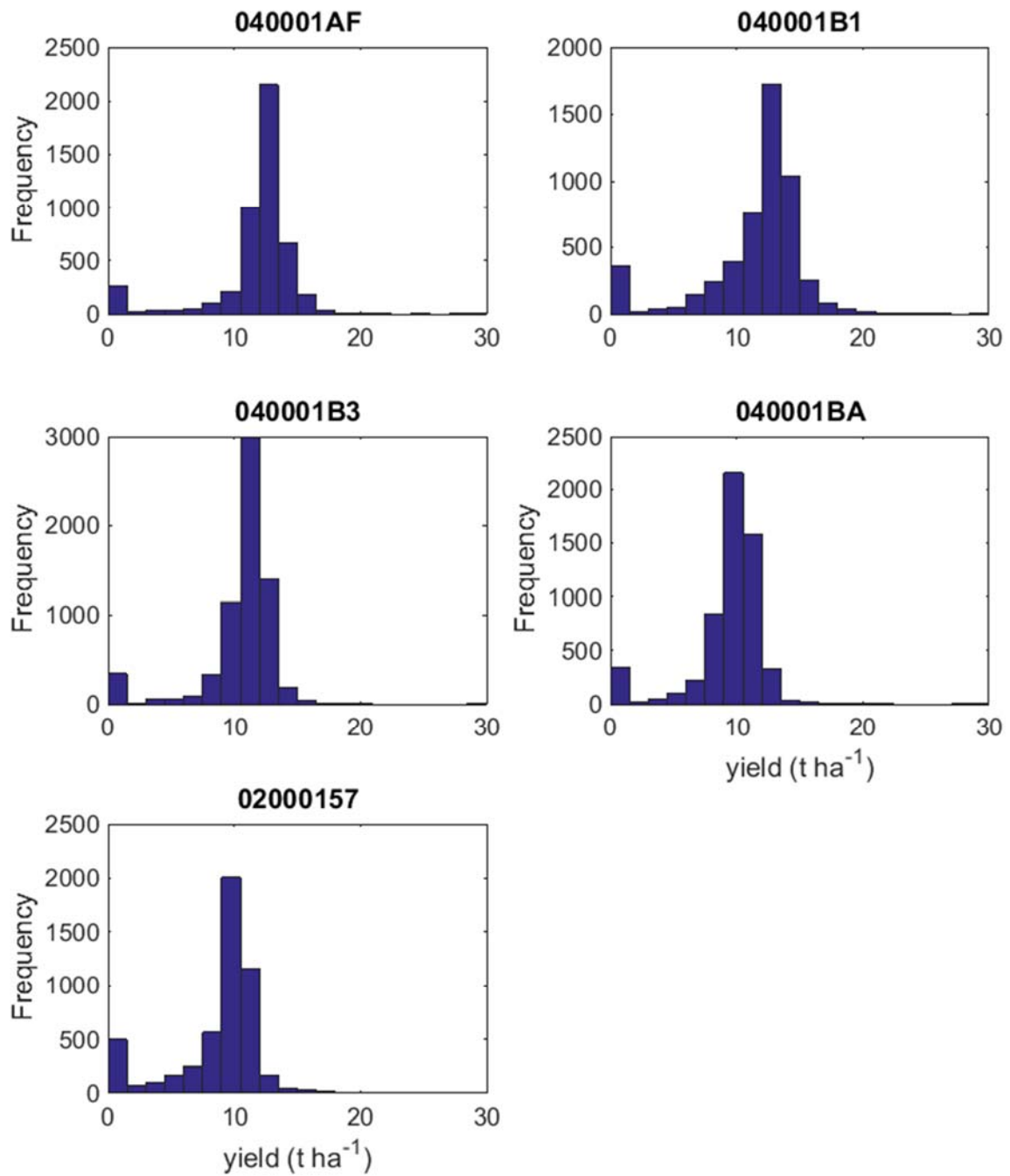


Figure 4.1.1. Histograms of raw yield monitor data (t ha<sup>-1</sup>) for five fields.

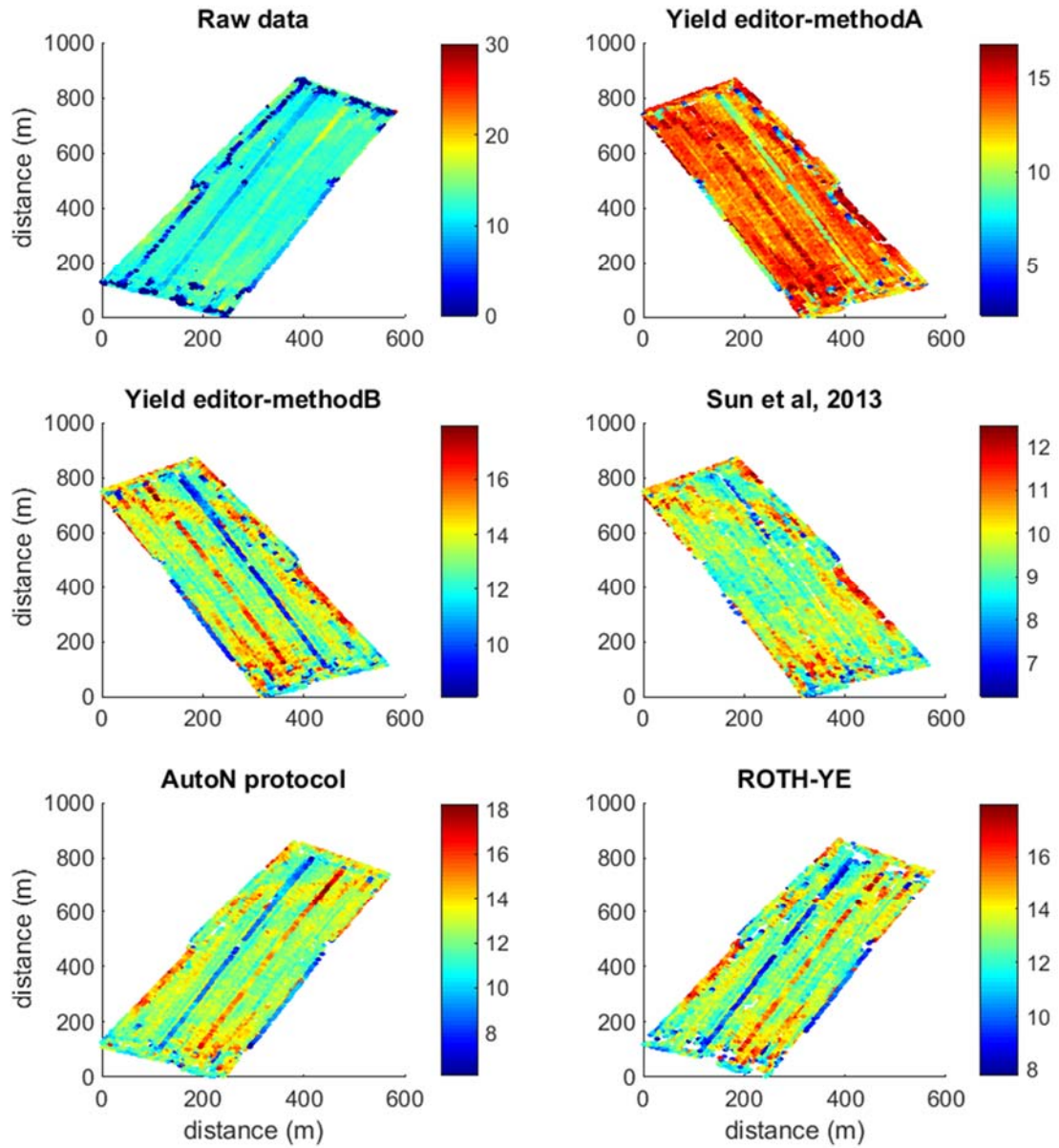


Figure 4.1.2. Raw and cleaned yield monitor data (t ha<sup>-1</sup>) for field 040001AF using different yield cleaning software

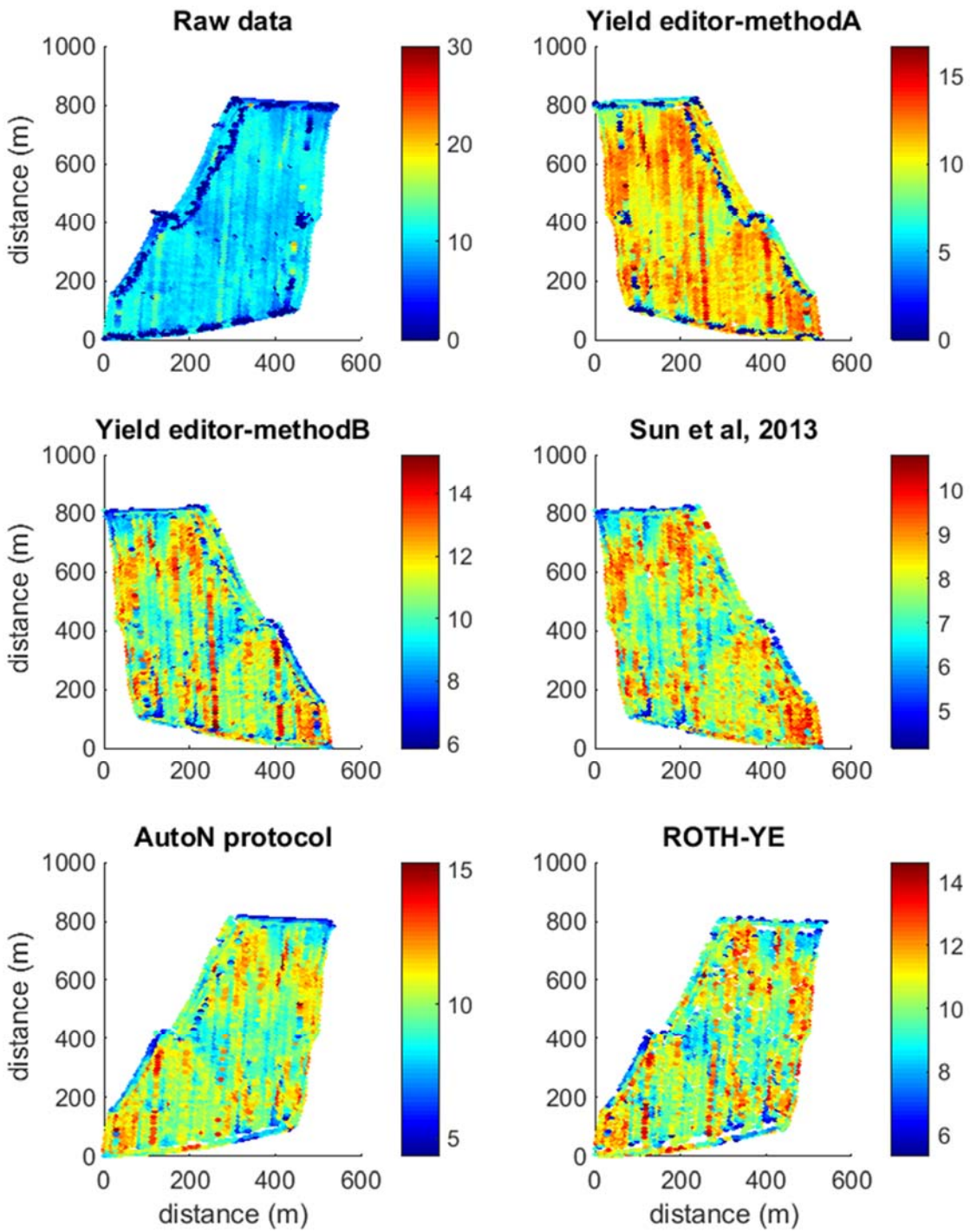


Figure 4.1.3 Raw and cleaned yield maps for site 040001BA using different yield cleaning software.

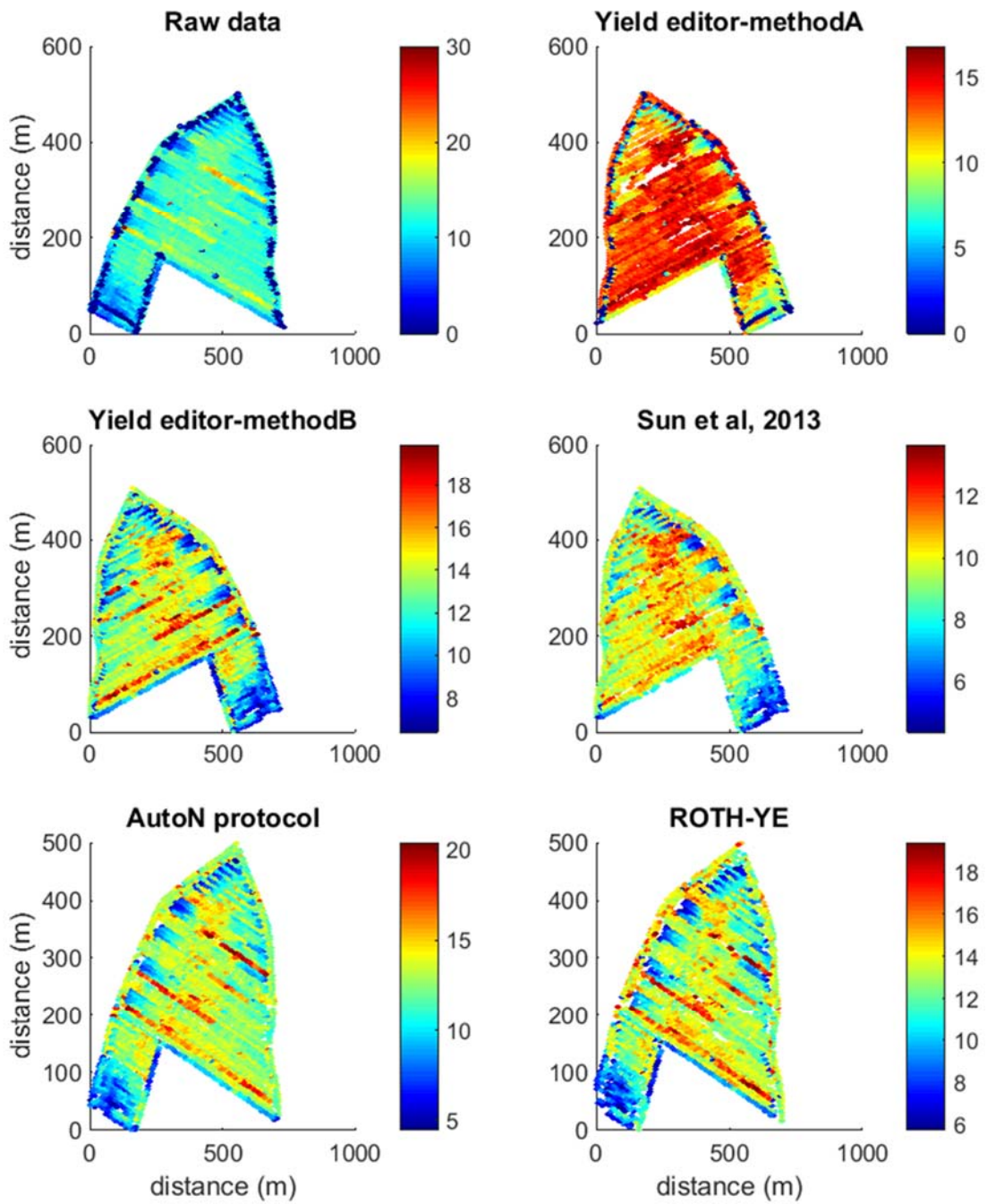


Figure 4.1.4. Cleaned yield maps for site 040001B1 using different yield cleaning software.

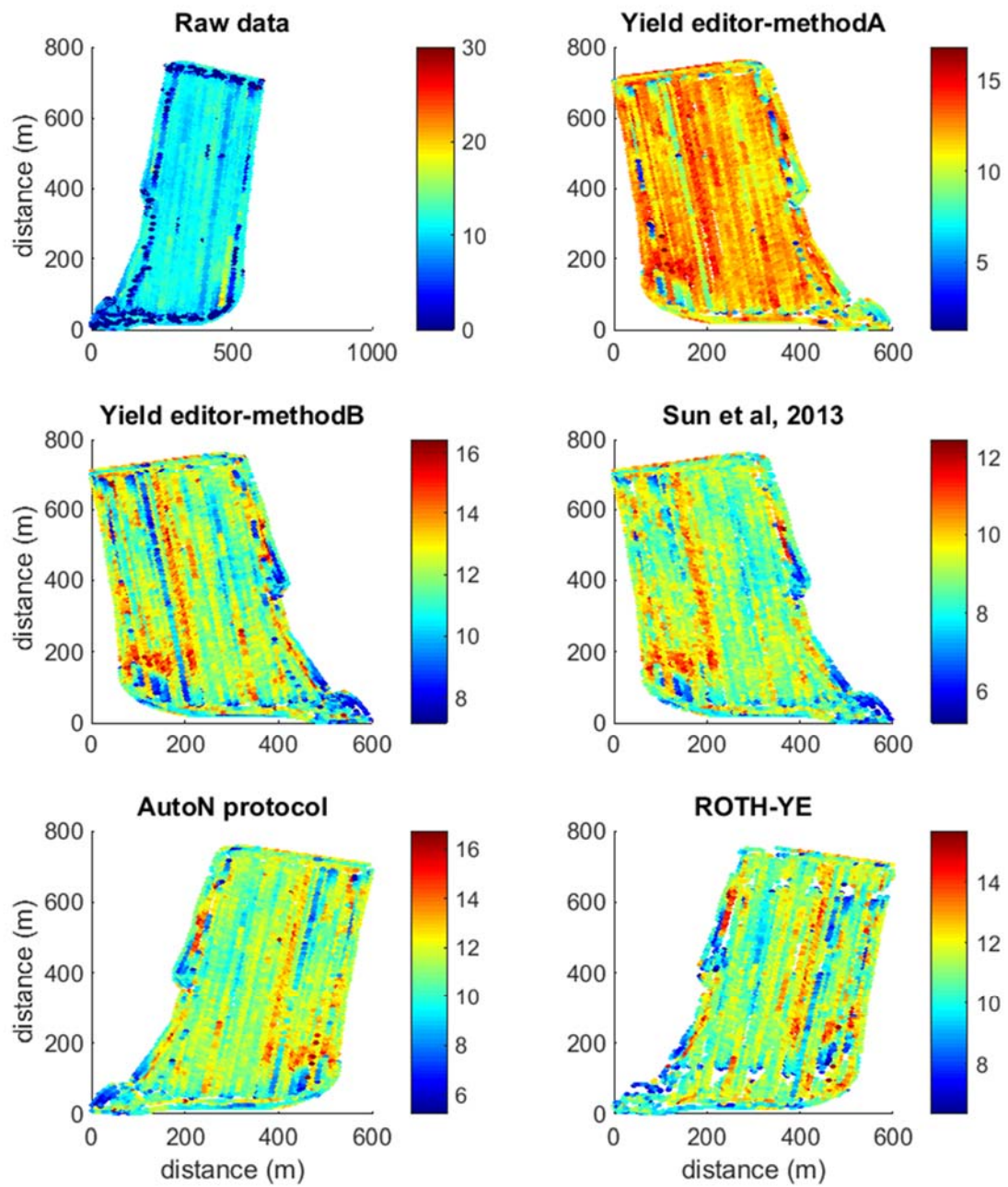


Figure 4.1.5. Cleaned yield maps for site 040001B3 using different yield cleaning software.

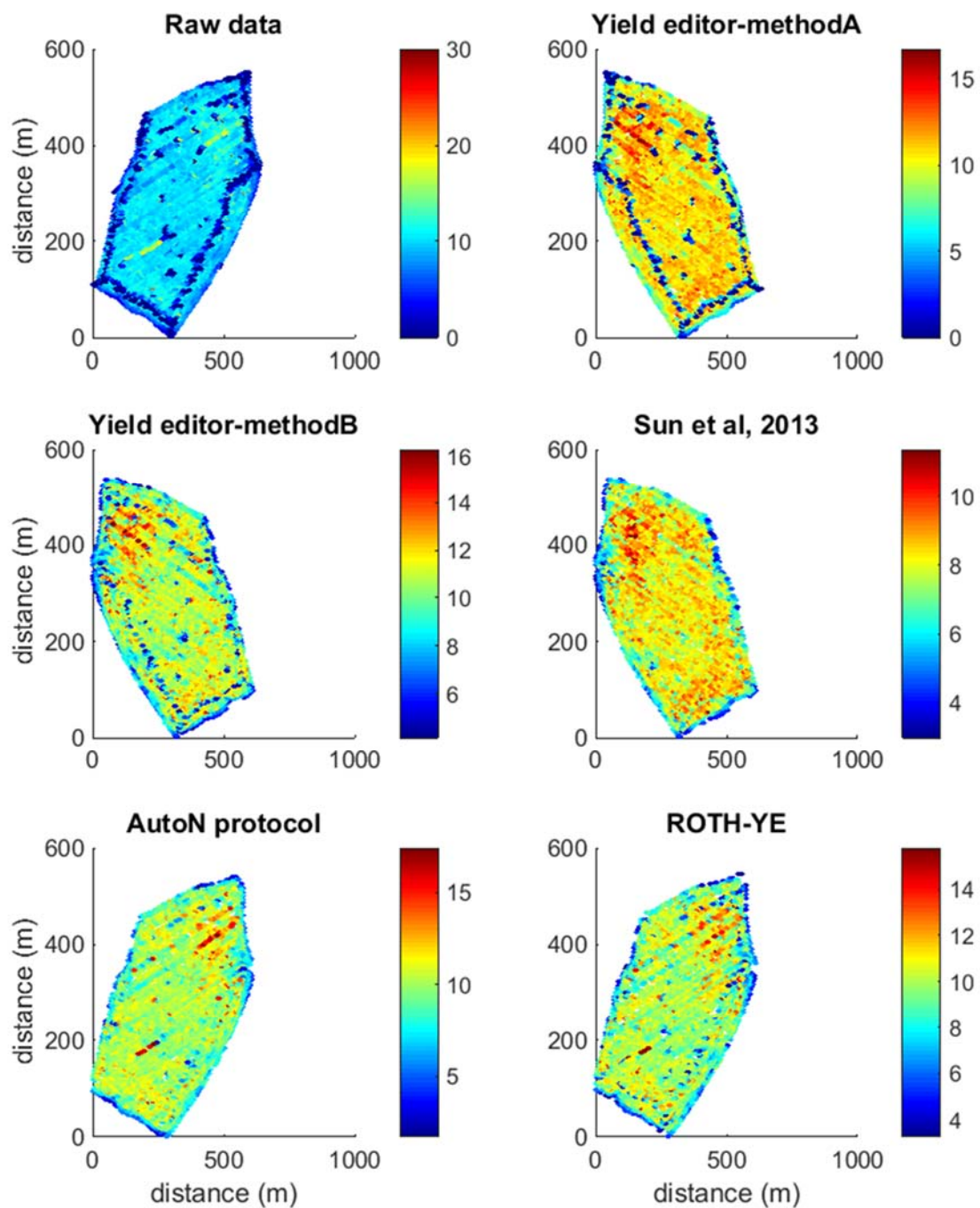


Figure 4.1.6. Raw and cleaned yield map for site 02000157 using different yield cleaning software.

Table 4.1.1. Summary statistics of the raw and cleaned yield monitor data from each field analysed with each program

Statistics						
	Raw data	Yield Editor		Sun et al.	Auto-N	ROTH-YE
		A	B			
<b>Field 040001AF</b>						
Mean (t ha <sup>-1</sup> )	11.7	13.2	13.4	9.6	12.6	13.1
STD	3.4	1.8	1.9	0.8	1.4	1.4
CV	0.29	0.14	0.11	0.09	0.11	0.11
N	4748	4093	4259	3790	4101	4097
Range (t ha <sup>-1</sup> )	0–30	2.3 –16.8	8–18	6-12.5	6–18.3	7.0–17.9
<b>Field 040001B1</b>						
Mean (t ha <sup>-1</sup> )	11.5	12.3	13.3	9.6	12.5	12.9
STD	4.05	3.5	2.3	1.5	2.2	2.2
CV	0.35	0.29	0.17	0.16	0.18	0.17
N	5187	4112	4623	4071	4435	4438
Range (t ha <sup>-1</sup> )	0–30	0-16.8	6.0-20.0	4.4-13.7	4.4-20.4	5.8-19.8
<b>Field 040001B3</b>						
Mean (t ha <sup>-1</sup> )	10.5	11.8	12.0	9.0	11.2	11.2
STD	3.02	1.67	1.4	0.96	1.4	1.3
CV	0.29	0.14	0.12	0.11	0.12	0.12
N	6660	5854	6054	5467	5743	5720
Range (t ha <sup>-1</sup> )	0–30.0	1.0-16.8	7-16.4	5.2-12.5	5.2-16.7	6.1-16.0
<b>Field 040001BA</b>						
Mean (t ha <sup>-1</sup> )	9.3	10.3	10.7	7.9	10.0	10.1
STD	2.9	2.6	1.5	1.0	1.44	1.4
CV	0.32	0.25	0.14	0.13	0.14	0.14
N	5705	5355	5145	4733	4753	4439
Range (t ha <sup>-1</sup> )	0–30	0-16.7	5.9-15.3	4.2-10.9	4.3-15.3	5.1-15
<b>Field 02000157</b>						
Mean (t ha <sup>-1</sup> )	8.8	9.7	10.4	7.9	9.8	9.7
STD	3.7	3.1	1.8	1.13	1.7	1.57
CV	0.41	0.32	0.18	0.14	0.18	0.16
N	5088	4338	4379	3837	4059	4047
Range (t ha <sup>-1</sup> )	0–32.2	0-16.7	4-16.3	3-11.4	1.8-17.4	3.0-15.8

## **4.2. Delineating management zones to understand the causes of yield variation**

We present the results for some selected fields in Figures 4.2.1.1 – 4.2.11.4. In each case, we show (i) the cleaned yield monitor data (cleaned using Roth-YE) that we have used in the cluster classification, (ii) the classification achieved from the smoothed fuzzy k-means cluster analysis (in most cases, we used the most recent four maps only ), (iii) the associated centroid values for each zone (i.e. the yield averages per zone) and (iv) the classification based on basic statistics (see section 3.2.1). We also present the results of the REML analysis to determine how much of the variation in the measured soil properties is explained by the cluster classification, and any other information that we had that might indicate causes for the difference in yield variation between the zones.

#### 4.2.1. Field-BD

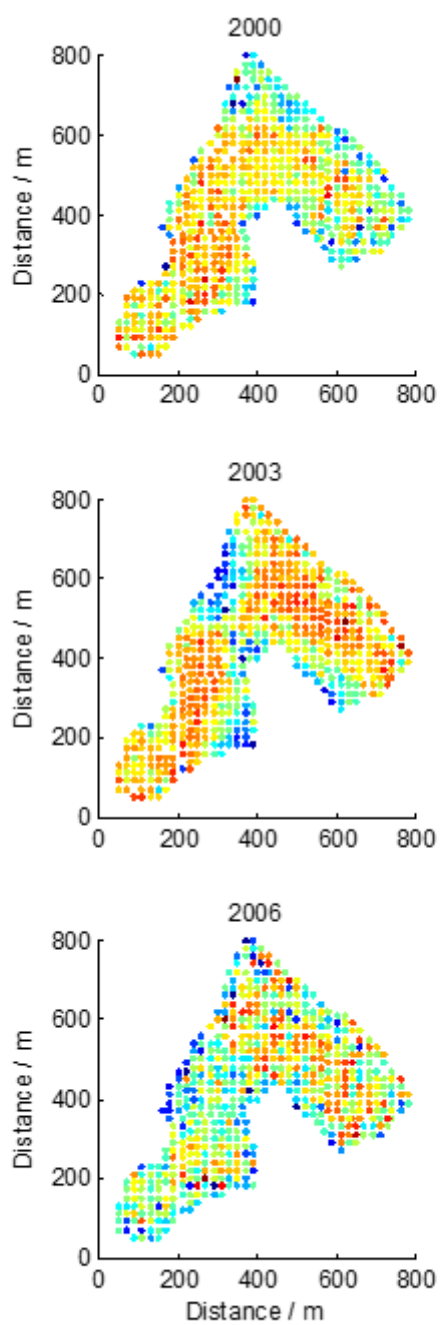


Figure 4.2.1.1 Cleaned yield maps of winter wheat from Field-BD.

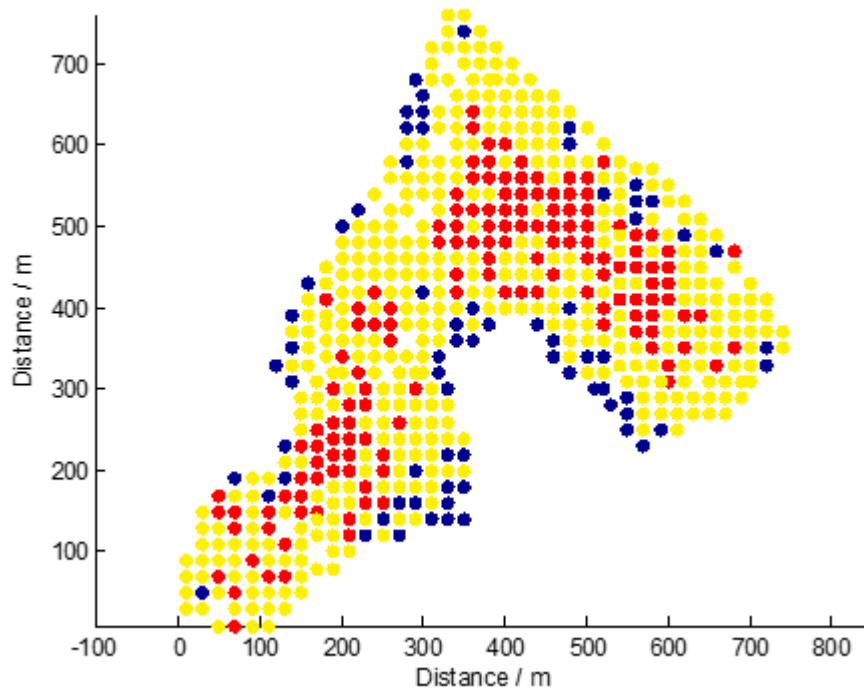


Figure 4.2.1.2 A map showing the areas of Field-BD that yielded better than average (red) in 2000, 2003 and 2006, worse than average (blue) or changed between better or worse than average between seasons (yellow).

Figure 4.2.1.3 shows the class of maximum membership at sites across the field which defines the zones. These correspond to the class centroids shown in Fig. 4.2.1.4, presented both using the raw data and standardised so that the yield average of the field is zero and the standard deviation is one. The centroid values show that Zone 2 yields consistently better than the other two, with the two poorer areas tending to be located at the towards the field margins. There is a broad similarity between the cluster classification and Fig. 4.2.1.2. Table 4.2.1 shows summary statistics for P and K in each zone. The results of the REML analysis showed that the cluster classification did not explain the spatial pattern in P and K ( $F_{2,17.5}=0.47$ ,  $p=0.633$  and  $F_{2,17.4}=1.78$ ,  $p=0.197$  respectively). We had no other field data from which to deduce a cause for the differences between the zones. However, season 2002—2003 (when Zone 3 yielded poorly) is associated with a wetter autumn than the other seasons and so this area might be prone to water logging.

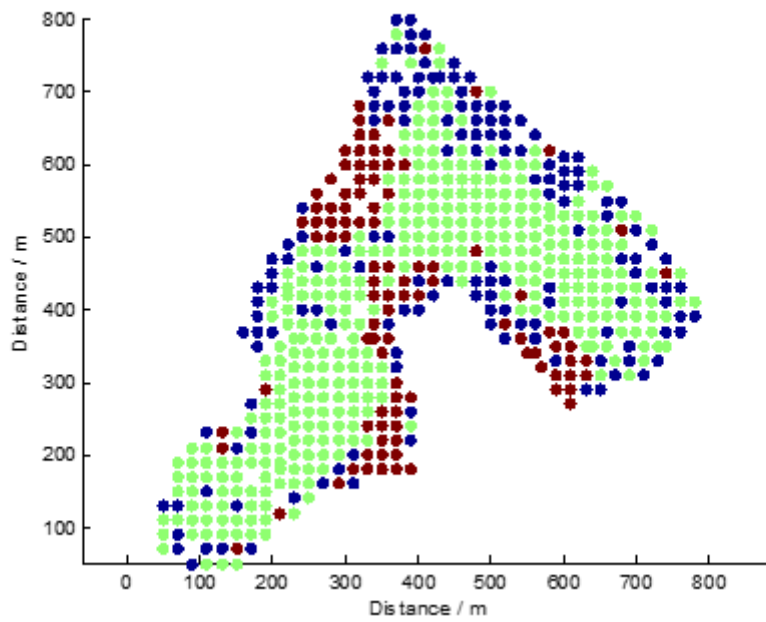


Figure 4.2.1.3 A map showing the cluster classification for Field-BD. Associated centroid values for each zone are shown in Fig. 4.2.4. Zone 1 is shown in blue, zone 2 in green and zone 3 in brown.

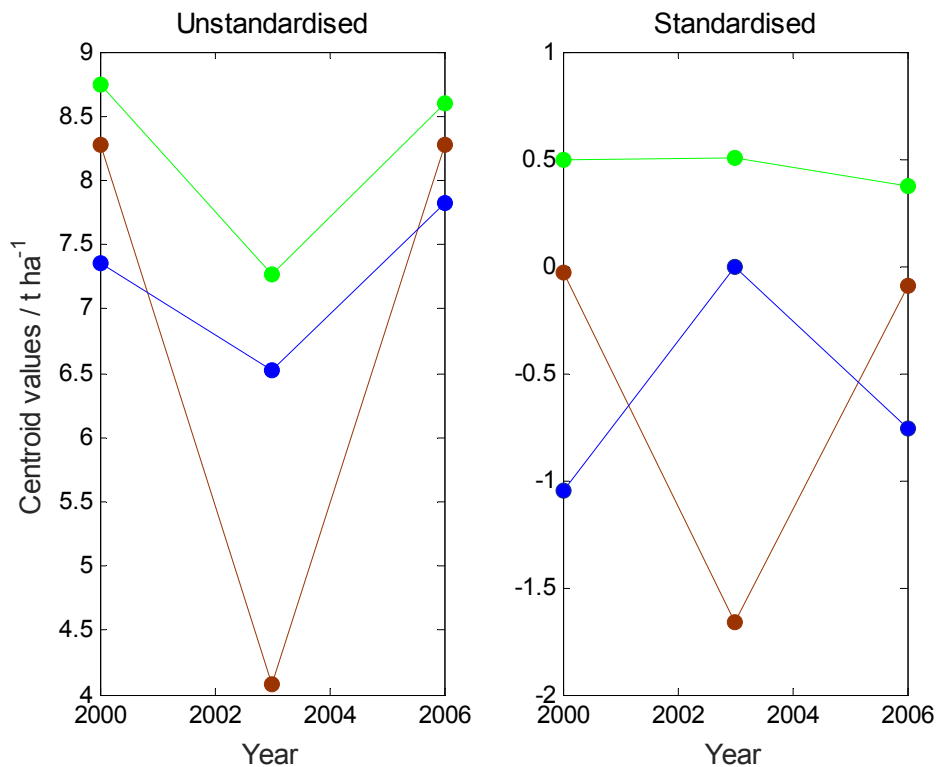


Figure 4.2.1.4 The class centroids across seasons for the cluster classes defined for Field-BD field. The centroids are shown in terms of (a) yield (t ha<sup>-1</sup>) and (b) standardised yield where the data is transformed so that the mean yield across the field is zero and the standard deviation is 1. Zone 1 is shown in blue, Zone 2 in green and Zone 3 in brown.

**Table 4.2.1: Summary statistics of measurements of P and K at Field-BD field according to zone.**

	<b>Mean</b>	<b>Minimum</b>	<b>Maximum</b>	<b>Standard deviation</b>
<b>Potassium</b>				
Total population	114.8	93.05	138.5	12.53
Zone 1	114.1	104.0	120.8	6.752
Zone 2	113.1	93.05	137.7	13.14
Zone 3	120.3	103.2	138.5	14.59
<b>Phosphorus</b>				
Total population	19.27	12.8	31.2	3.99
Zone 1	18.7	16.6	21.2	1.888
Zone 2	19.91	12.8	31.2	4.839
Zone 3	17.8	16.0	21.2	2.107

#### 4.2.2 Field-BF

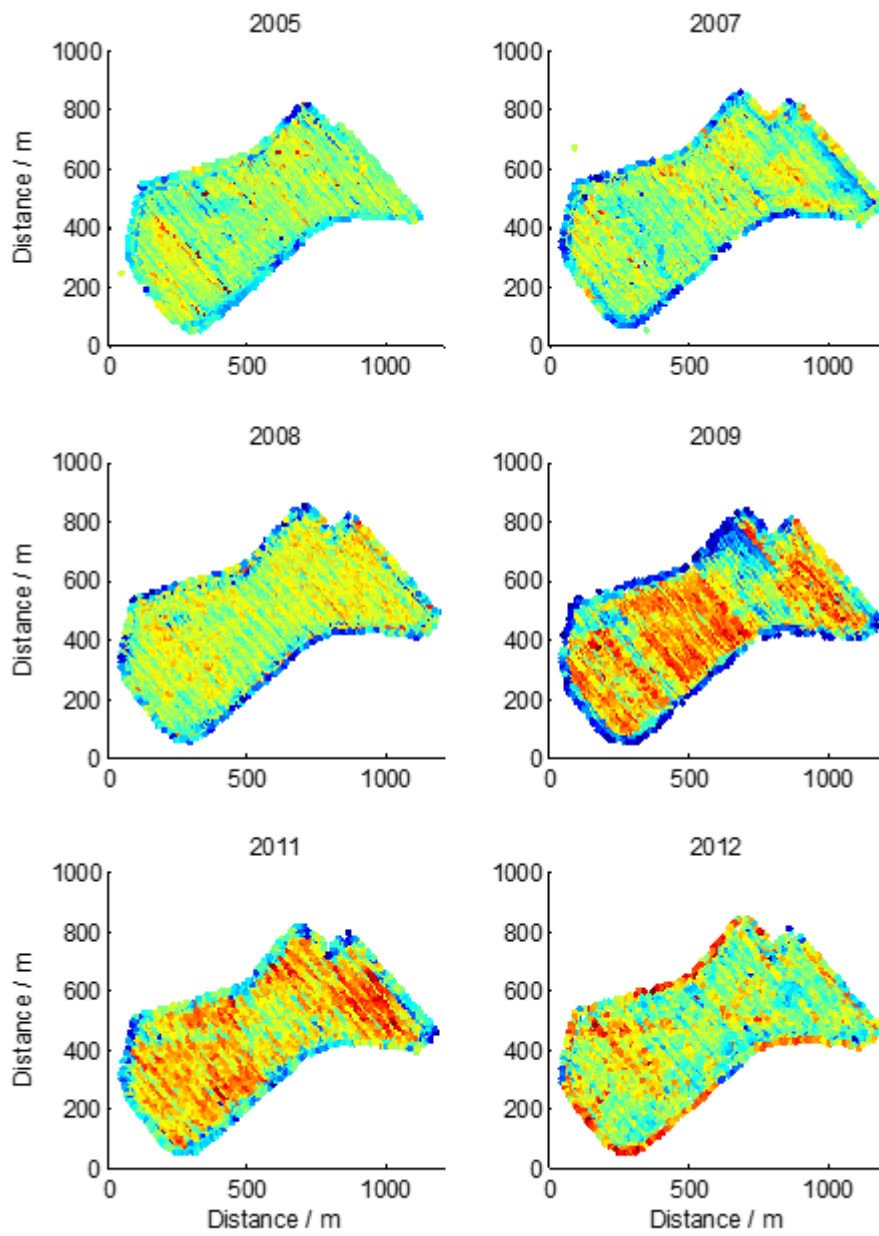


Figure 4.2.2.1 Cleaned yield maps of winter wheat from Field-BF.

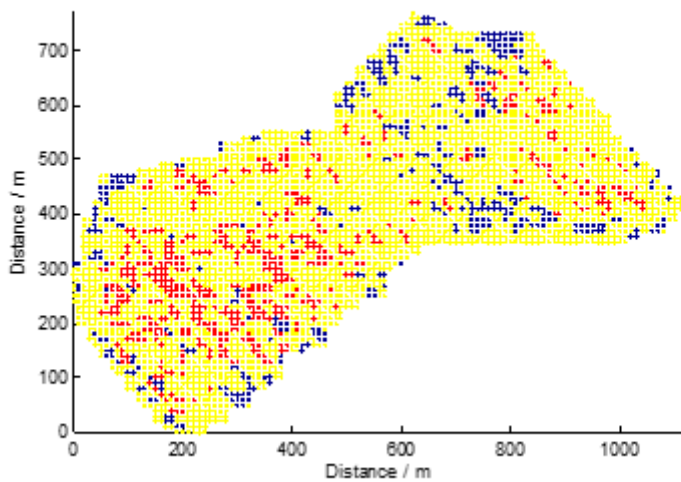


Figure 4.2.2.2. A map showing the areas of Field-BF that yielded better than average (red) in 2009, 2011 and 2012, worse than average (blue) or changed between better or worse than average between seasons (yellow).

Figure 4.2.2.3 shows the class of maximum membership at sites across the field which defines the zones. These correspond to the class centroids shown in 4.2.2.4. The differences between Zones 1 –3 are very small, and in practice these zones do not warrant further investigation. The centroid values show that Zone 3 yields consistently better than the others for three of the four seasons. There is some similarity Zone 3 and the location of the points identified as doing better than average (Fig. 4.2.2.2). Table 4.2.2 shows summary statistics for K, P Mg and pH in each zone. The results of the REML analysis showed that the cluster classification did not explain the spatial pattern in these nutrients ( $F_{3,43}=1.65$ ,  $p=0.192$ ,  $F_{3,36}=1.78$ ,  $p=0.168$ ,  $F_{3,43}=1.11$ ,  $p=0.356$  and  $F_{3,41.7}=1.71$ ,  $p=0.18$  respectively). We also had data on EC, which can act as a proxy for water, and we found that the cluster classification could not be explained by this either ( $F_{3,60}=1.11$ ,  $p=0.374$ ).

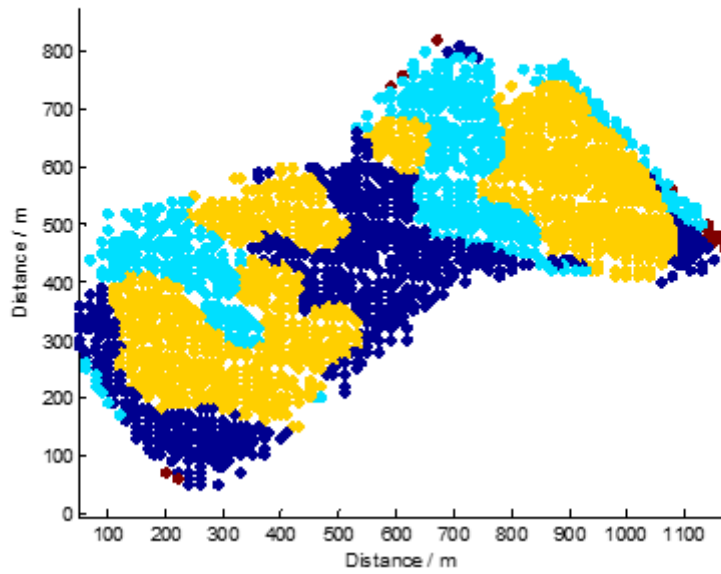
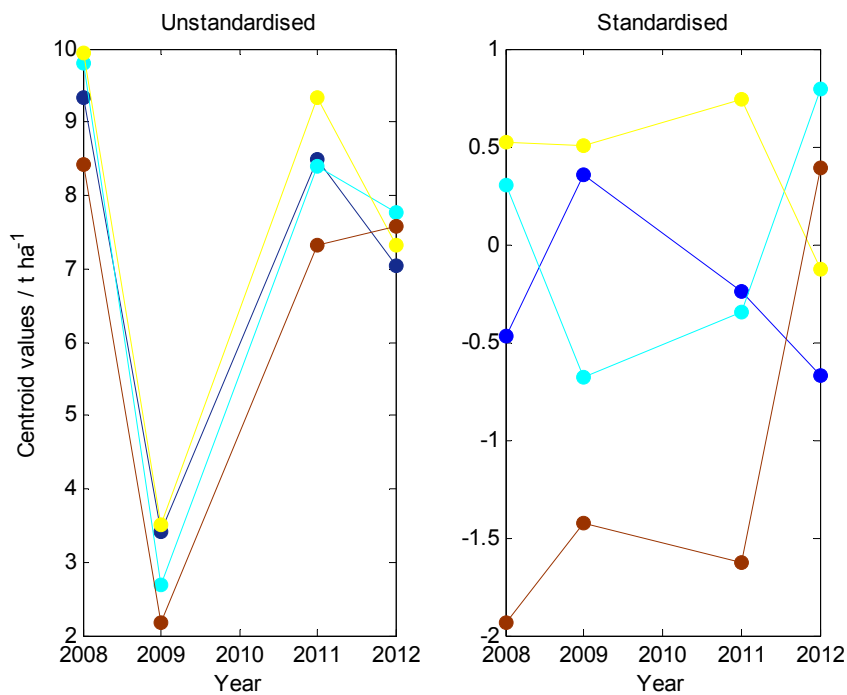


Figure 4.2.2.3 A map showing the cluster classification for Field-BF. Associated centroid values for each zone are show in in Fig. 4.2.2.4. Zone 1 is shown in dark blue, Zone 2 in light blue and Zone 3 in yellow and Zone 4 in brown.



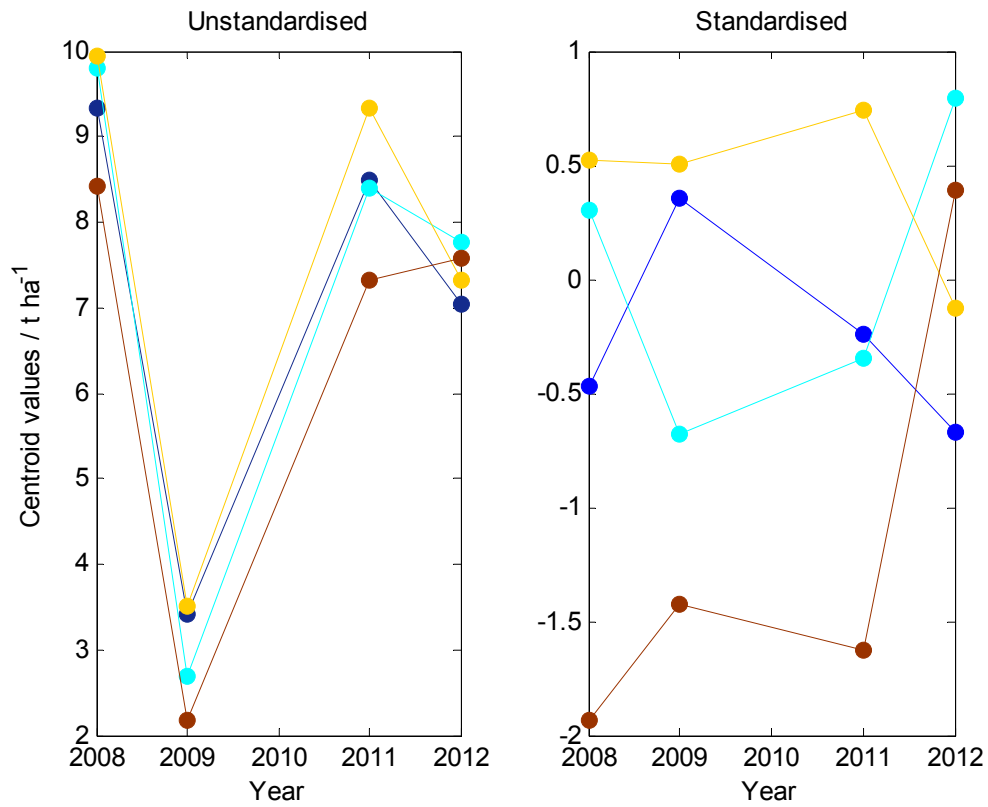


Figure 4.2.2.4 The class centroids across seasons for the cluster classes defined for Field-BF. The centroids are shown in terms of (a) yield ( $t\ ha^{-1}$ ) and (b) standardised yield. Zone 1 is shown in dark blue, Zone 2 in light blue and Zone 3 in yellow and Zone 4 in brown.

**Table 4.2.2: Summary statistics of measurements of P, K, Mg and pH at Field-BF according to zone**

	<b>Mean</b>	<b>Minimum</b>	<b>Maximum</b>	<b>Standard deviation</b>
<b>Potassium</b>				
Total population	209.4	157.9	296.5	30.52
Zone 1	221.5	169.2	296.5	36.0
Zone 2	206.6	162.8	276.6	36.95
Zone 3	203.0	157.9	248.7	23.34
Zone 4	211.1	211.1	211.1	–
<b>Phosphorus</b>				
Total population	27.54	17.0	49.4	7.501
Zone 1	24.96	17.6	49.4	7.988
Zone 2	31.58	21.8	38.8	5.414
Zone 3	27.65	17.0	44.2	7.617
Zone 4	24.8	24.8	24.8	–
<b>Magnesium</b>				
Total population	94.51	68.7	113.8	9.366
Zone 1	97.73	79.35	112.7	9.669
Zone 2	89.95	68.7	98.95	9.641
Zone 3	94.56	82.75	113.8	8.685
Zone 4	97.2	97.2	97.2	–
<b>pH</b>				
Total population	7.810	7.31	8.26	0.153
Zone 1	7.818	7.61	8.06	0.122
Zone 2	7.886	7.69	8.26	0.177
Zone 3	7.775	7.31	8.03	0.159
Zone 4	7.81	7.81	7.81	–

### 4.2.3 Field-CC

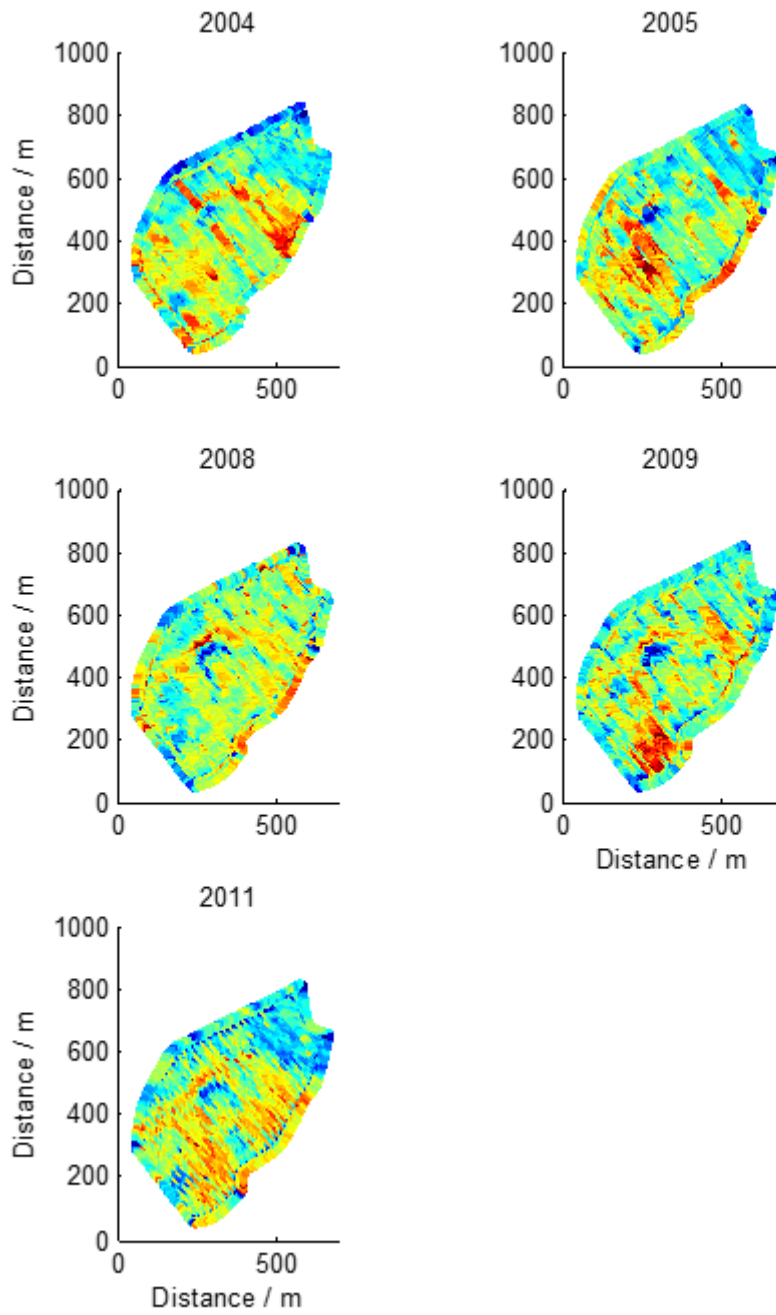


Figure 4.2.3.1 Cleaned yield maps of winter wheat from Field-CC.

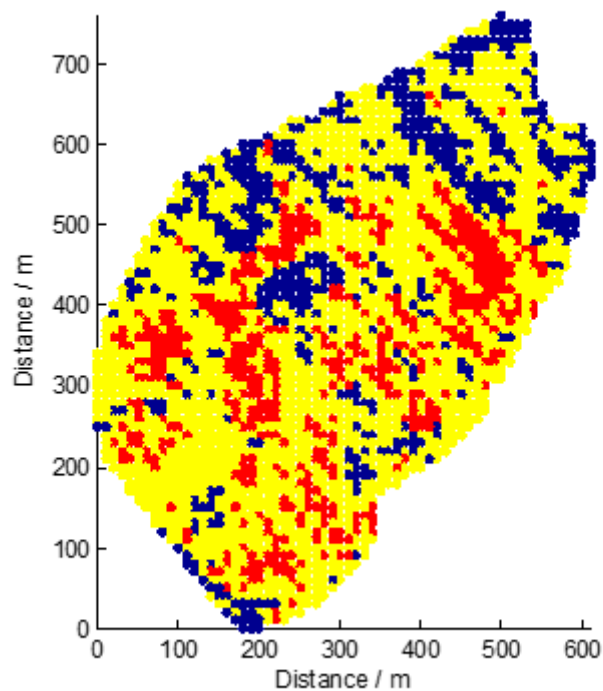


Figure 4.2.3.2. A map showing the areas of Field-CC that yielded better than average (red) in 2008, 2009 and 2011, worse than average (blue) or changed between better or worse than average between seasons (yellow).

Figure 4.2.3.3 shows the class of maximum membership at sites across the field which define the zones. These correspond to the class centroids shown in 4.2.3.4. The centroid values show that Zone 1 yields consistently better than Zone 2. There is a broad similarity between the cluster classification and Fig. 4.2.3.2. The summary statistics for P, K, Mg and pH are shown in Table 4.2.3 both for the total population and according to cluster class. Our REML analysis showed there was no evidence to relate the cluster classification with these soil properties (K –  $F_{1,28}=0.14$ ,  $p=0.712$ , P –  $F_{1,28}=0.09$ ,  $p=0.769$ , Mg –  $F_{1,33}=0.33$ ,  $p=0.571$ , pH – Wald statistic,  $\chi^2=0.79$ , 28 df,  $P = 0.382$ ).

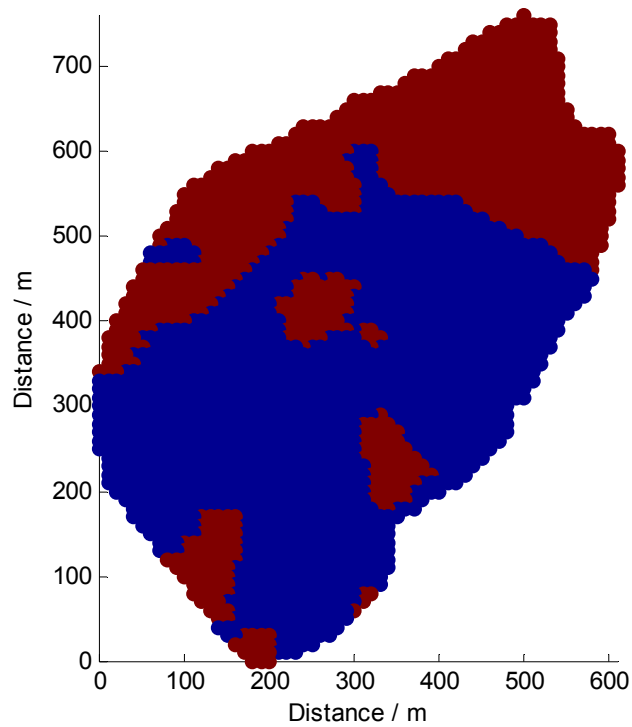


Figure 4.2.3.3 A map showing the cluster classification for Field-CC. Associated centroid values for each zone are shown in Fig. 4.2.3.4. Zone 1 is shown in blue, Zone 2 in brown.

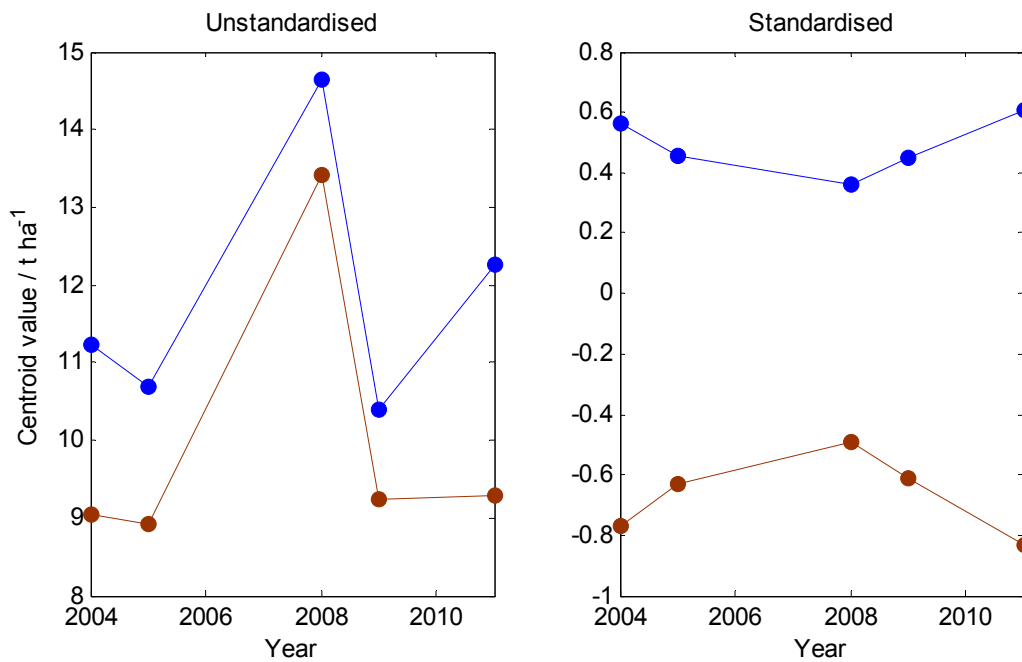
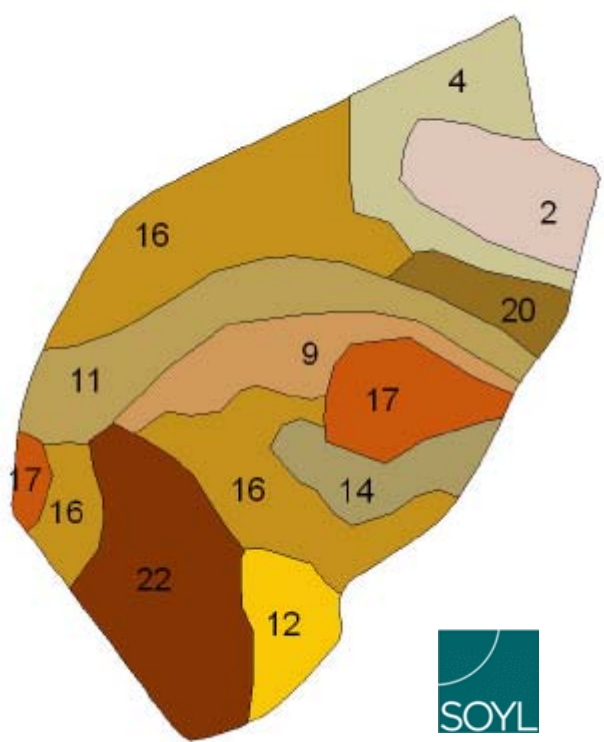


Figure 4.2.3.4. The class centroids across seasons for the cluster classes defined for Field-CC field. The centroids are shown in terms of (a) yield (t ha<sup>-1</sup>) and (b) standardised yield. Zone 1 is shown in blue, Zone 2 in brown.

**Table 4.2.3: Summary statistics of measurements of P, K, Mg and pH at Field-CC for the total population and according to zone.**

	<b>Mean</b>	<b>Minimum</b>	<b>Maximum</b>	<b>Standard deviation</b>
<b>Potassium</b>				
Total population	120.1	92.1	160.4	18.26
Zone 1	121.0	94.3	160.4	17.84
Zone 2	118.3	92.1	156.2	19.92
<b>Phosphorus</b>				
Total population	21.8	15.8	35.6	4.8
Zone 1	22.0	15.8	35.6	4.80
Zone 2	21.4	16.2	34.0	5.05
<b>Magnesium</b>				
Total population	38.4	20.8	67.3	9.89
Zone 1	39.1	23.0	67.3	10.09
Zone 2	36.9	20.8	50.5	9.84
<b>pH</b>				
Total population	7.5	6.4	8.2	0.56
Zone 1	7.6	6.5	8.2	0.53
Zone 2	7.4	6.4	8.2	0.63

For this field we also had a map of soil classes (Fig 4.2.3.5) and elevation data (Fig 4.2.3.6). The north-east section of the field is medium texture with the rest of the field allocated to heavy texture. The field is particularly stony in the north-east and also across a strip through the centre (soil class 9). The part of the field with lighter texture is associated with the poorer yielding area. The elevation map shows that Zone 2 generally relates to the local maxima in elevation. This suggests that perhaps the smaller yield result from reduced water availability, exposure or less available nitrogen resulting from the interaction of soil and water.



Soils classes:

1 is light texture

2–8 are medium texture

9–22 are heavy texture

Stoniness:

2, 4, 9 and 20 High

Other Moderate

Figure 4.2.3.5: A map, produced by SOYL, of soil indicating soil texture and stoniness for Field-CC.

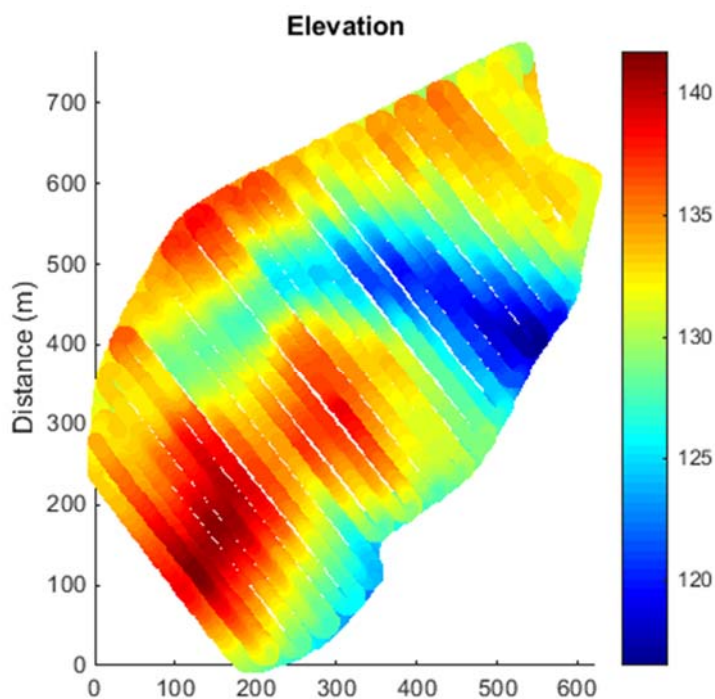


Figure 4.2.3.6: Elevation map for Field-CC (m above sea level).

#### 4.2.4 Field-CP

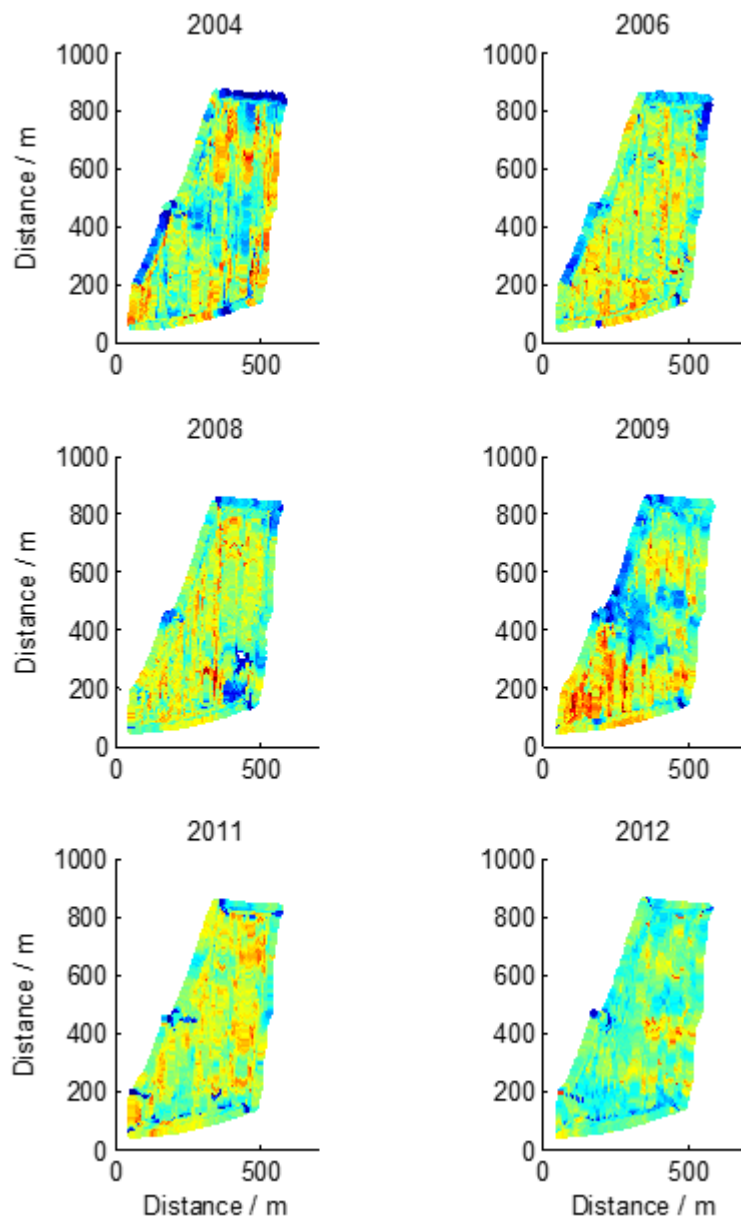


Figure 4.2.4.1 Cleaned yield maps of winter wheat from Field-CP.

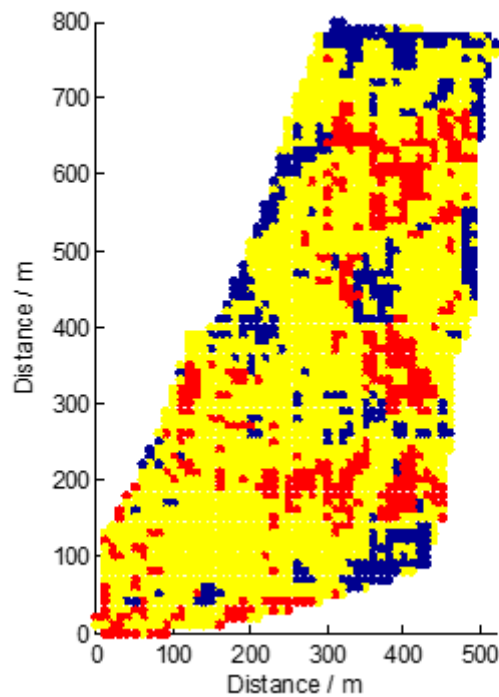


Figure 4.2.4.2. A map showing the areas of Field-CP that yielded better than average (red) in 2009, 2011 and 2012, worse than average (blue) or changed between better or worse than average between seasons (yellow).

Figure 4.2.4.3 shows the class of maximum membership at sites across the field. These correspond to the class centroids shown in 4.2.4.4. The centroid values show that Zone 3 generally yields the best and Zone 1 the worst. This is indicated to some extent on Fig. 4.2.4.2. Table 4.2.4 shows summary statistics for P, K, Mg and pH in each zone. The results of the REML analysis showed that the cluster classification did not explain the spatial pattern in P ( $F_{2,25.0}=0.02$ ,  $p=0.980$ ), however it did explain some of the variation in the other variables, particularly pH (K –  $F_{2,25.0}=4.58$ ,  $p=0.02$ , Mg –  $F_{2,25.0}=4.57$ ,  $p=0.02$ , and pH – Wald statistic,  $\chi^2=9.21$ , 2 df,  $P = 0.010$  ).

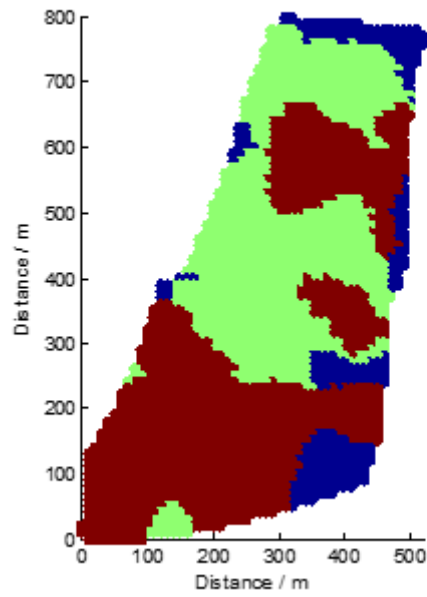


Figure 4.2.4.3. A map showing the cluster classification for Field-CP. Associated centroid values for each zone are shown in Fig. 4.2.4.4. Zone 1 is shown in blue, Zone 2 in green and Zone 3 in brown.

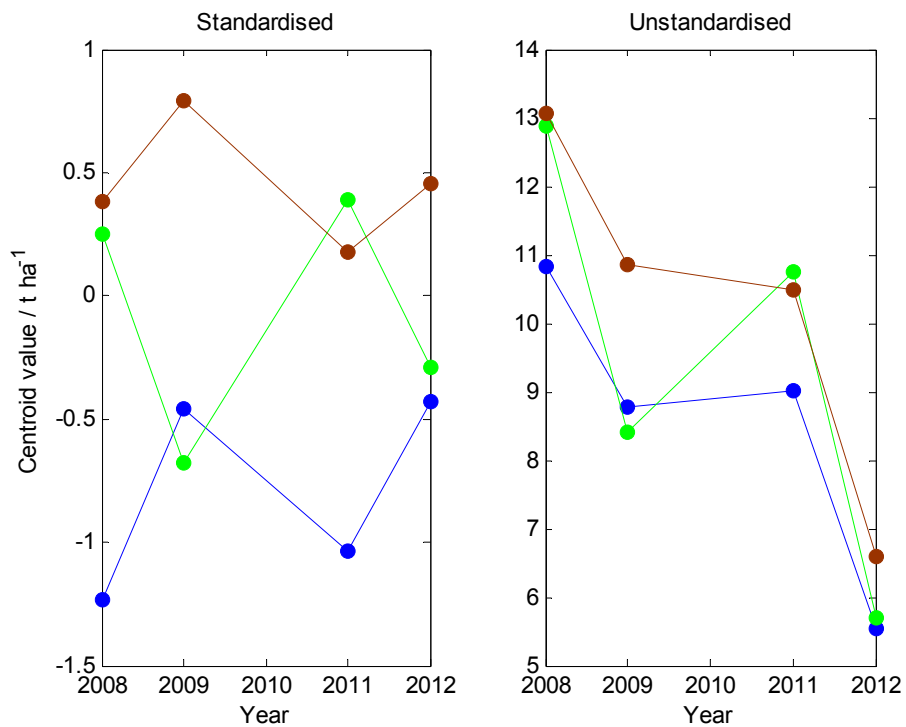


Figure 4.2.4.4. The class centroids across seasons for the cluster classes defined for Field-CP. The centroids are shown in terms of (a) standardised yield and (b) yield ( $t\ ha^{-1}$ ). Zone 1 is shown in blue, Zone 2 in green and Zone 3 in brown.

**Table 4.2.4 Summary statistics of measurements of P, Mg, pH and K at Field-CP field according to zone.**

	<b>Mean</b>	<b>Minimum</b>	<b>Maximum</b>	<b>Standard deviation</b>
<b>Potassium</b>				
Total population	145.1	109.5	206.7	25.49
Zone 1	145.3	126.0	172.8	24.44
Zone 2	146.3	109.5	206.7	28.85
Zone 3	144.2	109.5	206.7	25.49
<b>Phosphorus</b>				
Total population	22.4	14.2	43.2	6.399
Zone 1	31.67	21.4	43.2	10.96
Zone 2	21.93	16.4	30.0	4.737
Zone 3	20.79	14.2	32.4	5.147
<b>Magnesium</b>				
Total population	53.98	35.25	75.2	10.37
Zone 1	43.43	35.55	48.3	6.89
Zone 2	59.78	43.05	75.2	7.644
Zone 3	51.68	35.25	66.1	10.55
<b>pH</b>				
Total population	7.174	5.61	8.25	0.714
Zone 1	7.03	6.87	7.16	0.147
Zone 2	6.634	5.61	7.89	0.556
Zone 3	7.629	6.29	8.28	0.585

#### 4.2.5 Field-ER

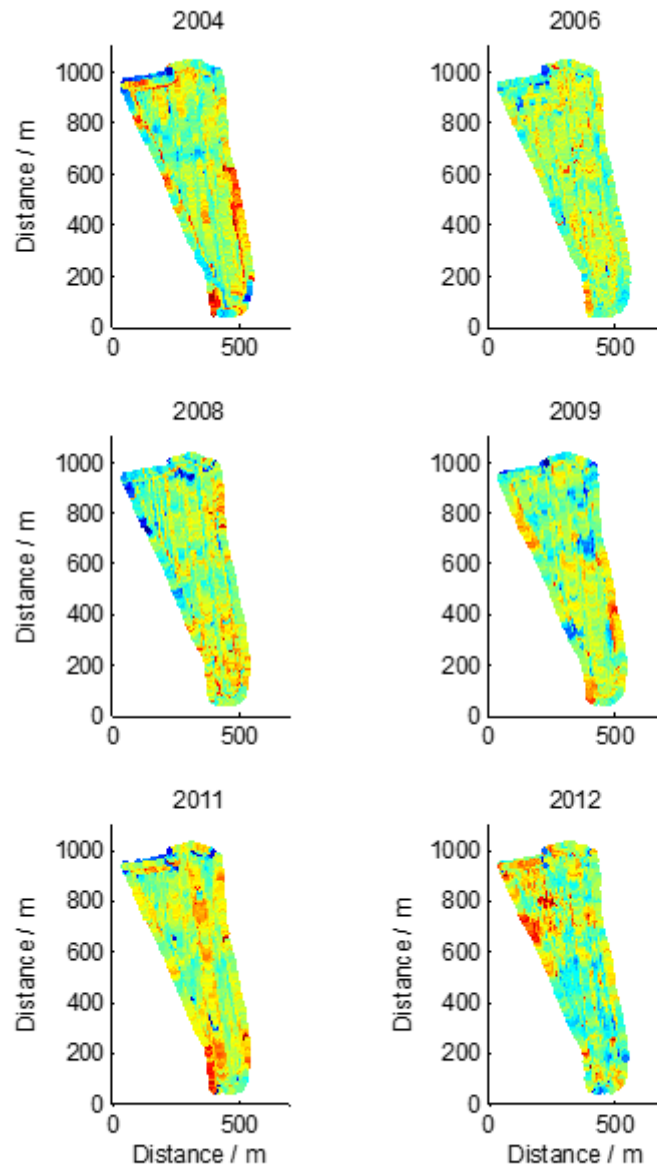


Figure 4.2.5.1 Cleaned yield maps of winter wheat from Field-ER.

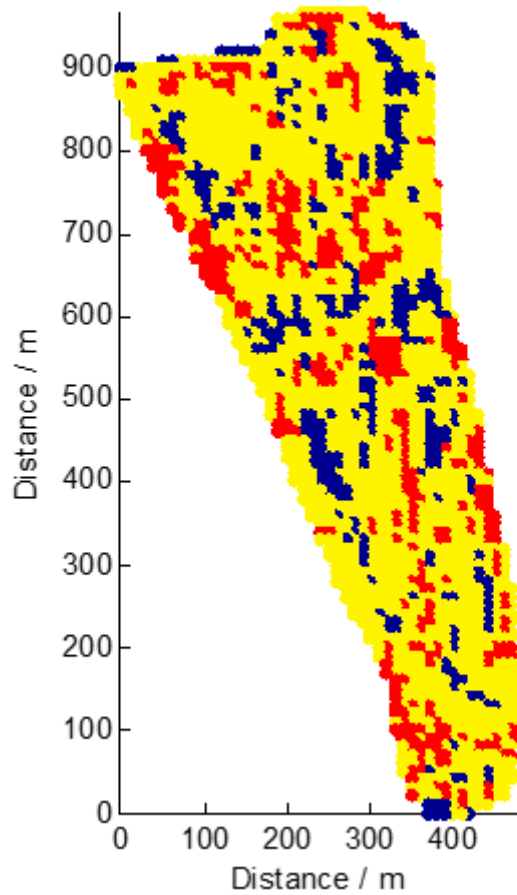


Figure 4.2.5.2. A map showing the parts of Field-ER that yielded better (red), worse (blue) or fluctuated (yellow) compared to the average yield for seasons in 2009, 2011 and 2012.

Figure 4.2.5.3 shows the class of maximum membership at sites across the field. These correspond to the class centroids shown in figure 4.2.5.4. The centroid values show that Zone 2 generally yields the least. Table 4.2.5 shows summary statistics for P, K, Mg and pH in each zone. The results of the REML analysis showed that the cluster classification did not explain the spatial pattern in P ( $F_{2,21.0}=1.41$ ,  $p=0.265$ ), however it did explain some of the variation in the other variables, particularly Mg ( $K - F_{2,21.0}=0.1$ ,  $p=0.901$ ,  $Mg - F_{2,21.0}=2.75$ ,  $p=0.087$ , and  $pH - F_{2,21.0}=0.92$ ,  $p=0.413$ ).

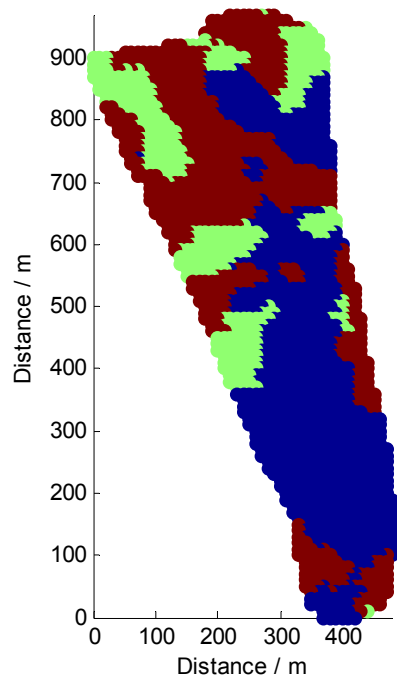


Figure 4.2.5.3. A map showing the cluster classification for Field-ER. Associated centroid values for each zone are shown in in Fig. 4.2.5.4. Zone 1 is shown in blue, Zone 2 in green and Zone 3 in brown.

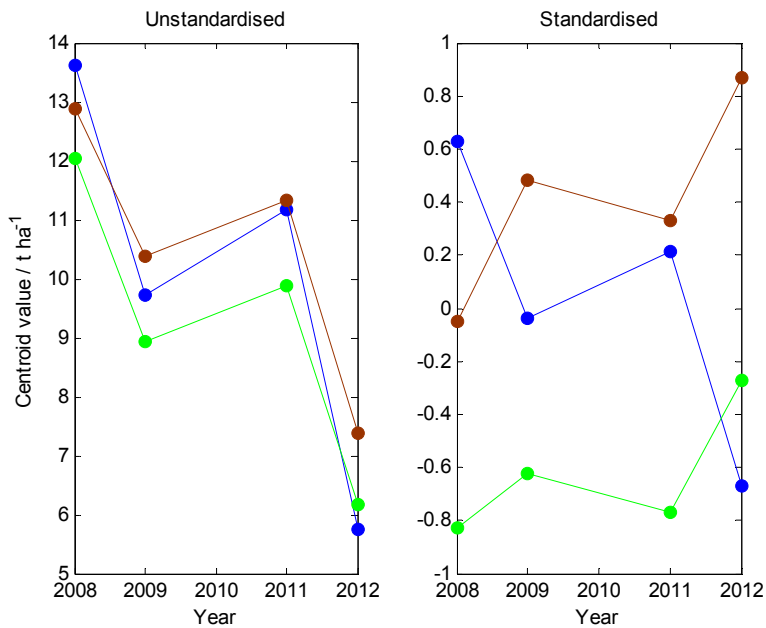


Figure 4.2.5.4. The class centroids for the cluster classes defined for Field-ER across seasons. The centroids are shown in terms of (a) yield ( $t\ ha^{-1}$ ) and (b) standardised yield. Zone 1 is shown in blue, Zone 2 in green and Zone 3 in brown.

**Table 4.2.5. Summary statistics of measurements of P, K, Mg and pH at Field-ER according to zone.**

	<b>Mean</b>	<b>Minimum</b>	<b>Maximum</b>	<b>Standard deviation</b>
<b>Potassium</b>				
Total population	145.5	112.5	208.3	22.33
Zone 1	142.8	117.6	185.4	19.69
Zone 2	146.3	113.2	179.3	24.12
Zone 3	147.6	112.5	208.3	25.66
<b>Phosphorus</b>				
Total population	21.7	14.0	28.0	4.1444
Zone 1	20.0	15.4	24.8	3.243
Zone 2	21.88	17.0	26.8	4.518
Zone 3	23.14	14.0	28.0	4.501
<b>Magnesium</b>				
Total population	48.02	38.2	66.5	7.489
Zone 1	47.92	40.0	62.15	7.826
Zone 2	48.02	38.20	66.5	9.121
Zone 3	45.1	38.2	51.45	4.707
<b>pH</b>				
Total population	7.880	6.54	8.3	0.457
Zone 1	7.837	6.54	8.24	0.537
Zone 2	7.686	6.98	8.22	0.605
Zone 3	8.015	7.44	8.3	0.266

#### 4.2.6 Field-EL

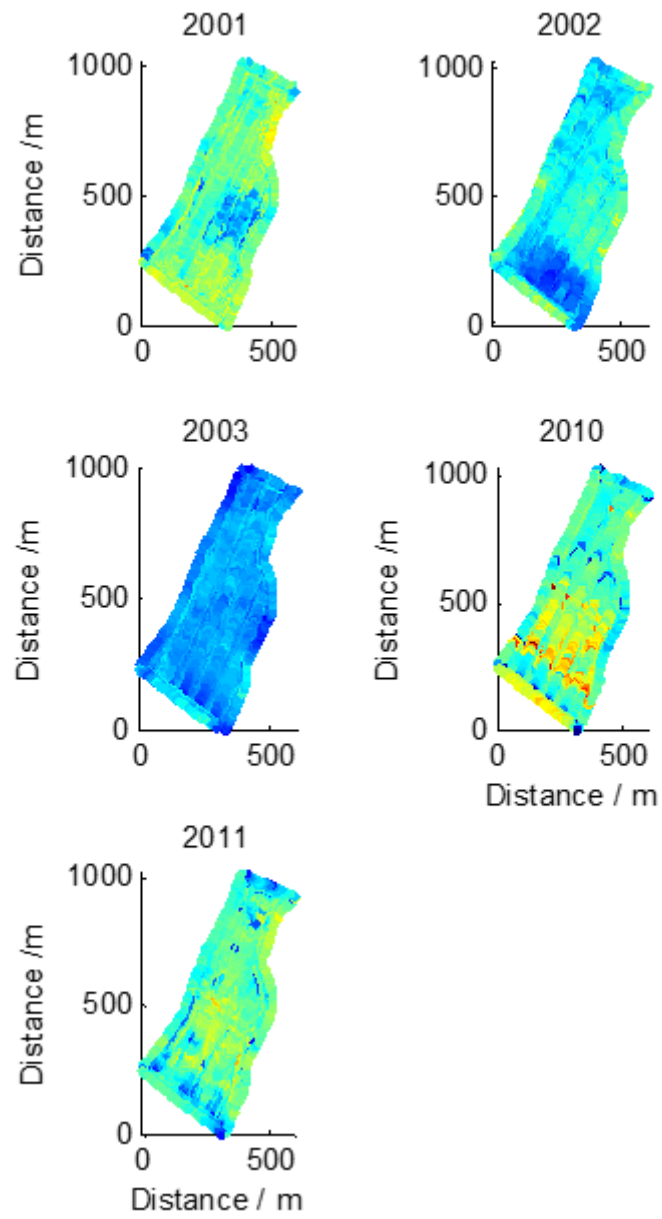


Figure 4.2.6.1 Cleaned yield maps of winter wheat from Field-EL.

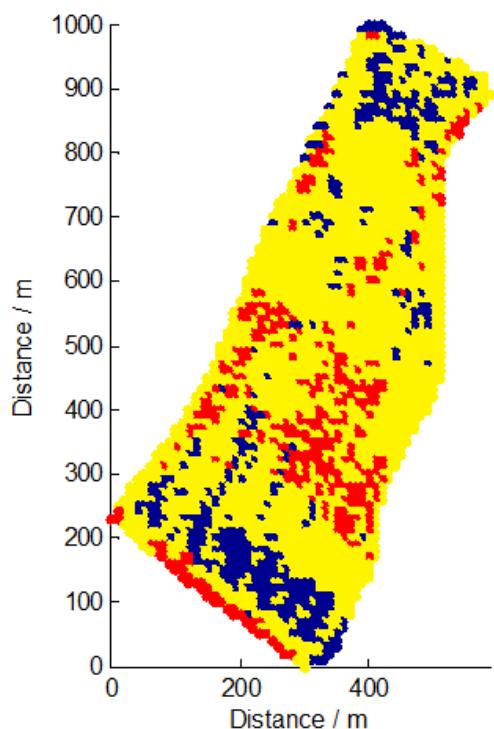


Fig. 4.2.6.2 A map showing the areas of Field-EL field that yielded better than average (red) in 2003, 2010 and 2011, worse than average (blue) or changed between better or worse than average between seasons (yellow).

Figure 4.2.6.3 shows the class of maximum membership at sites across the field. These

correspond to the class centroids shown in 4.2.6.4. The centroid values show Zone 3 tends to be the worst in most years. This accords with Fig. 4.2.6.2. The summary statistics for P, K, Mg and pH are shown in Table 4.2.6 both for the total population and according to zone. The REML analysis showed that the cluster classification did not explain the variation in K, P or Mg ( $F_{3,14.9}=1.31$ ,  $p=0.309$ ; Wald statistic,  $\chi^2=0.65$ , 3 df,  $p = 0.585$  and  $F_{3,25}=0.62$ ,  $p=0.610$  respectively), but there is significant evidence that the zones explain the variation in pH ( $F_{3,18.6}=3.48$ ,  $p=0.037$ ). The mean values for pH for each zone were similar to one another, however, and so unlikely that the variation in pH directly caused of the yield variation. It is more likely that some other factor influenced the yield variation and also affected the soil pH. A map of elevation shows that the lowest part of the field is the part associated with poorer yields (Zone 3). In its worst year (2002) the autumn rainfall was much greater than the other years (90 mm average per month compared with <65 mm) and so yield variation between zones might, in part, be related to this.

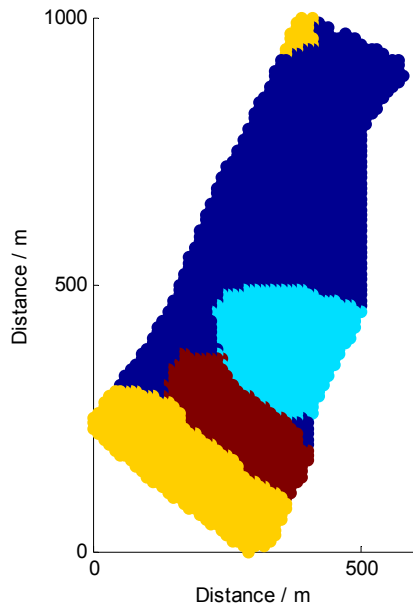


Figure 4.2.6.3. A map showing the cluster classification for Field-EL. Associated centroid values for each zone are shown in Fig. 4.2.6.4. Zone 1 is shown in dark blue, Zone 2 in light blue, Zone 3 in yellow and Zone 4 in brown.

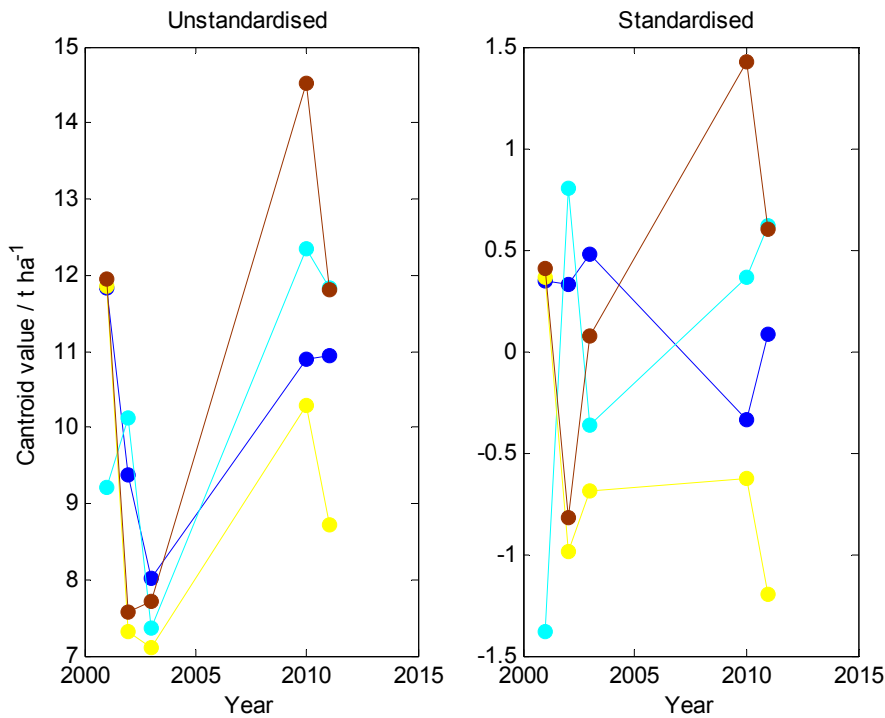


Figure 4.2.6.4. The class centroids across seasons for the cluster classes defined for Field-EL. The centroids are shown in terms of (a) yield ( $t\ ha^{-1}$ ) and (b) standardised yield. Zone 1 is shown in dark blue, Zone 2 in light blue, Zone 3 in yellow and Zone 4 in brown.

**Table 4.2.6 Summary statistics of measurements of P, K, Mg and pH at Field-EL for the total population and according to zone.**

	<b>Mean</b>	<b>Minimum</b>	<b>Maximum</b>	<b>Standard deviation</b>
<b>Potassium</b>				
Total population	157.1	110.5	217.1	28.43
Zone 1	154.2	110.5	205.4	25.31
Zone 2	167.6	136.9	217.1	35.42
Zone 3	136.8	114.5	160.3	17.13
Zone 4	180.4	139.3	208.3	29.21
<b>Phosphorus</b>				
Total population	22.38	13.4	32.8	4.585
Zone 1	22.91	13.4	32.6	5.011
Zone 2	24.76	21.8	32.8	4.681
Zone 3	20.28	16.0	26.2	4.095
Zone 4	20.05	19.0	22.0	1.418
<b>Magnesium</b>				
Total population	53.79	24.75	72.65	12.39
Zone 1	54.63	24.75	71.6	14.45
Zone 2	58.05	50.95	69.35	6.943
Zone 3	47.57	40.6	62.6	8.629
Zone 4	53.11	40.75	72.65	13.97
<b>pH</b>				
Total population	8.177	7.89	8.39	0.148
Zone 1	8.183	8.04	8.39	0.125
Zone 2	8.026	7.98	8.13	0.0615
Zone 3	8.226	7.89	8.36	0.192
Zone 4	8.28	8.09	8.39	0.143

#### 4.2.7 Field-HM

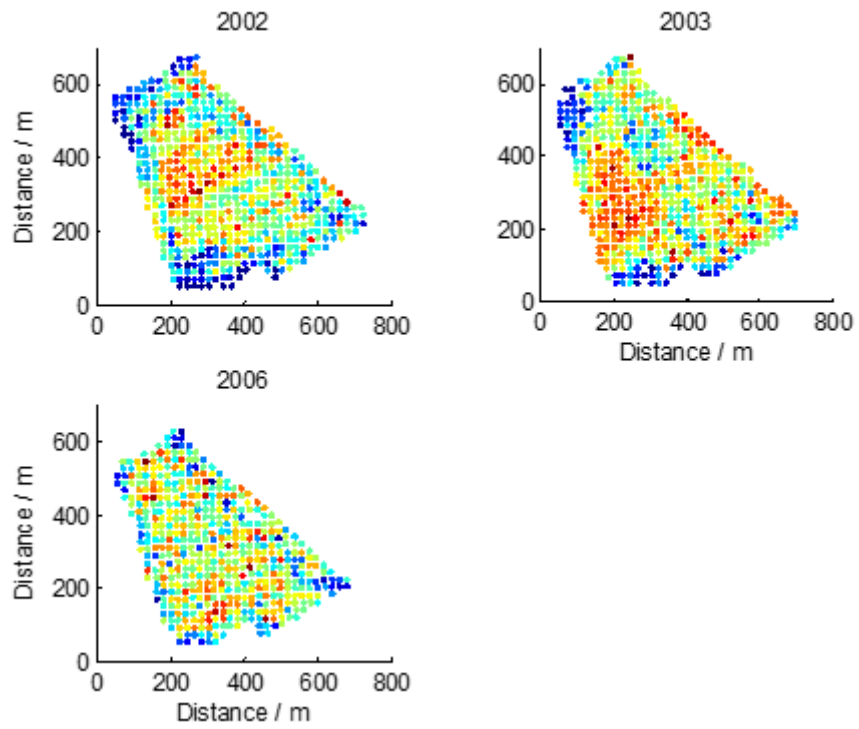


Figure 4.2.7.1 Cleaned yield maps of winter wheat from Field-HM field.

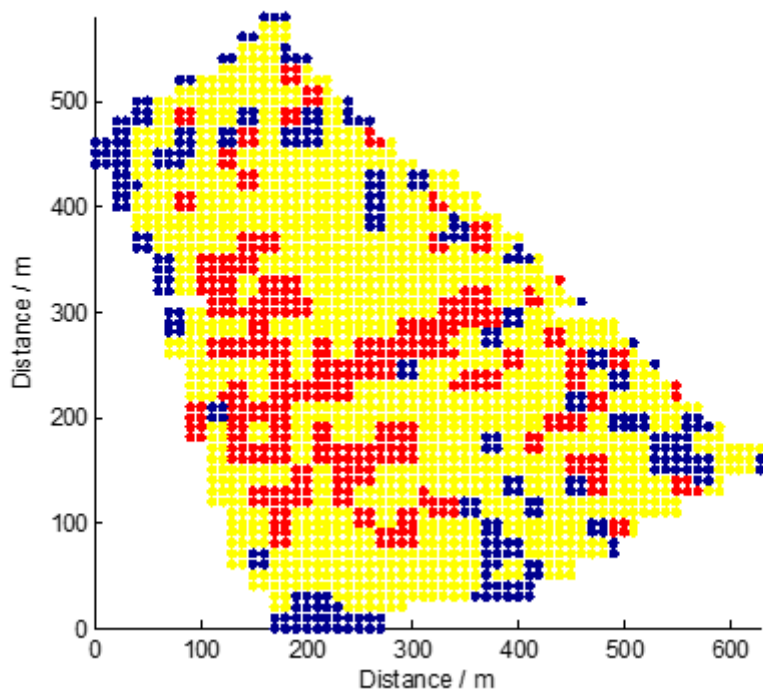


Figure 4.2.7.2. A map showing the areas of Field-HM that yielded better than average (red) in 2002, 2003 and 2006, worse than average (blue) or changed between better or worse than average between seasons (yellow).

Figure 4.2.7.3 shows the class of maximum membership at sites across the field. These correspond to the class centroids shown in 4.2.7.4. The centroid values show that Zone 4 tends to yield the least and Zone 2 the most. This can be seen to some extent in Fig. 4.2.7.2. No other information was available for this field.

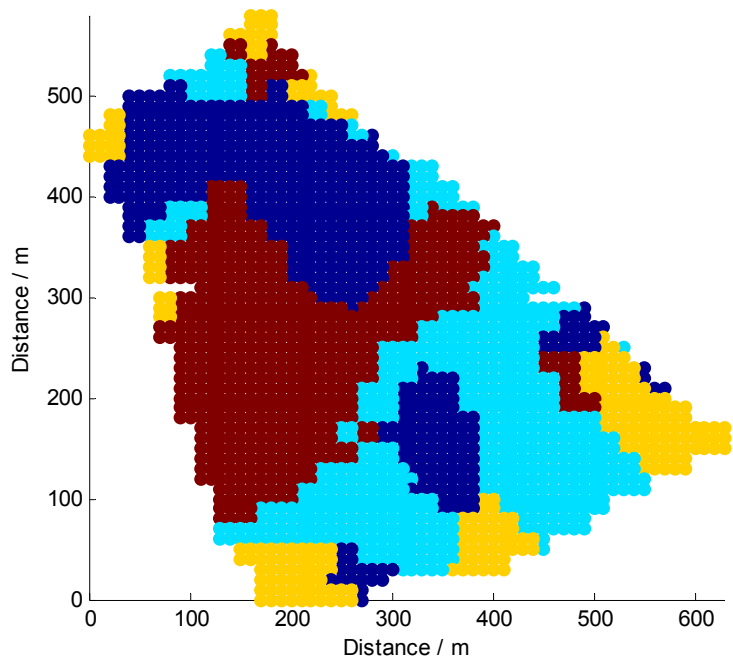


Figure 4.2.7.3 A map showing the cluster classification for Field-HM. Associated centroid values for each zone are show in in Fig. 4.2.7.4. Zone 1 is shown in dark blue, Zone 2 in light blue Zone 3 in yellow and Zone 4 in brown.

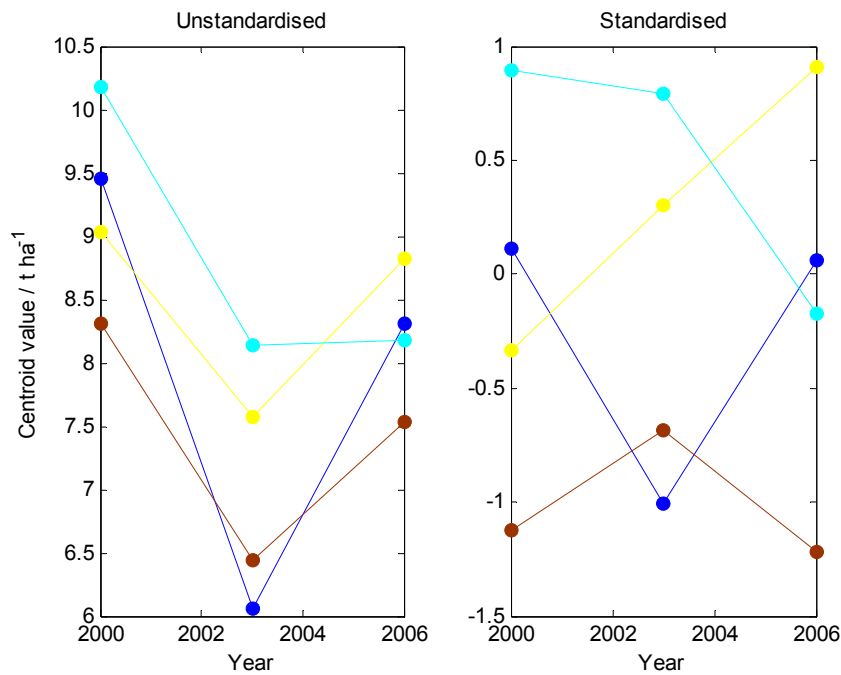


Figure 4.2.7.4. The class centroids across seasons for the cluster classes defined for Field-HM. The centroids are shown in terms of (a) yield (t ha<sup>-1</sup>) and (b) standardised yield. Zone 1 is shown in dark blue, Zone 2 in light blue Zone 3 in yellow and Zone 4 in brown.

#### 4.2.8 Field-HS

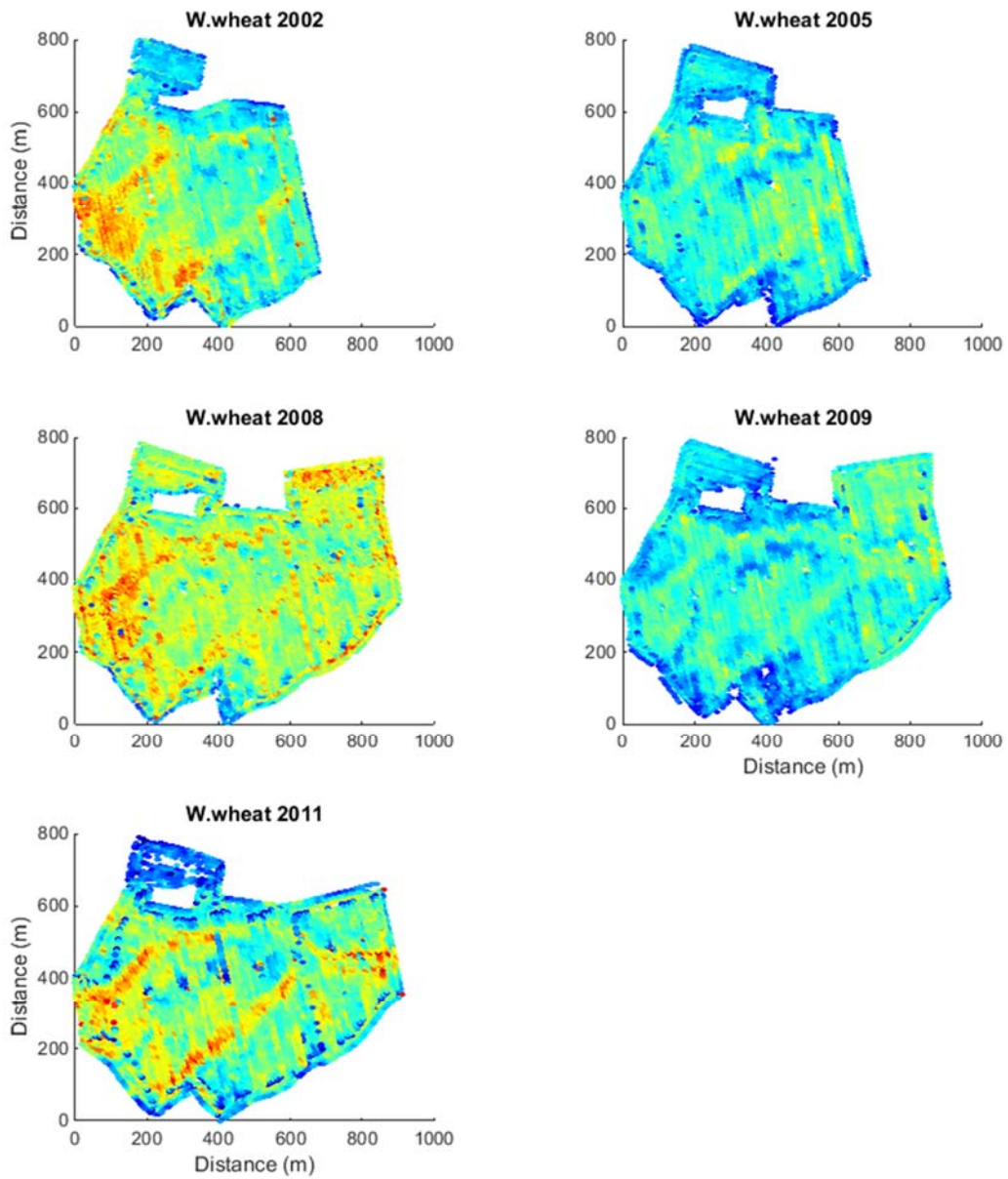


Figure 4.2.8.1. Cleaned yield maps of winter wheat from Field-HS. Note that the maps are of yield monitor data and in some seasons only part of the field was harvested (compare 2011 with 2002,2005,2008 and 2009)

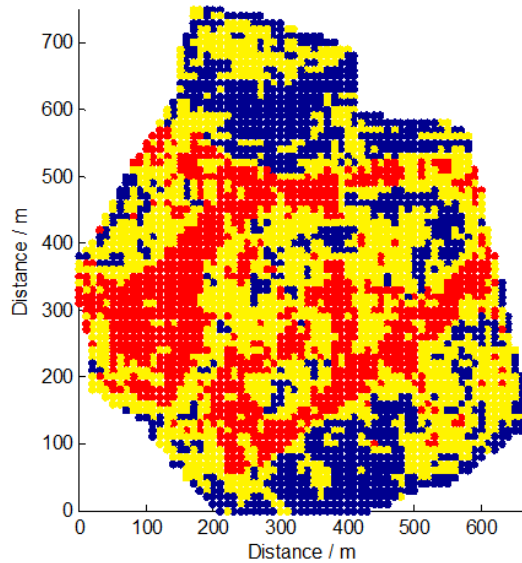


Figure 4.2.8.2. A map showing the areas of Field-HS that yielded better than average (red), worse than average (blue) or changed between better or worse than average between seasons (yellow).

Figure 4.2.8.3 shows the class of maximum membership at sites across the field. These correspond to the class centroids shown in 4.2.8.4. The centroid values show that Zone 2 yields consistently better than Zone 1. There is a broad similarity between the cluster classification and Fig. 4.2.8.2. The summary statistics for P, K, Mg and pH are shown in Table 4.2.8 both for the total population and according to zone. Our REML analysis showed there was no evidence to relate the cluster classification with these soil properties (K –  $\chi^2=0.02$ , 1 df,  $p = 0.881$ , P –  $F_{1,34}=2.57$ ,  $p=0.118$ , Mg – Wald statistic,  $\chi^2=0.04$ , 1 df,  $P = 0.838$ , pH – Wald statistic,  $\chi^2=0.48$ , 1 df,  $P = 0.489$ ). Maps of soil type and elevation did not correspond to the cluster zones and so gave no further insight into the underlying cause for the differences between zones.

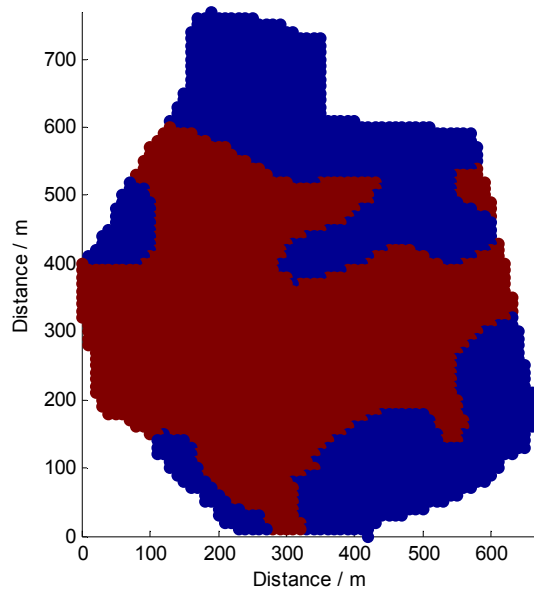


Figure 4.2.8.3 A map showing the cluster classification for Field-HS. Associated centroid values for each zone are show in in Fig. 4.2.8.4. Zone 1 is shown in blue and Zone 2 in brown.

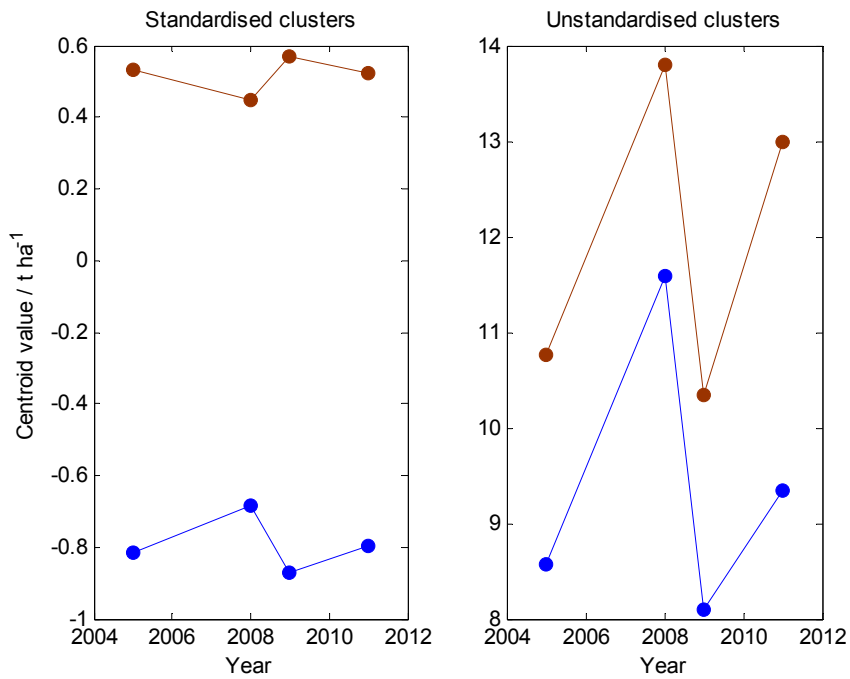


Figure 4.2.8.4. The class centroids across seasons for the cluster classes defined for Field-HS. The centroids are shown in terms of (a) yield ( $t\ ha^{-1}$ ) and (b) standardised yield. Zone 1 is shown in blue and Zone 2 in brown.

**Table 4.2.8 Summary statistics of measurements of P, K, Mg and pH at Field-HS for the total population and according to zone.**

	<b>Mean</b>	<b>Minimum</b>	<b>Maximum</b>	<b>Standard deviation</b>
<b>Potassium</b>				
Total population	156.1	86.15	353.6	55.71
Zone 1	153.9	93.3	242.4	39.64
Zone 2	157.3	86.15	353.6	63.85
<b>Phosphorus</b>				
Total population	26.0	11.6	80	12.08
Zone 1	21.8	14.4	26.6	3.682
Zone 2	28.37	11.6	80	14.43
<b>Magnesium</b>				
Total population	46.95	23.1	83.6	13.45
Zone 1	46.03	23.10	83.60	17.48
Zone 2	47.46	30.9	78.45	10.98
<b>pH</b>				
Total population	7.503	5.88	8.26	0.702
Zone 1	7.518	5.88	8.26	0.788
Zone 2	7.495	5.97	8.19	0.667

4.2.9 Field-LM

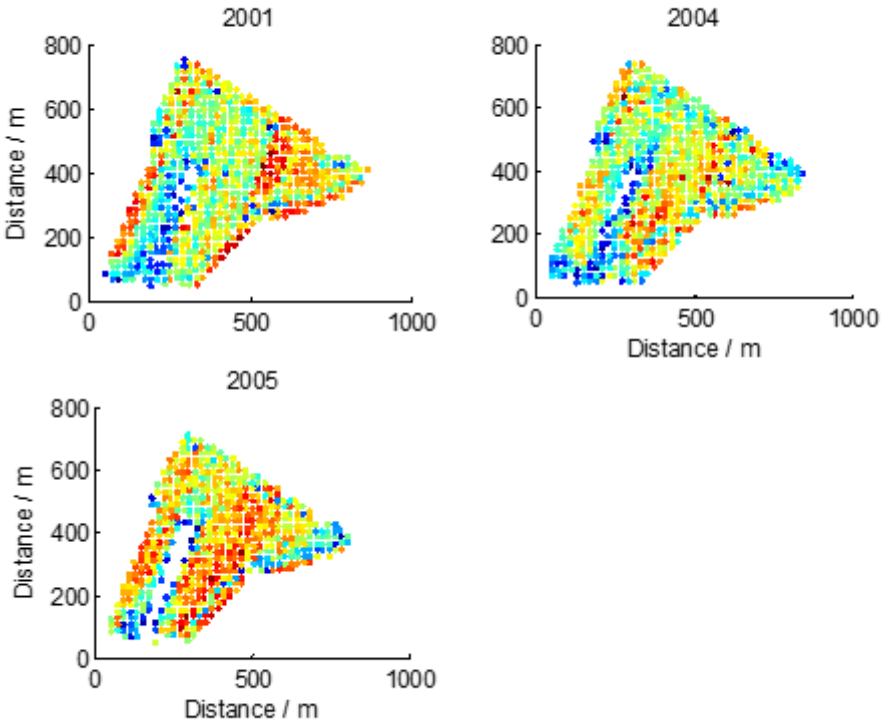


Figure 4.2.9.1 Cleaned yield maps of winter wheat from Field-LM.

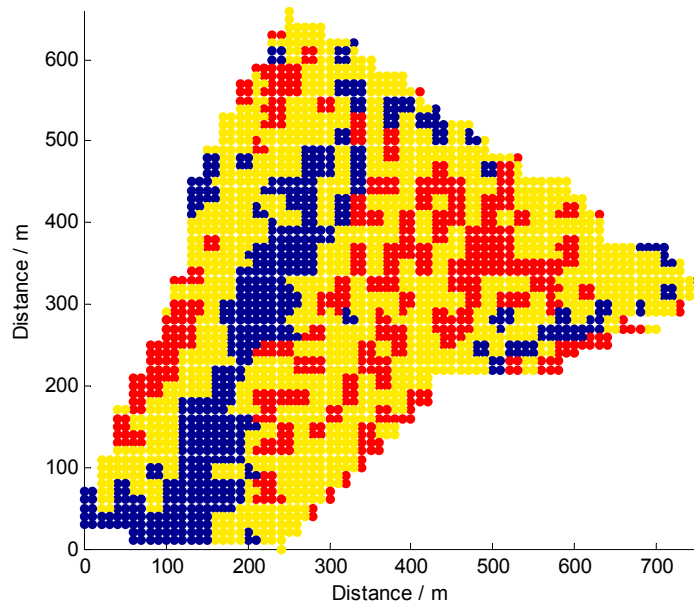


Figure 4.2.9.2. A map showing the areas of Field-LM that yielded better than average (red) in 2001, 2004 and 2005, worse than average (blue) or changed between better or worse than average between seasons (yellow).

Figure 4.2.9.3 shows the class of maximum membership at sites across the field. These correspond to the class centroids shown in 4.2.9.4. The centroid values show that Zone 2 yields consistently better than Zone 1. There is a similarity between the cluster classification and Fig. 4.2.8.2. The summary statistics for P and K are shown in Table 4.2.9, both for the total population and according to zone. Our REML analysis showed there was no evidence to relate the cluster classification with these soil properties ( $K - F_{1,24}=1.80, p=0.192$ ,  $P - F_{1,22.7}=1.87, p=0.185$ ). We had no further information on this field.

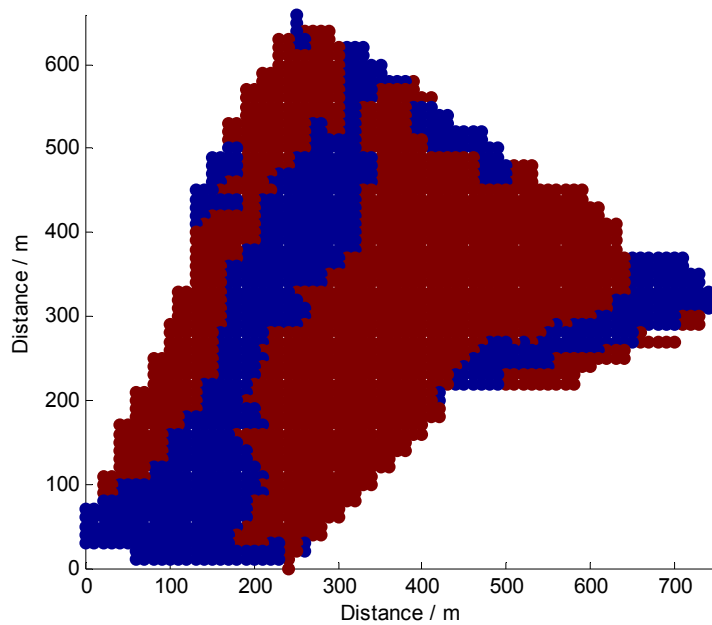


Figure 4.2.9.3 A map showing the cluster classification for Field-LM. Associated centroid values for each zone are shown in Fig. 4.2.9.4. Zone 1 is shown in blue, zone 2 in brown.

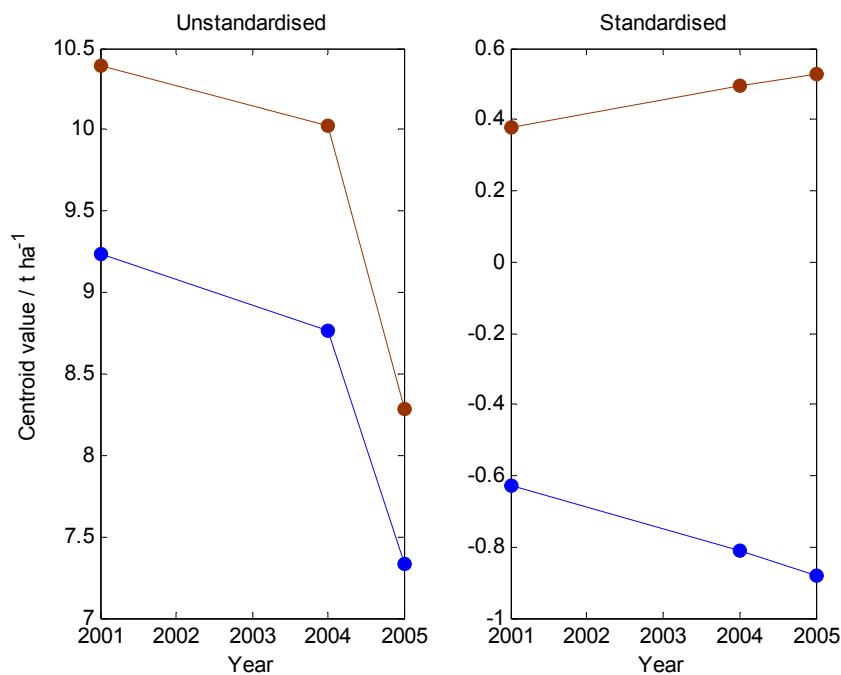


Figure 4.2.9.4 The class centroids across seasons for the cluster classes defined for Field-LM. The centroids are shown in terms of (a) yield (t ha<sup>-1</sup>) and (b) standardised yield. Zone 1 is shown in blue, zone 2 in brown.

**Table 4.2.9 Summary statistics of measurements of P and K, at Field-LM for the total population and according to zone.**

	<b>Mean</b>	<b>Minimum</b>	<b>Maximum</b>	<b>Standard deviation</b>
<b>Potassium</b>				
Total population	141.3	92.85	179.8	24.49
Zone 1	151.7	121.5	176.9	18.02
Zone 2	137.4	92.85	179.8	25.82
<b>Phosphorus</b>				
Total population	28.04	18.8	52.2	6.795
Zone 1	27.2	18.8	37.2	5.654
Zone 2	28.35	20.6	52.2	7.287

#### 4.2.10 Field-PA

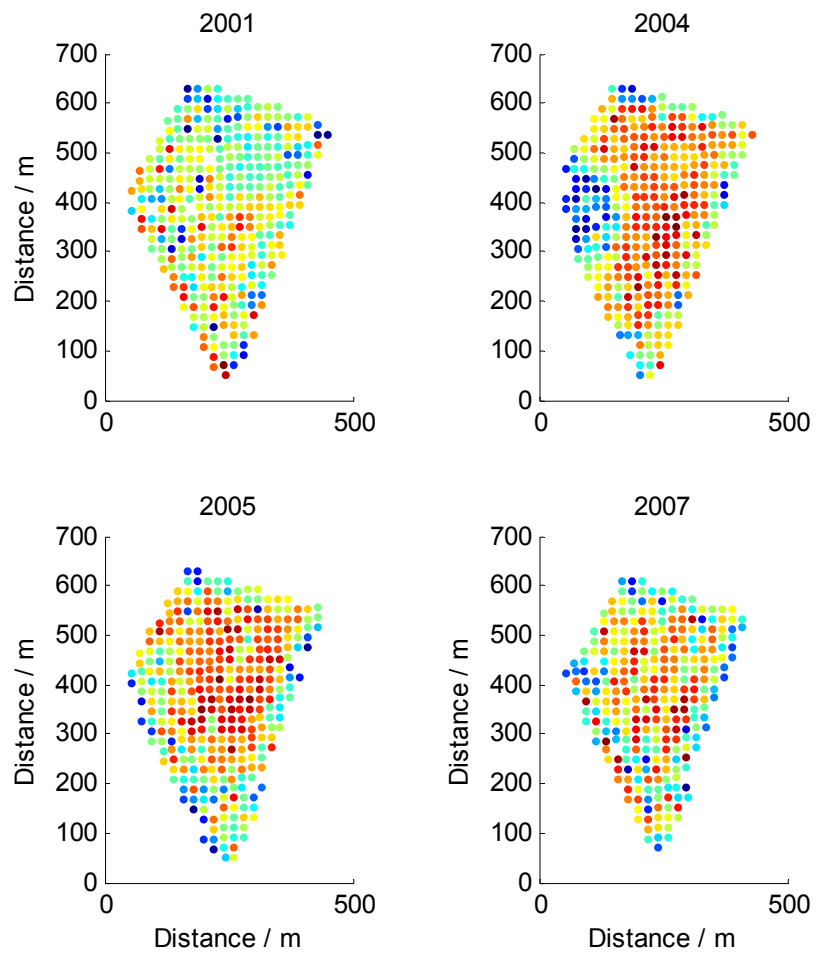


Figure 4.2.10.1 Cleaned yield maps of winter wheat from Field-PA.

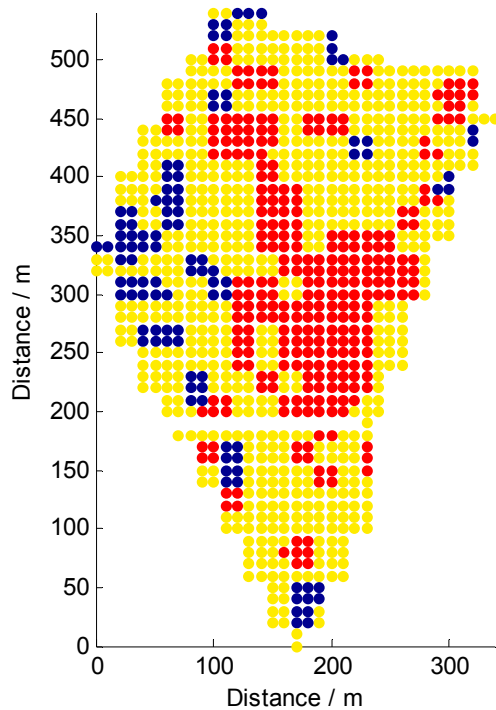


Figure 4.2.10.2. A map showing the areas of Field-PA that yielded better than average (red) in 2004, 2005 and 2007, worse than average (blue) or changed between better or worse than average between seasons (yellow).

Figure 4.2.10.3 shows the class of maximum membership at sites across the field. These correspond to the class centroids shown in 4.2.10.4. The centroid values show that Zone 1 yields consistently better than the other two Zones. Zone 3, which generally relates to the field margins, yields least well except in 2004 when Zone 2 is has a very low yield. There is a broad similarity between the cluster classification and the map produced from the simpler approach (Fig. 4.2.10.2.). We had no further information on this field, but the cause of the lower yields that are associated with the centre of the field in 2004 in Zone 2 are likely to be obvious to the farmer.

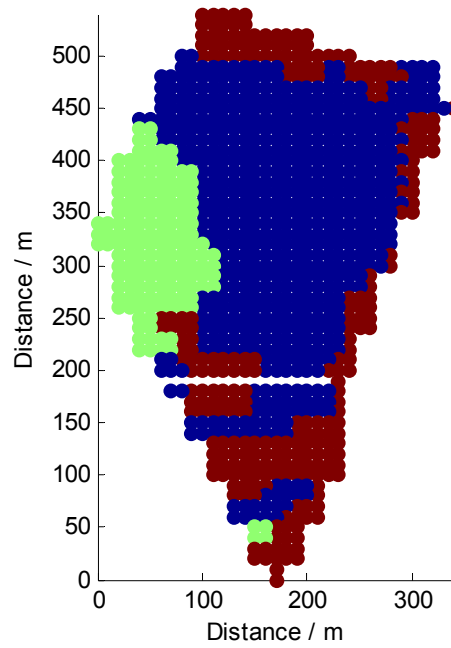


Figure 4.2.10.3 A map showing the cluster classification for Field-PA. Associated centroid values for each zone are shown in Fig. 4.2.10.4. Zone 1 is shown in blue, Zone 2 in green and Zone 3 in brown.

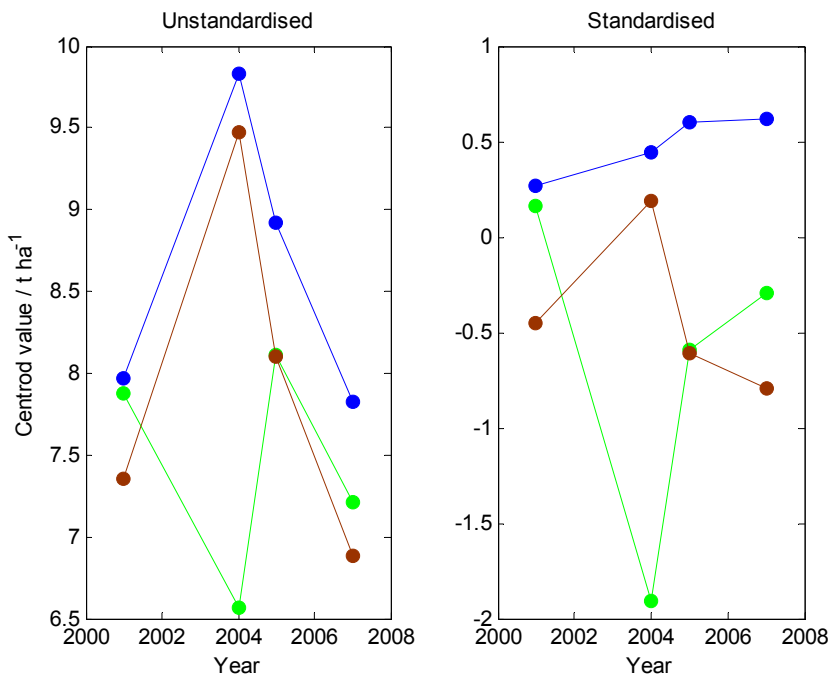


Figure 4.2.10.4. The class centroids across seasons for the cluster classes defined for Field-PA. The centroids are shown in terms of (a) yield (t ha<sup>-1</sup>) and (b) standardised yield. Zone 1 is shown in blue, Zone 2 in green and Zone 3 in brown.

4.2.11 Field-TK

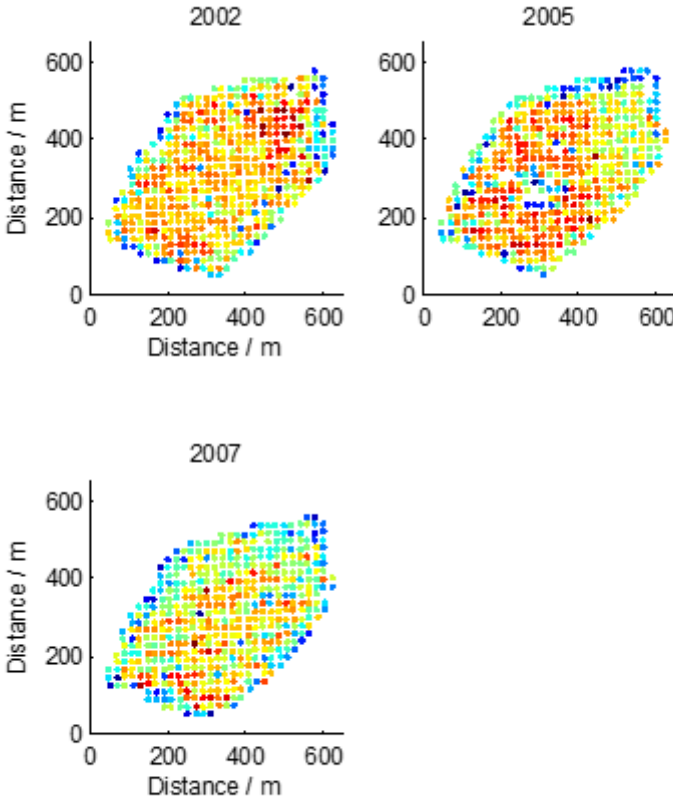


Figure 4.2.11.1 Cleaned yield maps of winter wheat from Field-TK.

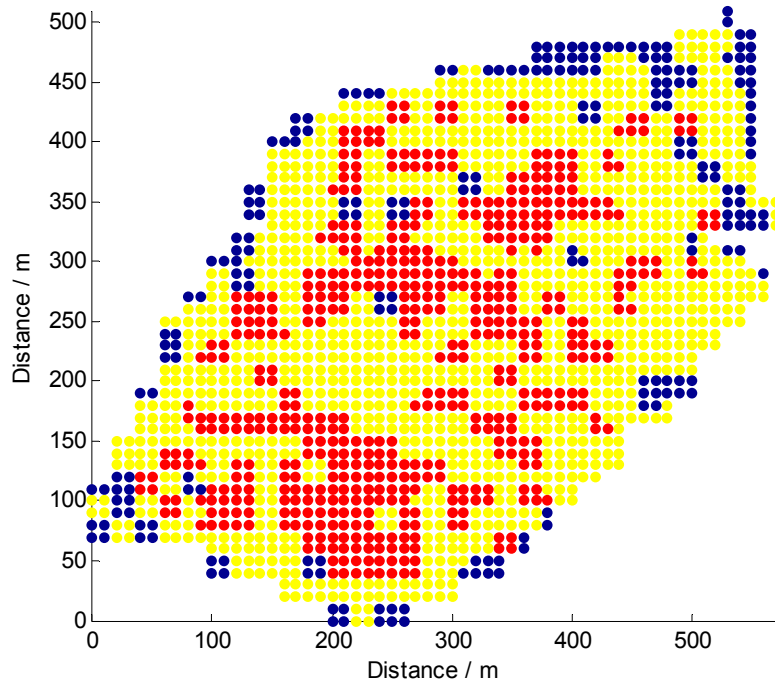


Figure 4.2.11.2. A map showing the areas of Field-TK that yielded better than average (red) in 2002, 2005 and 2007, worse than average (blue) or changed between better or worse than average between seasons (yellow).

Figure 4.2.11.3 shows the class of maximum membership at sites across the field. These correspond to the class centroids shown in 4.2.11.4. This is a simple case where the field margins (Zone 2) yield consistently less well than the field centre.

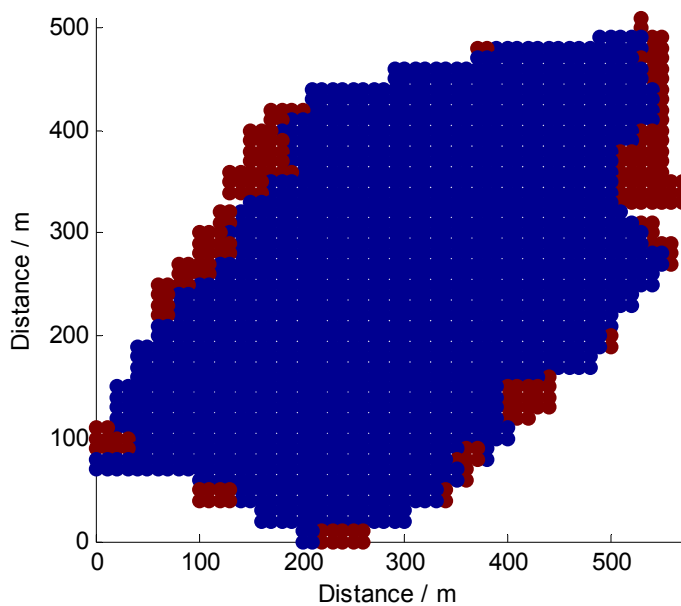


Figure 4.2.11.3. A map showing the cluster classification for Field-TK. Associated centroid values for each zone are shown in Fig. 4.2.11.4. Zone 1 is shown in blue, zone 2 in brown.

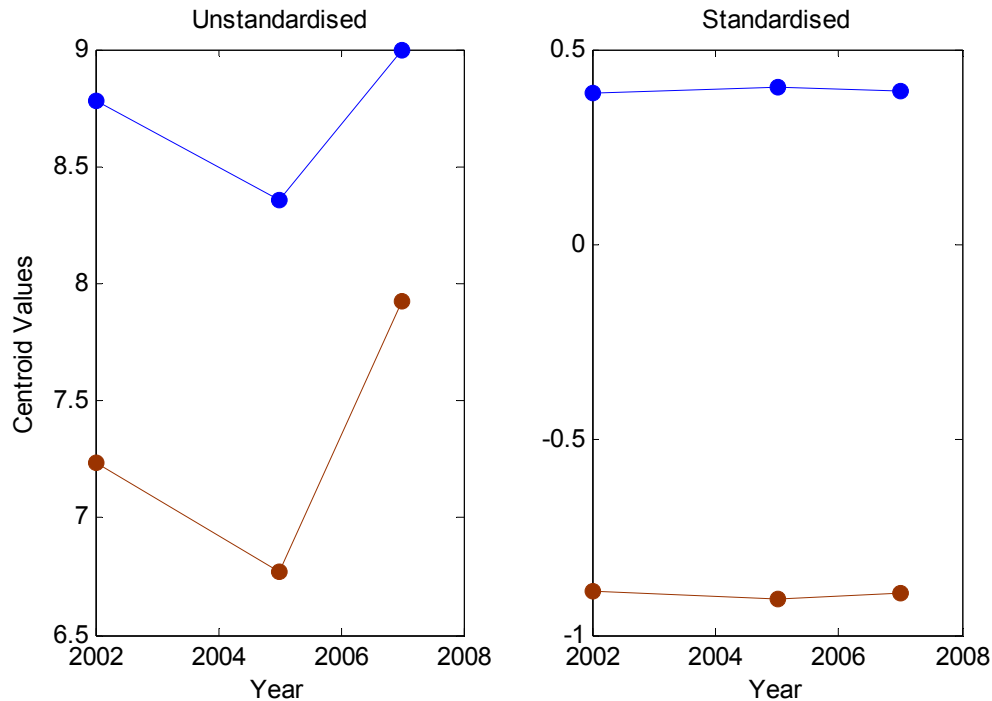


Figure 4.2.11.4. The class centroids across seasons for the cluster classes defined for Field-LM. The centroids are shown in terms of (a) yield (t ha<sup>-1</sup>) and (b) standardised yield. Zone 1 is shown in blue, zone 2 in brown.

### 4.3. Compare measuring soil nutrients by different sampling methods

#### 4.3.1. Comparison of $P$ estimated by the sampling schemes

For each realisation, we computed the difference in profit margin given by the zone-based ( $\Delta_{\text{zone}}$ ) and grid based ( $\Delta_{\text{grid}}$ ) schemes compared with that of the field-based ( $\Delta_{\text{field}}$ ) scheme. Thus, the differences are  $(\Delta_{\text{grid}} - \Delta_{\text{field}})$  and  $(\Delta_{\text{zone}} - \Delta_{\text{field}})$  for the grid-based and zone-based values, respectively. Table 4.3.1 reports the means and standard errors for these differences, which are also shown in Figure 4.3.1. In all cases, the grid-based estimates gave larger profits than did the zone-based estimates. This was largely because the cluster classes were not significant factors in explaining the variation in the nutrients (see Section 4.2 and Appendix 8.3). The smallest differences between the zone-based estimate and the grid-based one were for the fields with the largest differences in mean concentrations of  $P$  between zones (Field-GP and Field-RH). Field-BD had the smallest mean of  $\Delta_{\text{zone}} - \Delta_{\text{field}}$ , and this is likely to result from both the small difference in mean values of  $P$  between the zones,  $s\beta(1)$ ,  $s\beta(2)$  and  $s\beta(3)$ , and the short-range variation (effective range 63.0 m) which is smaller than the distance across feasible management zones. The largest mean profits were for Field-LM and Field-MC which have a long spatial structure with values of  $P$  in a treatable range (i.e. values on the incline of the dose response curve shown in Figure 3.3.2).

The distributions of  $\Delta_{\text{zone}} - \Delta_{\text{field}}$  are more symmetrically distributed than for  $\Delta_{\text{grid}} - \Delta_{\text{field}}$  for all fields except for Field-RH, (as illustrated in Figure 4.3.1). The distributions of  $\Delta_{\text{grid}} - \Delta_{\text{field}}$  are positively skewed. For Field-RH and Field-GP a large number of realisations had values of  $\hat{z}_{\text{field}}$  and  $\hat{z}_{\text{zone}}$  that were not limiting (99% and 66% respectively). This resulted in recommendations of no fertilizer application, and so  $\Delta_{\text{zone}} - \Delta_{\text{field}}$  is simply the difference in sampling costs. These correspond to the large peaks in the distributions of  $\Delta_{\text{grid}} - \Delta_{\text{field}}$ . We also computed the difference in excess fertilizer applied when estimates were based on the zone-based ( $\hat{z}_{\text{zone}}$ ) and grid based ( $\hat{z}_{\text{grid}}$ ) sampling schemes compared with the field-based ( $\hat{z}_{\text{field}}$ ) scheme. We define excess fertilizer as the amount applied over and above that which would have been applied if we had perfect knowledge of the true variation in P across the field. Table 4.3.1 reports the means and standard error for these differences ( $\hat{z}_{\text{zone}} - \hat{z}_{\text{field}}$ ) and ( $\hat{z}_{\text{grid}} - \hat{z}_{\text{field}}$ )

There was no consistent pattern to the mean responses. In some fields (Field-ER, Field-GP and Field-RH) the field-based sampling resulted in less of an excess than the zone-based sampling with positive differences and in some fields (Field-BD, Field-GP and Field-RH) the field-based sampling resulted in less of an excess than the grid-based sampling (Table 4.3.1). Similarly there was no consistent pattern between grid- and zone-based sampling.

#### *4.3.2. Assessing the extent to which yield maps can be used to predict the most appropriate sampling scheme*

The parameters for the models fitted by multiple linear regressions are listed in Table 4.3.2 along with percentage of explained variance. For Field-GP, Field-MC and Field-RH the regression model was fitted to the subset of realisations where  $\hat{z}_{\text{field}}$  or  $\hat{z}_{\text{zone}}$  were limiting. The models fitted to  $\Delta_{\text{zone}} - \Delta_{\text{field}}$  explained very little of the variation in the data. The variation in  $\Delta_{\text{grid}} - \Delta_{\text{field}}$  was better explained, although the value for Field-BD were still small. The realisations for this site were generated from the model with a small effective range and the nugget to sill ratios of the realisations were in general larger than other sites (at least 37% larger, data not shown) indicating a relatively large component of unstructured variance.

Table 4.3.1. Simulated field averages of soil P concentrations with the average difference in net profit for zone- and grid-based sampling compared with the field-based across all simulations.

Fields	The range of simulated field averages of P (mg kg <sup>-1</sup> )	Mean net profit (£ ha <sup>-1</sup> )				Mean excess nutrient (kg ha <sup>-1</sup> )			
		Zone – Field		Grid – Field		Zone – Field		Grid – Field	
		profit	SE	profit	SE	Excess nutrient	SE	Excess nutrient	SE
Field-BD	19-21	-13	0.81	12.1	0.75	-2.49	0.17	1.07	0.17
Field-ER	17-25	0.93	0.23	14.8	0.21	0.14	0.11	-1.9	0.10
Field-GP	48-131	2.6	0.36	10.3	0.46	0.14	0.02	0.64	0.02
Field-LM	22-30	12.9	1.2	57.7	1.4	-2.7	0.22	-0.35	0.22
Field-MC	7-34	16.7	1.05	46.9	1.11	-2.06	0.16	-0.10	0.16
Field-RH	81-90	-0.18	0.05	2.4	0.08	0.07	0.01	0.98	0.01

Table 4.3.2. The percentage variance accounted for and model parameters for the multiple linear regression models (Equation 17) fitted to the  $\Delta_{\text{zone}} - \Delta_{\text{field}}$  and  $\Delta_{\text{grid}} - \Delta_{\text{field}}$  data

Field name	Model Parameters				Percentage variance accounted for
	b0	b1	b2	b3	
Zone sampling					
Field-BD	-7.61	-0.1907	-7.82	0.1552	0.1
Field-ER	-2.072	-0.0082	4.275	-0.00428	2.1
Field-GP*	-7.2	0.018	12.53	-0.0075	16.0
Field-LM	-4.03	0.0008	3.882	0.00084	6.7
Field-MC	-17.4	0.253	11.61	-0.0378	3.8
Field-RH*	189.64	-1.55	-25.98	0.25	10.2
Grid Sampling					
Field-BD	6.01	-0.013	-10.03	0.2322	0.5
Field-ER	5.762	0.00653	6.629	0.01229	18.7
Field-GP	-8.065	-0.00326	5.3	0.02439	50.2
Field-LM	-9.03	0.1492	10.046	-0.00218	33.9
Field-MC	4.6542	-0.0205	-1.0646	0.0049	45.0
Field-RH	-7.117	0.09547	1.3406	0.01446	21.9

\*Model only fitted to realisations where estimated P was limiting

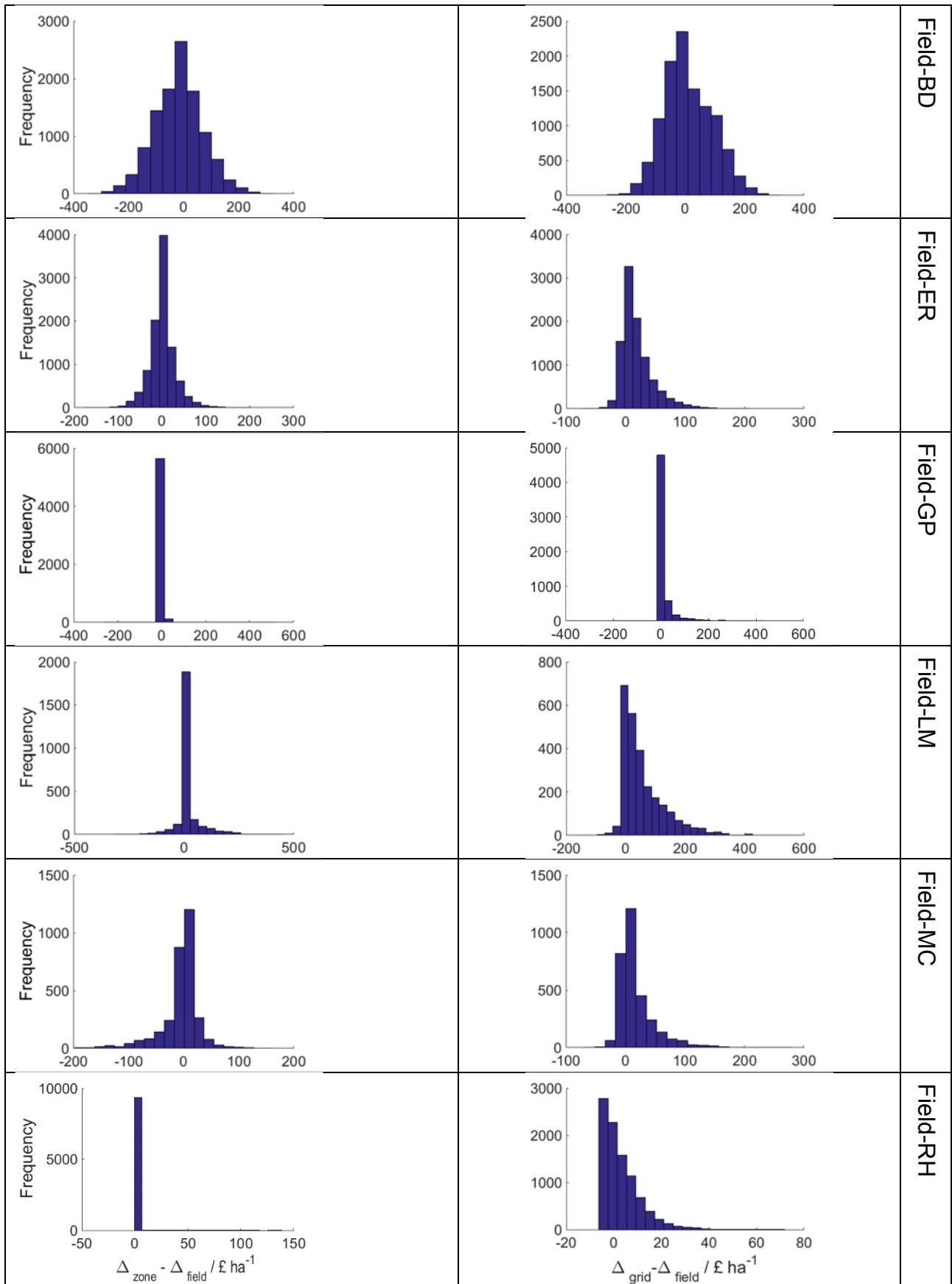
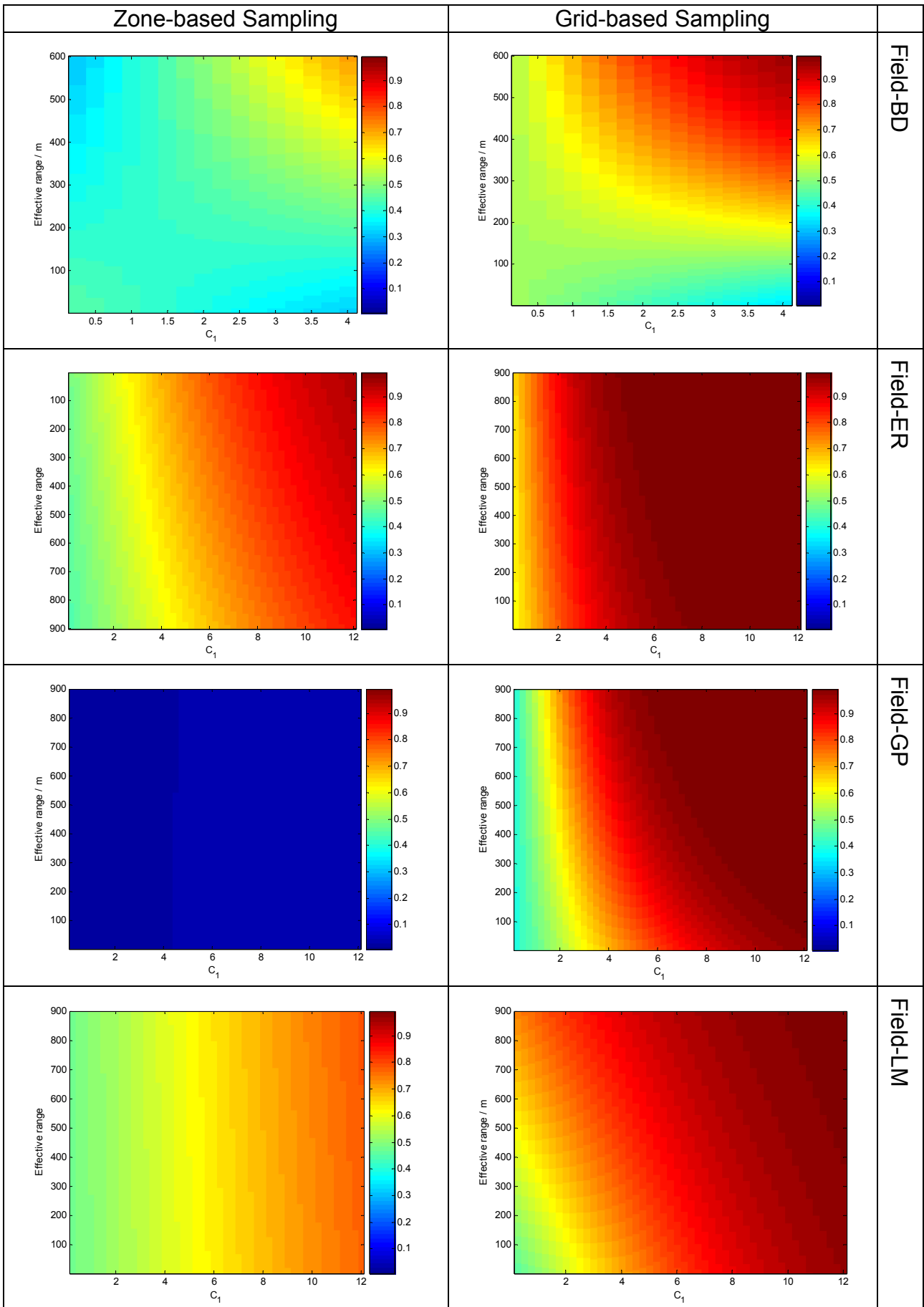


Figure 4.3.1. Histograms of  $\Delta_{\text{zone}} - \Delta_{\text{field}}$  and  $\Delta_{\text{grid}} - \Delta_{\text{field}}$



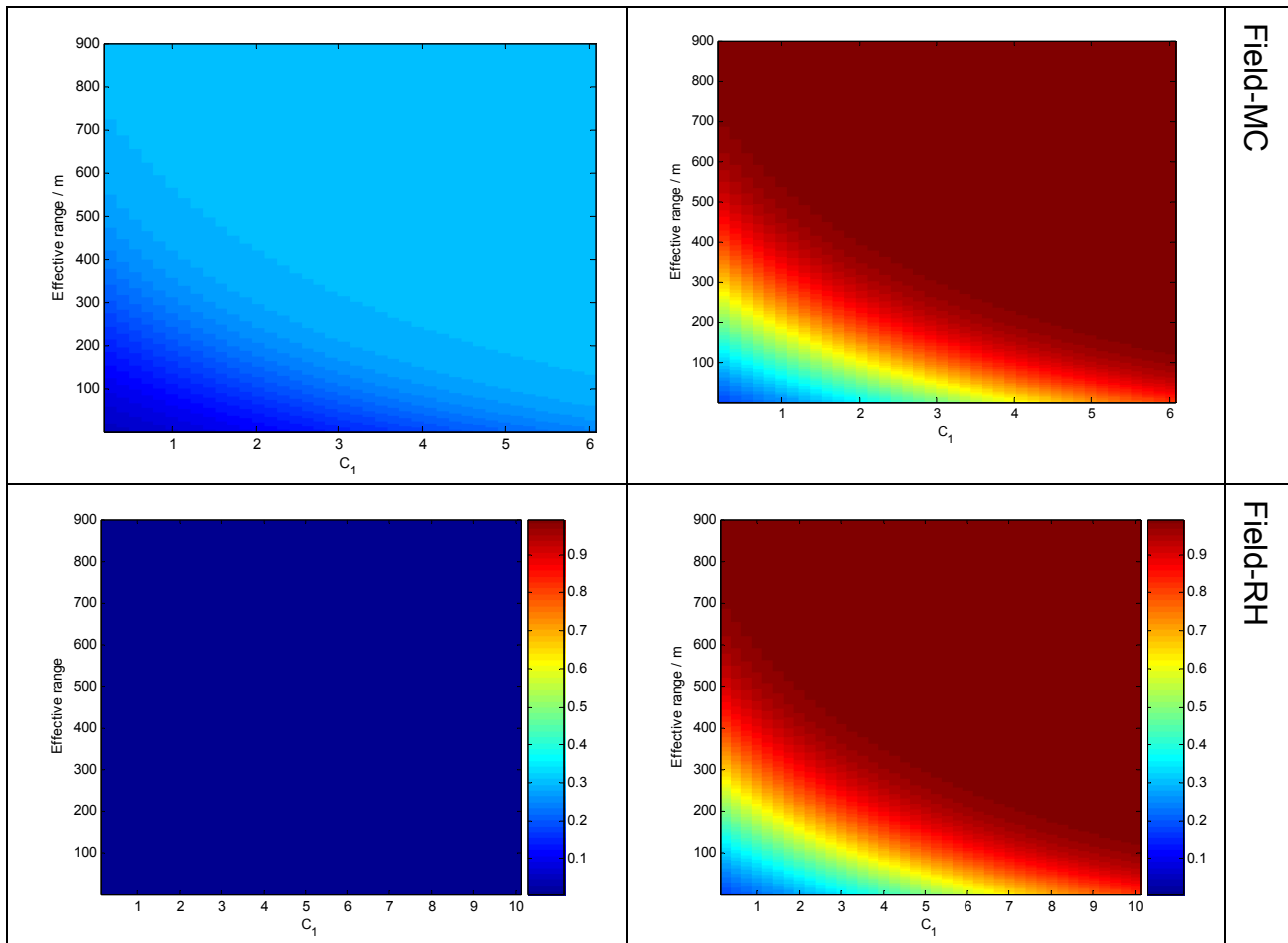


Figure 4.3.2. Maps showing the probability that zone-based and grid-based sampling are more profitable than field-based sampling.

Figure 4.3.2 shows the probability that  $\Delta_{\text{zone}}$  and  $\Delta_{\text{grid}}$  are larger than  $\Delta_{\text{field}}$ . In all cases the probability increases with both  $c_1$  and the effective range ( $3a$ ). This is also true of  $\Delta_{\text{zone}} - \Delta_{\text{field}}$  for Field-GP and Field-RH, but these sites are dominated by simulations where  $\hat{z}_{\text{field}}$  and  $\hat{z}_{\text{zone}}$  were not limiting, and so the effects are negligible. The multiple linear regressions showed that the effective range and  $c_1$  explained very little of the variation in the excess fertilizer data,  $\hat{z}_{\text{zone}} - \hat{z}_{\text{field}}$  and  $\hat{z}_{\text{grid}} - \hat{z}_{\text{field}}$  (Table 4.3.3).

Table 4.3.3. The percentage variance accounted for and model parameters for the multiple linear regression models (Equation 17) fitted to the  $\hat{z}_{\text{zone}} - \hat{z}_{\text{field}}$  and  $\hat{z}_{\text{grid}} - \hat{z}_{\text{field}}$  data.

Field name	Model Parameters				Percentage variance accounted for
	b0	b1	b2	b3	
Zone sampling					
Field-BD	-1.660	-0.0116	-1.079	0.01682	0.0
Field-ER	2.117	-0.00997	-0.843	0.00362	0.3
Field-GP*	0.54	0.00007	0.711	-0.00191	1.5
Field-LM	0.884	-0.00276	-0.761	0.000096	6.9
Field-MC*	6.21	-0.0044	-3.373	0.00874	13.0
Field-RH*	6.89	0.012	-0.261	0.01548	1.1
Grid Sampling					
Field-BD	0.139	0.0121	-0.363	0.00785	0.0
Field-ER	5.762	0.00653	6.629	0.01229	0.4
Field-GP	-0.0935	0.001977	0.3965	0.000888	12.6
Field-LM	1.796	0.00439	0.441	-0.001309	6.0
Field-MC	3.716	-0.00554	-1.104	0.001731	8.4
Field-RH	3.1403	0.00735	0.1193	0.00828	3.0

\*Model only fitted to realisations where estimated P was limiting

#### 4.4. Usefulness of yield maps to manage soil variation at the scale of soil management zones

##### 4.4.1. Potential for variable rate (PVRM) based on Lark et al. (2003)

For each one of the fields, we calculated the variance ratio (VR) and standard deviation (SD) for the winter wheat yield monitor files across different years and used the average to calculate the PVRM rank for each field (Table 4.4.1) using the decision tree (Figure 3.4.2). In this study, more than half of the fields have a PVRM rank of 3 with average VR values of greater than 2.0. The remaining fields have a PVRM rank of 2 or 1 depending on the average VR, average SD and average NCE according to the decision tree in Figure 3.4.2. Detailed results of the PVRM analysis for each of the fields for different years are given in the Appendix 8.4.

Table 4.4.1. PVRM parameters for different fields

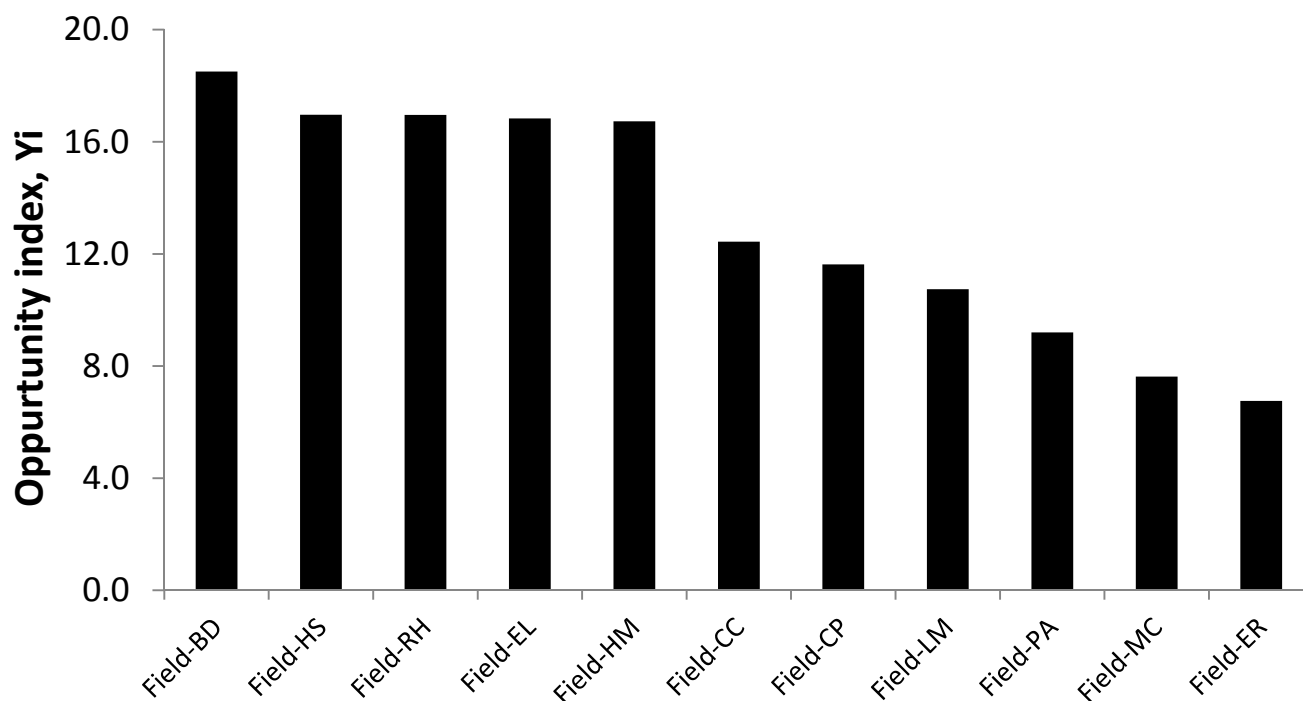
Field	Average effective range	Average NCE	Average SD	Average VR	PVRM rank
Field-BD	310.0	0.15	0.7	2.3	3
Field-CC	174.3	0.17	1.2	2.2	3
Field-CP	204.3	0.33	0.9	2.4	3
Field-ER	65.2	0.38	0.8	1.9	1
Field-EL	322.1	0.22	1.2	2.5	3
Field-HM	402.2	0.24	0.5	1.5	1
Field-HS	312.4	0.17	1.5	2.6	3
Field-LM	191.7	0.17	0.6	1.7	1
Field-MC	154.0	0.12	0.7	1.5	3
Field-PA	252.5	0.26	0.52	2.0	3
Field-RH	395.8	0.13	0.6	1.5	1

#### 4.4.2. Opportunity index ( $Y_i$ )

The Opportunity index (i.e. the presence of spatial variation which can be managed) was calculated for each field across different years using the magnitude ( $M_v$ ) and the spatial structure ( $S_v$ ) of yield variation and are given in Appendix 8.5. Field-HS gave the highest average coefficient of variation ( $aC_v$ ) (13.4) followed by Field-BD (11.4), Field-EL (11.3), Field-CC (10.8) and the remaining fields (Table 4.4.2). The median  $aC_v$  ( $aC_{v50}$ ) over all the fields was 10. The average  $Y_i$  for different fields calculated using the  $Y_i$  for different years ranges from 6.8 to 18.5 with a mean of 13.0 (Table 4.4.2). The fields are arranged in the order of their decreasing  $Y_i$  in Figure 4.4.1. The highest  $Y_i$  is for Field-HS and the lowest is for Field-ER.

Table 4.4.2. Opportunity index for different fields

Field	Average mean yield ( $\bar{y}$ )	Average Coefficient of variation ( $aC_v$ )	Average magnitude of variation ( $M_v$ )	Average Spatial structure of the yield variation ( $S_v$ )	Average opportunity index ( $Y_i$ )
Field-BD	7.6	11.4	1.1	258.3	17.0
Field-CC	11.1	10.8	1.1	145.3	12.4
Field-CP	10.6	8.8	0.9	170.2	11.6
Field-ER	10.3	8.7	0.9	54.3	6.8
Field-EL	10.1	11.3	1.1	268.3	16.8
Field-HM	8.2	8.4	0.8	335.3	16.7
Field-HS	11.2	13.4	1.3	260.5	18.5
Field-LM	8.9	7.4	0.7	159.8	10.7
Field-MC	10.4	8.2	0.8	75.8	7.6
Field-PA	8.2	8.2	0.8	149.1	10.7
Field-RH	7.8	8.7	0.9	330.0	17.0
<b>Mean</b>	<b>9.5</b>	<b>9.6</b>	<b>1.0</b>	<b>197.9</b>	<b>13.1</b>



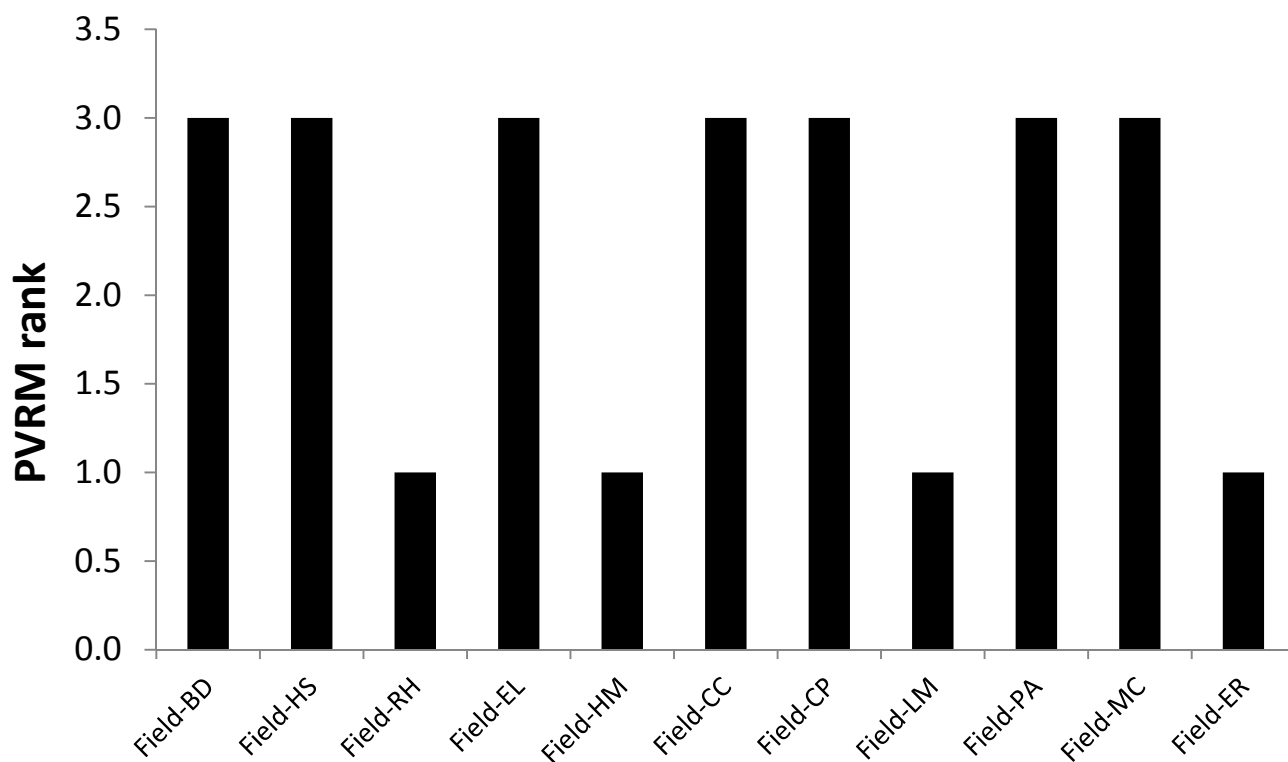


Figure 4.4.1. Opportunity index ( $Y_i$ ) and PVRM ranks for each field in the descending order of  $Y_i$ .

Comparing the results from the method by Lark et al. (2003) with the opportunity index, we see that they do not accord exactly. To explore this further we considered the ratio of dispersion variances (VR) for each site (Figure 4.4.2). Here we see some broad agreement between the two methods with the smaller ratings for two methods given to Field-LM, Field-PA, Field-MC and Field-ER. The two obvious exceptions are Field-RH and Field-HM, which have a small VR and a large opportunity index. Closer inspection shows that the value for the opportunity index is inflated by the large range that affect the  $S_v$  values for these sites.

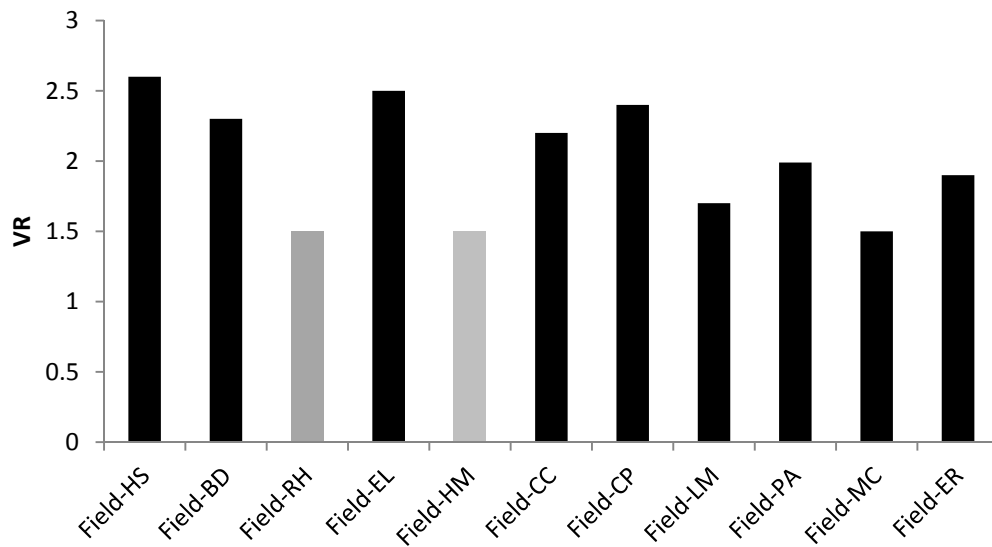


Figure 4.4.2. The average ratio of dispersion variance ( $VR$ ) for each field in the descending order of  $Y_i$ .

#### 4.4.1. Variable Rate Management Score

Our analysis showed that out of the five metrics (Table 4.4.1) we proposed, the best for explaining the variation in profit from variable rate management was

$$M_s = c_1 \log(r)$$

We note that the results in Table 4.4.1. are from simulations based on the scaled variation in the fields and so do not represent the true variation as quantified in Figure 4.4.3. The results from this metric are shown in Figure. 4.4.3. This score had a similar trend to the opportunity index with Field-LM, Field-PA, Field-MC and Field-ER scoring lower values. Under this system the scores of Field-RH and Field-HM gave a lower ranking than they achieved with the opportunity index.

Table 4.4.1. The percentage variance in profit from variable rate management accounted for by each of the metrics for the potential for variable rate management.

Fields which simulations were based on	$rc_1$	$V_R S_B$	$c_1 \sqrt{r}$	$V_R \sqrt{S_B}$	$c_1 \log(r)$
Field-BD	0.2	0.4	0.1	0.3	0.1
Field-LM	31.5	33.4	34.7	29.9	35.6
Field-MC	42.5	21.3	44.5	10.9	44.2
Field-ER	19.2	15.6	21.8	15.6	22.3
Field-GP	45.5	38.1	46.2	19.1	46.3

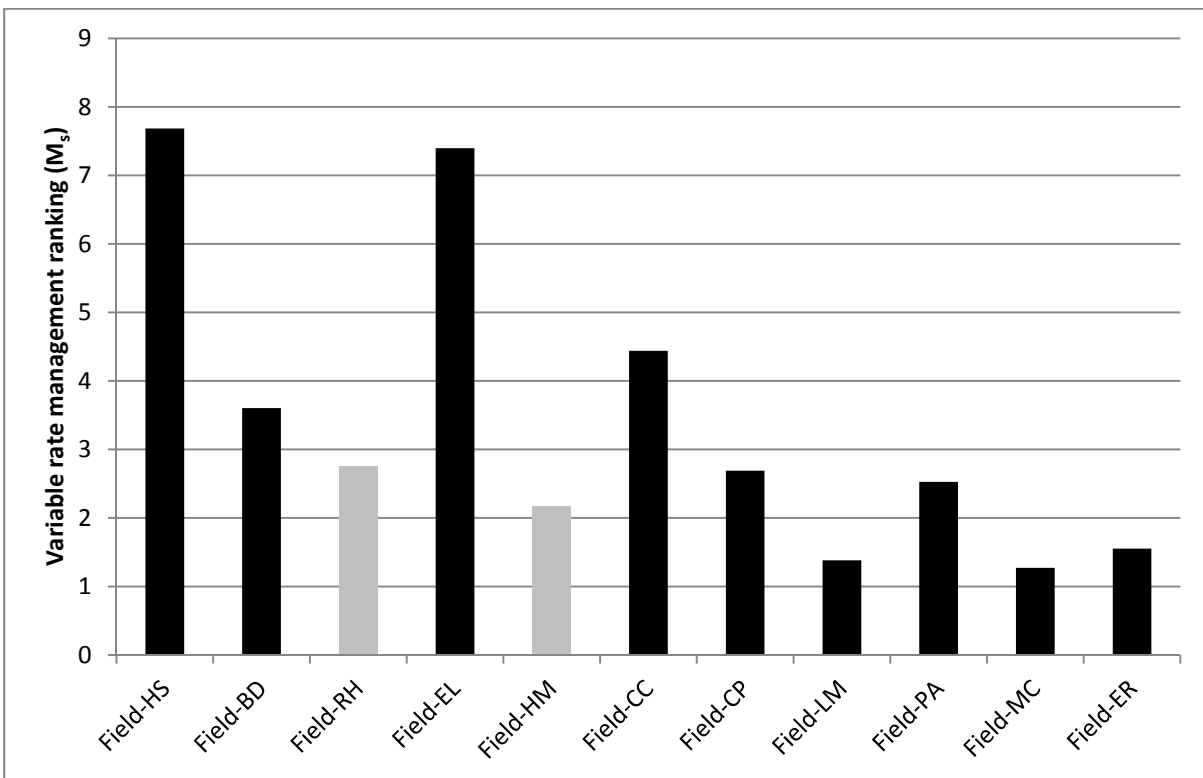


Figure 4.4.3. Variable rate management ranking ( $M_s$ ) for each field in the descending order of  $Y_i$ .

## 5. Discussion

### 5.1 Comparison of yield cleaning software

A good yield cleaning program should have a balance of removing the outliers and artefacts without losing the information on the variation in the field. From the results of the above case studies Yield

Editor, Auto-N and ROTH-YE tend to remove fewer points than the Sun *et al.* (2013), which has a local standard deviation filter to remove local outliers. This removes fine scale variation that other methods preserve including some artefacts that are obvious on visual inspection such as the line of low yielding values in Figure. 4.1.2.

The projections in Yield Editor (Sudduth and Drummond, 2007) and the program by Sun *et al.* (2013) that are used to transform longitude and latitude to Easting and Northing are unsuitable for the UK as maps of the yield become distorted. For Yield Editor there is the additional issue that our raw monitor data (which is typical of that which UK farmers would collect) was not in the correct format. Yield was not recorded in terms of flow rate and the units were recorded as metric values than imperial. Additionally in our files there was no information on pass number and so we had to estimate this from other data. All of these factors led us to conclude that neither Yield Editor nor the program by Sun *et al.* (2013) were suitable for use by UK farmers.

Both the yield-monitor cleaning program developed for the Auto-N project and the program developed in this project (Roth-YE) are suitable for UK conditions and give reliable results. The Auto-N program was developed in Excel for scientists to analyse data, and was not developed for wider use. Therefore, although it is a sound approach it is not user friendly and the parameter values are fixed. Roth-YE is based on similar algorithms to the Auto-N code and so unsurprisingly gave similar results. The main advantages of Roth-YE are that it contains a novel flow delay filter and it allows the user to inspect the data and change default filter settings using it's easy to use interface. Our results suggest that Roth-YE could be improved further by including a local standard deviation filter such as the one described in Sun *et al.* (2013).

Commercially available software developed for inspecting yield monitor data often smooths the yield monitor data producing an attractive map of variation. Whilst this has its place and can be useful to farmers, often important variation is lost through the process. A free-ware program similar Roth YE (updated to include a local standard deviation filter) would therefore be of value to farmers as it only removes suspect data points and so retains a lot more of the actual variation in the yield that is important for further analysis such as classification of management zones or assessing field variation and so the potential for variable rate management.

## **5.2 Delineating management zones to understand the causes of yield variation**

When yield mapping first started it was expected that parts of the field would consistently yield well, while others would yield less well. This was shown often not to be the case (Blackmore *et al.*, 2003). Therefore a method such as smoothed fuzzy k-means cluster analysis is ideally suited to delimiting management zones from yield monitor data. It produces zones which are generally spatially coherent and internally homogeneous. The great advantage of this method over those that identify zones that

always yield better or worse than average is that it is able to detect zones within which the points vary similarly from season to season. This allows us to detect areas that, for example, might be prone to drought and so do well in wet years but not in dry years.

In the examples we considered, very few of the zones were related to differences in the measured soil nutrients, which was not surprising because our data came from well managed fields. In some cases, there was evidence that the zones were driven by water availability but we were unable to do further exploration to confirm this.

In practice, classifying the field into zones that vary distinctly from one another is useful for farmers, as it helps them to identify differences in response across the field and quantifies the magnitude of these. Where zones are distinct (quantified by the normalized classification entropy) and yield differences between zones substantial, the farmer should seek an understanding of the causes so that he or she can adjust management practices accordingly. These causes may be obvious to the farmer or require further investigation, for example by soil sampling.

### **5.3 Compare measuring soil nutrients by different sampling methods**

We have investigated, through simulation, the cost-effectiveness of three management scales and sampling strategies commonly used to guide fertilizer recommendations. We aimed to see if the variation captured in yield monitor data could be used to determine which sampling strategy would be best in any given situation. We have shown that the advantages of using grid- and zone-based sampling strategies over field-based ones vary from field to field. In our simulations, on average, the grid-based sampling performed better than the zone-based sampling. This was largely because the underlying zones were largely not driven by variation in P, which is likely to be the case for many fields in the UK. In practice, many farmers would be able to explain the observed differences between proposed management zones and so be able to predict whether the zones were determined by differences in nutrient availability. This would provide valuable information on whether zone-based sampling was sensible.

The probability of grid-based sampling being more profitable increases with both increases in the effective range and sill variance,  $c_1$  of the nutrient measurements. Larger values of  $c_1$  imply large variability of nutrients, and a farmer might wish to apply fertilizer differentially in accord. This is feasible in practice only if the effective range is also large, and for two reasons. One is the difficulty of varying the application at a fine scale; the other is the cost of sampling and soil analysis on grids fine enough to map the concentration of the nutrient in the soil. Our results are based on current (2016) prices of wheat and fertilizer and sampling costs, which are subject to variation. Therefore the absolute values shown should not be applied in other contexts, although the principles hold.

## 5.4 Usefulness of yield maps to manage soil variation at the scale of soil management zones

We compared three methodologies that use yield maps to indicate whether a given field is suitable for variable rate management. All of these methods aim to determine whether fields have large enough variation for variable rate management to be cost effective and whether the variation is at a scale large enough to be managed. To do this all three approaches use metrics of the variogram of the yield monitor data. The variogram gives an excellent summary of the yield variation but the question is how best to use it to inform on the potential for variable rate management.

Lark *et al.* (2003) used two metrics of the variogram in their decision tree. The first was a variance ratio ( $VR$ ) that compares the dispersion variance in a 1ha block with the variance in a 0.01 ha block. If the variation in the yield is totally unstructured (i.e. the variogram is all nugget) then the ratio is one (its minimum value). The larger the ratio the stronger the spatial structure. This measure depends on the ratio of the sill to nugget and the range. The second is a standard deviation measure that quantifies the structured variation (which depends on the  $c_1$  parameter of the variogram). We note that Lark *et al.* (2003) decision tree was not designed to be used standalone but with expert knowledge and that some of the decision nodes are counterintuitive. We ranked each of our fields for its potential for variable rate management (PVRM) based on the approach of Lark *et al.* (2003). Out of the 11 fields studied, more than half of the fields had a rank of 3 and had a potential for variable rate management.

The measures that Pringle *et al.* (2003) use are essentially a measure of the structured variation ( $M_v$ ) and so similar to Lark *et al.*'s standard deviation and a measure of the range ( $S_v$ ). All other factors in the Pringle *et al.*'s approach (e.g. the characteristics of the variable rate machinery) are likely to be consistent between a single farmer's fields. We calculated an opportunity index ( $Y_i$ ) for variable rate management (Pringle *et al.*, 2003; de Oliveira, 2009) for each field. The larger the value of  $Y_i$  the greater the scope for variable rate management. We observed that the dependence of one of the metrics ( $S_v$ ) on the range parameter tended to over-inflate the ranking of fields with large range although they had only small variation (e.g.: Field-HM, Field-RH). De Oliveira (2009) propose that a value above 6.0 shows the field is suitable for variable rate management. According to this criterion, all of the fields we have considered in this study can be considered for variable rate management as the  $Y_i$  value ranges from about 7–19. However, it is not clear whether this critical value is country specific and so not suitable for the UK.

It is very difficult to determine thresholds for the variogram metrics over which variable rate management would be cost effective. This is both because of changes in costs of management, and because (as we showed in section 4.3) there is no consistent relationship between the variogram

parameters and profitability between fields (see Figure 4.3.2) because each field's variation will be driven by a combination of slightly different factors. Sun *et al.* (2013), who also use this methodology, suggest the farmer ranks his or her fields based on  $Y_i$  and we believe that this is a more pragmatic approach.

The metric that we propose, the variable rate management score ( $M_s = c_1 \log(r)$ ), combines the  $c_1$  parameter with the range of the variogram ( $r$ ). A small value of  $c_1$  would indicate that the variation was too small for variable rate management to be worthwhile, whilst a small range would indicate that variable rate management was impractical. This metric accords reasonably well with the rankings given by the opportunity index, but does not overinflate the scores of fields that have variograms with a large range yet small variances. Of those metrics we considered,  $M_s$  seems to be the most reliable for ranking fields for the potential for variable rate management. We caution that a large score does not necessarily indicate that variable rate management is cost effective, only that the farmer would be wise to try and understand the causes of the observed variation to see if it could be managed more efficiently.

## 6. Conclusions

Field data on crop yields and soil properties from a number of farms in the UK were collated in this study to investigate the potential of yield maps for informing farm management decisions. Yield monitor data contain useful information on the variability of the field, but, often contain noise associated with artefacts and random errors. Yield cleaning software can eliminate these erroneous data. ***ROTH-YE developed in this project, specifically to clean the yield data from UK farms, is equivalent to or better than any of the other yield cleaning software we considered, although could be improved further by the addition of a filter to remove local outliers.***

Cleaned yield data were used to create management zones whose yields varied distinctly from one another. In only a few of the fields we studied were the zones related to differences in the measured soil nutrients. This may have been because much of our data came from well-managed fields. In some instances, there was evidence that differences in water availability substantially influenced the differences between zones. ***In practice identifying these zones is useful for the farmer as it highlights and quantifies differences in yield that should be explored further. By understanding the causes of the differences, the farmer will be able to manage his or her fields more effectively.***

Our investigation of different sampling approaches showed that the economic benefit of grid- and zone-based sampling over field-based varies from field to field. On average, grid-based sampling performed better than zone-based sampling. ***We found that the variation captured in yield monitor data can help to inform on which sampling scheme is most appropriate. By***

***forming variograms from yield maps we can use the quantification of the spatially structured variation to indicate when each sampling scheme is likely to be most cost effective.***

The spatial variation captured by the variogram of the yield monitor data can help to determine whether spatially variable management is cost effective. We considered a decision tree to assess the 'Potential for variable rate management' by Lark *et al.* (2003) and the Opportunity index by de Oliveira (2009). We found parts of the Lark *et al.*(2003) were counterintuitive due to the way the tree was derived and that the Opportunity index was over sensitive to the range of the variogram of the yield monitor data. We proposed a new metric for variable rate management that we believe can be used by a farmer to rank his fields in order of the potential for variable rate management. It is very difficult to determine thresholds for these metrics over which variable rate management would be cost effective. Therefore, ***we believe it is best if the farmer ranks his or her fields according to a measure such as the management score we proposed to determine which fields are most likely to respond profitable to variable rate management. We caution that a large score does not necessarily indicate that variable rate management is cost effective, only that the farmer would be wise to try and understand the causes of the observed variation to see if it could be managed more efficiently.***

## 6.1. Guidance for farmers

The principles described here could be integrated to help farmers to the most from their yield data.

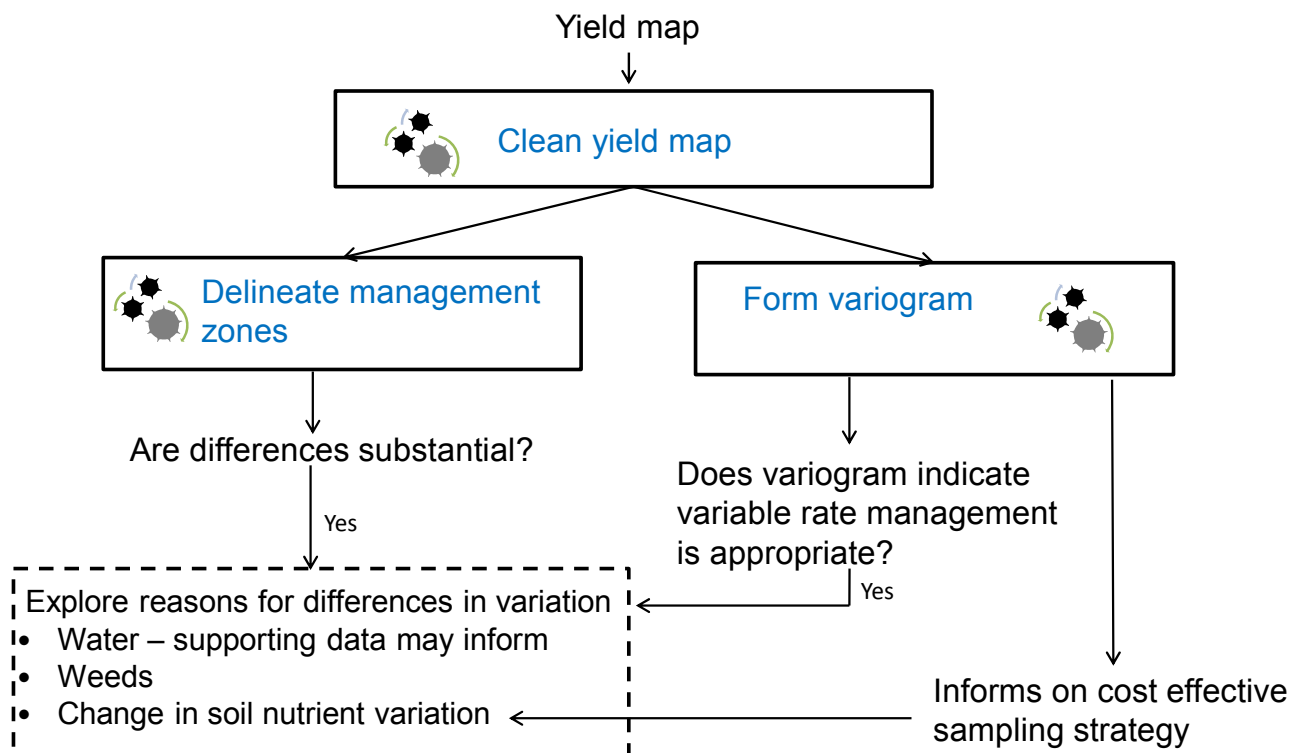


Figure 6. Guidance for farmers on the use of yield maps for variable rate management in the field (The symbols in the boxes indicate the use of computers to process the algorithms).

Following the logical steps laid out in Figure 6 farmers should

- (i) Clean their yield monitor data to remove artefacts and outliers, without smoothing out important variation. A program such as Roth-YE is ideally suited to this. The clean yield map will give the farmer an indication of the range of yields in the field and are needed for steps (ii) and (iii) below.
- (ii) Inspect the yield maps before further use. Only use monitor data that forms coherent maps (e.g. winter wheat, oats and barley) avoid poorer data typically associated with maps of oil seeds or peas and beans or maps with large gaps in them.
- (iii) Use the cleaned maps in a spatially smoothed cluster analysis to delineate management zones. This will allow farmers to identify parts of the field that vary differently from one another across seasons. When differences in yields between zones are reasonably large, the farmer should seek to understand these differences using a combination of his or her expert knowledge, other sensor data, historic weather data and perhaps soil sampling.

- (iv) Form variograms using recent (up to last five) years yield monitor data to get a picture closer to the current situation in the field. Variograms of the yield monitor summarise important features of the yield variation in the field, and this can be assumed to be a proxy for soil conditions. Therefore, metrics based on the variogram can be used to decide (i) when variable-rate application of fertilizer might be cost effective and (ii) what sampling strategy is best to apply to determine the nutrient status of the field.

## **6.2. Future research and knowledge transfer**

### *6.2.1. Integrating farmer's knowledge with hard data to inform management zones.*

In the methods above, we describe how to delineate management zones based on yield monitor data. Once these zones are defined other data can be used to determine what is driving the differences. Farmers will also often have a sound theory for the reasons for the observed variation in yields. Using mathematical techniques this 'soft data' could be incorporated with the measured data (the hard data) to improve the delineation of management zones and the understanding of what drives them.

### *6.2.2. Validation of soil management zones by the yield determining factors at field*

In this study, fields were divided in to two-to-four management zones based on the spatial variance of the yield determining factors. In only a few of the fields were zones related to the differences in measured soil nutrients. A number of other factors (e.g. texture effect on water holding capacity, pH and other nutrients like nitrogen, potassium, calcium, magnesium), may be driving the variation in the field. We need to validate these soil management zones by the evaluation of yield determining factors in the field to explain the variation in the yield between the soil management zones.

### *6.2.3. Investigate new methods of sampling*

In evaluating the different sampling approaches, we have considered only three methods: field, zone, and grid-based. There could be other approaches of sampling. For example if a yield map shows that one area of the field is more variable than another, would it be prudent to sample more intensively in the more variable zone?

### *6.2.4. Developing an integrated model that farmers can use*

The methods described here rely on several computer programs working as stand-alone versions. Currently these are working prototypes, which need further development to be robust enough to give to farmers to use themselves. Although some of the components (e.g. yield cleaning program) have user interfaces. Ideally, the methods described here should be integrated into a single program, which can do all the different tasks starting from yield cleaning, creating management zones and

assessing these fields for variable rate management. This could be made accessible to farmers through any web based platforms (e.g. AHDB website).

## 7. References

- Arslan, S., Colvin, T.S., 2002. Grain Yield Mapping: Yield Sensing, Yield Reconstruction, and Errors. *Precision Agric* 3, 135-154.
- Blackmore, S., Godwin, R.J., Fountas, S., 2003. The Analysis of Spatial and Temporal Trends in Yield Map Data over Six Years. *Biosystems Engineering* 84, 455-466.
- de Oliveira, R.P., 2009. Contributions towards decision support for site-specific crop management - A study of aspects influencing the development of knowledge-intensive differential management decisions. Faculty of Agriculture, Food and Natural Resources, Australian Centre for Precision Agriculture. University of Sydney, <http://hdl.handle.net/2123/7204>.
- Dunn, J.C., 1976. Indices of partition fuzziness and the detection of clusters in large data sets. In: Gupta, M.M. (Ed.), *Fuzzy Automata and Decision Process*. Elsevier, New York.
- Griffin, T.W., 2010. The spatial analysis of yield data. In: Oliver, M.A. (Ed.), *Geostatistical applications for precision agriculture*. Springer.
- Johnston, A.E., 2005. Phosphorus nutrition in arable crops.
- Johnston, A.E., Goulding, K.W.T., 1988. Rational potassium manuring for arable cropping systems. *Journal of the Science of Food and Agriculture* 46, 1-11.
- Kindred, D.R., Storer, K., Hatley, D., Ginsburg, D., Catalayud, A., Milne, A., Marchant, B., Miller, P., Sylvester-Bradley, R., 2015. Automating Nitrogen fertiliser Management for cereals (Auto-N) LINK Research Project LK09134: Reducing GHG emissions, nitrate pollution and lost productivity by fully automating N fertiliser management. Agriculture and Horticulture Development Board.
- Lark, R.M., 1998. Forming spatially coherent regions by classification of multi-variate data: an example from the analysis of maps of crop yield. *International Journal of Geographical Information Science* 12, 83-98.
- Lark, R.M., Wheeler, H.C., Bradley, R.I., Mayr, T.R., Dampney, P.M.R., 2003. Developing a cost effective procedure for investigating within-field variation of soil conditions. Project Report No.296. HGCA.
- Marchant, B.P., Dailey, A.G., Lark, R.M., 2012. Cost effective sampling strategies for soil management. Project Report No. 485. Home Grown Cereals Authority. [http://cereals.ahdb.org.uk/media/252472/pr485\\_summary.pdf](http://cereals.ahdb.org.uk/media/252472/pr485_summary.pdf). Last accessed January 2016.
- Milford, G.F.J., Johnston, A.E., 2007. Potassium and nitrogen interactions. In: *Proceedings No 615. International Fertiliser Society*. pp. 1-22.
- Milne, A.E., Webster, R., Ginsburg, D., Kindred, D., 2012. Spatial multivariate classification of an arable field into compact management zones based on past crop yields. *Comput Electron Agr* 80, 17-30.
- Ordnance-Survey, 2015. A guide to coordinate systems in Great Britain-An introduction to mapping coordinate systems and the use of GPS datasets with Ordnance Survey mapping.
- Patterson, H.D., Thompson, R., 1971. Recovery of inter-block Information when block sizes are unequal. *Biometrika* 58, 545-554.

- Payne, R.W., Murray, D.A., Harding, S.A., 2011. An Introduction to the GenStat Command Language (14th Edition). VSN International, Hemel Hempstead, UK.
- Pringle, M.J., McBratney, A.B., Whelan, B.M., Taylor, J.A., 2003. A preliminary approach to assessing the opportunity for site-specific crop management in a field, using yield monitor data. *Agr Syst* 76, 273-292.
- Searey, S.W., Schueller, J.K., Bac, Y.H., Borgelt, S.C., Stout, B.A., 1989. Mapping of spatially variable yield during grain combining. *Transactions of the American Society of Agricultural Engineers* 32, 826-829. *Transactions of the American Society of Agricultural Engineers* 32, 826-829.
- Simbahan, G.C., Dobermann, A., Ping, J.L., 2004. Site-specific management - Screening yield monitor data improves grain yield maps. *Agron J* 96, 1091-1102.
- Stafford, J.V., Ambler, B., Lark, R.M., Catt, J., 1996. Mapping and interpreting the yield variation in cereal crops. *Comput Electron Agr* 14, 101-119.
- Sudduth, K.A., Drummond, S.T., 2007. Yield Editor: Software for removing errors from crop yield maps. *Agron J* 99, 1471-1482.
- Sun, W., Whelan, B., McBratney, A., Minasny, B., 2013. An integrated framework for software to provide yield data cleaning and estimation of an opportunity index for site-specific crop management. *Precision Agric* 14, 376-391.
- Syers, J.K., Johnston, A.E., Curtin, D., 2008. Efficiency of soil and fertilizer phosphorus use: reconciling changing concepts of soil phosphorus behaviour with agronomic information. *Bulletin* 18. FAO, Rome. <ftp://ftp.fao.org/docrep/fao/010/a1595e/a1595e00.pdf>. Last accessed january 2016. .
- Webster, R., 1985. Quantitative Spatial Analysis of Soil in the Field. In: Stewart, B.A. (Ed.), *Advances in Soil Science*. Springer New York, New York, NY, pp. 1-70.
- Webster, R., Oliver, M.A., 2001. *Geostatistics for environmental scientista*. John Wiley and Sons, Ltd., Chichester.
- Webster, R., Oliver, M.A., 2007. *Geostatistics for Environmental Scientists*, 2nd edition. John Wiley & Sons, Chichester.

## 8. Appendices

### 8.1. Description of variogram

A variogram is a function of the expected mean squared difference between random variables at places separated in a space of one, two or three dimensions:

$$\gamma(h) = \frac{1}{2} E [Z(x) - Z(x + h)]^2$$

where  $Z(x)$  and  $Z(x + h)$  are variable  $Z$  at positions  $x$  and  $x + h$  separated by the vector  $h$  for all  $h$ . It characterizes the similarity, or dissimilarity, between places in terms of separation in both distance and direction. If  $Z$  is spatially correlated then  $\gamma(h)$  increases (the places become increasingly dissimilar) as the separating distance increases.

Experimental variograms are often calculated by the method of moments:

$$\hat{\gamma}(h) = \frac{1}{2m(h)} \sum_{j=1}^{m(h)} \{z^*(x) - z^*(x + h)\}^2$$

where  $z^*(x)$  and  $z^*(x + h)$  are the simulated values at positions  $x$  and  $x + h$  separated by the lag  $h$ , which in the isotropic case is the scalar distance  $h$ , and  $m(h)$  is the number of comparisons at that lag. By changing  $h$  we obtained the ordered set to which we can fit variogram models. Several authorised variogram models are described by Webster and Oliver (2001). Examples include

The spherical model:

$$\gamma(h) = c_0 + c_1 \left\{ 1.5 \left( \frac{h}{r} \right) - 0.5 \left( \frac{h}{r} \right)^3 \right\} \quad \text{if } h \leq r$$

$$\gamma(h) = c_0 + c_1 \quad \text{otherwise}$$

where  $c_0$  and  $c_1$  are the nugget and spatially correlated parameters of the variance,  $r$  is the range parameter.

The exponential model:

$$\gamma(h) = c_0 + c_1 \left\{ 1 - \exp \left( -\frac{h}{a} \right) \right\}$$

here  $c_0$  and  $c_1$  are the nugget and spatially correlated parameters of the variance,  $a$  is the distance parameter and  $h = |h|$  is the separation in distance (or lag). The function approaches its maximum,

$c_0 + c_1$ , asymptotically, and the distance  $3a$  is often taken to be the effective range of the spatial correlation.

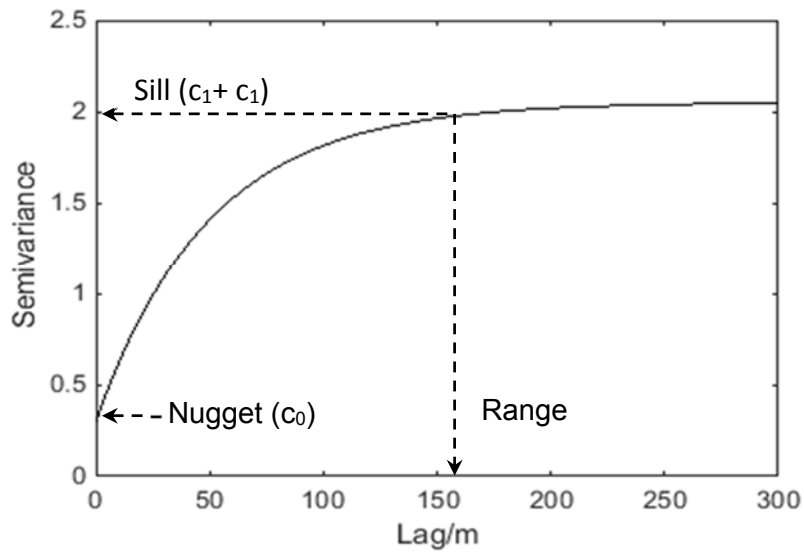


Figure 8.1. An exponential variogram with sill, nugget and effective range shown.

## 8.2. Mathematical symbols and abbreviations used.

Symbol	Meaning
$x \equiv \{x_1, x_2\}$	Spatial coordinates in two dimensions
$y$	Yield of crop
$\tilde{y}$	Standardized yield
$y_r$	Realized yield
$y_0$	Target yield
$z$	Quantity of phosphorus, P
$z^*$	Realization of $z$
$z_{\text{fert}}$	Quantity of fertilizer P
$z_{\text{soil}}$	Initial quantity of P in the soil
$z_{\text{total}}$	$z_{\text{fert}} + z_{\text{soil}}$
$k$	The number of classes in the k-means classification
<b>Variogram parameters</b>	
$c_0$	Nugget variance
$c_1$	Variance of spatially correlated structure
$a$	Distance parameter
<b>Costs</b>	
$G_{\text{wheat}}$	Price of grain, assumed to be £150 t <sup>-1</sup>
$G_{\text{fert}}$	Price of P fertilizer, assumed to be £0.31 kg <sup>-1</sup>
$G_{\text{sample}}$	Cost of soil analysis, assumed to be £5 sample <sup>-1</sup>

**8.3. Summary statistics for P in each field according to zone and the probability that the observed variation in P was explained by the classifications.**

	<b>Mean</b>	<b>Median</b>	<b>Minimum</b>	<b>Maximum</b>	<b>Standard deviation</b>	<b>F prob.</b>
<b>Field-BD</b>						
Total population	19.3	18.6	12.8	31.2	4.0	0.897
Zone 1	19.93	20.6	16.0	22.8	2.419	
Zone 2	19.2	16.8	12.8	31.2	5.530	
Zone 3	18.93	19.2	16.6	21.8	1.934	
<b>Field-ER</b>						
Total population	21.7	22.3	14	28	4.144	0.265
Zone 1	20.0	19	15.4	24.8	3.243	
Zone 2	23.1	24.5	14	28	4.501	
Zone 3	21.9	21.8	17	26.8	4.518	
<b>Field-GP</b>						
Total population	95.0	90.2	37.2	165.2	36.7	0.399
Zone 1	90.9	92.1	37.2	163.6	35.4	
Zone 2	106.2	103.4	49.8	165.2	39.8	
Zone 3	69.7	69.7	54.2	85.2	21.9	
<b>Field-LM</b>						
Total population	28.0	26.8	18.8	52.2	6.8	0.567
Zone 1	27.2	26.6	18.8	37.2	5.7	
Zone 2	28.4	27.0	20.6	52.2	7.3	
<b>Field-MC</b>						
Total population	16.9	15.4	11.6	34.8	6.1	0.449
Zone 1	16.1	13.6	11.6	34.8	6.7	
Zone 2	18.1	17.4	13	29.8	4.9	
<b>Field-RH</b>						
Total population	83.2	72.6	20.8	163.4	40.4	0.144
Zone 1	81.84	72.6	20.8	145.0	39.71	
Zone 2	59.48	51.0	40.8	97.0	22.63	
Zone 3	109.6	118.8	44.2	163.4	46.01	

#### 8.4. Parameters of different variograms models for various fields.

Field	Year	Model	Range		Sill		Nugget	VR**	SD††
			a1	a2	C1	C2			
Field-BD	2000	Exponential*	274.4	-	0.91	-	0.36	0.63	1.82
	2003	Double Spherical	190.5	386.9	2.20	0.95	0.28	1.23	4.00
	2006	Spherical	268.6	-	0.18	-	0.32	0.24	1.15
Field-CC	2004	Double Spherical	39.3	198.6	0.81	1.31	0.65	1.14	2.20
	2005	Double Spherical	42.4	234.8	1.16	1.01	0.94	1.19	1.97
	2008	Double Spherical	36.2	113.3	1.11	0.43	0.66	1.15	2.10
	2009	Double Spherical	44.6	165.9	0.73	0.25	0.30	0.89	2.42
	2011	Exponential*	158.9	-	3.11	-	1.13	1.38	2.10
Field-CP	2000	Double Spherical	17.6	415.3	0.50	0.52	0.44	0.77	1.54
	2003	Double Spherical	18.6	146.1	0.72	0.29	0.32	0.93	1.85
	2006	Double Spherical	33.5	235.4	0.37	0.16	0.40	0.64	1.63
	2008	Exponential*	93.6	-	1.19	-	0.67	0.96	1.84
	2009	Double Spherical	42.1	313.8	0.79	1.92	0.46	1.12	2.54
	2011	Double Spherical	22.4	103.9	0.92	0.26	-	1.04	3.10
	2012	Double Spherical	23.2	122.2	0.59	0.71	0.00	1.00	3.99
Field-ER	2004	Exponential*	65.5		0.44		0.83	0.61	1.30
	2006	Exponential*	52.3		0.36		0.34	0.57	1.52
	2008	Double Spherical	11.4	90.4	0.93	0.21		1.04	1.79
	2009	Exponential*	57.6		1.36		0.38	1.09	2.22
	2012	Exponential*	60.0		0.97		0.12	0.92	2.79
Field-EL	2001	Double Spherical	25.2	286.7	0.52	1.63	0.74	0.99	1.79
	2002	Double Spherical	16.1	656.0	0.69	3.93		1.10	3.10
	2003	Double Spherical	37.3	188.3	0.19	0.16	0.36	0.50	1.48
	2010	Double Spherical	21.8	156.5	3.03	1.60	0.09	1.94	3.00
	2011	Double Spherical	28.4	323.2	1.53	1.55	0.16	1.37	3.19
Field-HM	2000	Double Spherical	49.2	473.3	0.19	0.81	0.30	0.56	1.76
	2003	Double Spherical	128.1	499.6	0.50	0.85	0.49	0.67	1.71
	2006	Exponential*	233.7		0.07		0.27	0.19	1.11
Field-HS	2002	Double Spherical	64.8	347.9	1.52	2.52	1.17	1.38	2.13
	2005	Double Spherical	48.6	269.7	1.28	1.13	0.48	1.23	2.70
	2008	Double Spherical	22.3	187.6	2.71	0.99		1.75	3.03

	2009	Double Spherical	64.7	443.0	1.31	0.90	0.53	1.13	2.50
	2011	Double Spherical	56.5	313.8	3.22	2.33	1.50	1.86	2.42
Field-LM	2001	Double Spherical	128.4	323.7	0.59	0.33	0.64	0.66	1.55
	2004	Exponential	143.1	-	0.91	-	0.31	0.77	2.18
	2005	Spherical	181.2	-	0.28	-	0.21	0.35	1.48
	2007	Spherical	118.6	-	0.30	-	0.23	0.43	1.65
Field-MC	2002	Exponential*	96.2	-	0.82	-	0.60	0.79	1.68
	2005	Power†	138.0	-	0.02	-	0.44	0.47	1.32
	2008	Double Spherical	39.4	227.9	0.37	0.54	0.65	0.74	1.59
Field-PA	2004	Spherical	229.1	-	2.49	-	0.27	0.88	2.92
	2005	Double Spherical	57.5	278.7	0.11	0.39	0.17	0.46	1.92
	2007	Spherical	249.6	-	0.20		0.33	0.24	1.15
Field-RH	2000	Double Spherical	10.1	411.5	0.67	1.11	0.0	0.94	1.86
	2006	Power†	380.0		0.32		0.39	0.18	1.07

\*Effective range = lag distance \* 2.966;

†Effective range 95% of the half of the maximum length of the field

\*\*VR: Variance ratio; ††SD: Standard deviation

### 8.5. Opportunity index ( $Y_i$ ) and its components for different years for different fields.

Field	Year	X_mean	aCv	Mv	Sv	$Y_i$
Field-BD	2000	8.2	9.3	0.9	228.3	14.6
	2003	6.3	19.2	1.9	322.5	24.9
	2006	8.3	5.8	0.6	224.2	11.4
Field-CC	2004	10.3	11.8	1.2	165.8	14.0
	2005	10.0	12.5	1.3	195.8	15.7
	2008	14.2	7.6	0.8	94.17	8.5
	2009	10.0	8.1	0.8	138.3	10.6
	2011	11.1	13.7	1.4	132.5	13.5
Field-CP	2000	12.6	6.6	0.7	345.8	15.1
	2003	12.3	6.8	0.7	121.7	9.1
	2006	10.5	6.8	0.7	195.8	11.5
	2008	12.5	7.9	0.8	78.3	7.9
	2009	9.6	12.5	1.3	261.7	18.1
	2011	10.4	7.8	0.8	86.7	8.2
	2012	6.1	13.1	1.3	101.7	11.5
Field-ER	2004	11.7	8.8	0.9	55.0	7.0
	2006	10.3	6.0	0.6	43.3	5.1
	2008	13.0	6.4	0.6	75.0	6.9
	2009	9.8	10.0	1.0	48.3	6.9
	2012	6.5	12.2	1.2	50.0	7.8
Field-EL	2001	11.4	9.7	1.0	239.2	15.2
	2002	9.0	12.8	1.3	546.7	26.4
	2003	7.6	8.1	0.8	156.7	11.3
	2010	11.7	14.2	1.4	130.0	13.6
	2011	10.8	11.6	1.2	269.2	17.6
Field-HM	2000	9.2	7.7	0.8	394.2	17.5
	2003	7.1	12.4	1.2	416.7	22.7
	2006	8.3	5.1	0.5	195.0	10.0
Field-HS	2002	11.7	15.1	1.5	290.0	20.9
	2005	9.9	12.3	1.2	225.0	16.6
	2008	13.1	11.1	1.1	156.7	13.2
	2009	9.9	11.9	1.2	369.2	20.9
	2011	11.6	16.8	1.7	261.7	20.9
Field-LM	2001	9.9	9.0	0.9	270.0	15.6
	2004	9.4	8.2	0.8	119.2	9.9

	2005	7.9	6.2	0.6	150.8	9.6
	2007	8.3	6.2	0.6	99.2	7.8
Field-MC	2002	10.2	9.6	1.0	80.0	8.7
	2005	9.7	7.2	0.7	115.0	9.1
	2008	11.4	7.8	0.8	32.5	5.0
Field-PA	2004	9.0	11.5	1.1	190.8	14.8
	2005	8.4	6.5	0.6	48.3	5.6
	2007	7.4	6.6	0.7	208.3	11.7
Field-RH	2000	8.9	9.9	1.0	343.3	18.5
	2006	6.7	7.5	0.8	316.7	15.5